



Ca' Foscari
University
of Venice

Master's Degree in
Conservation Science and Technology
for Cultural Heritage

-
Ca' Foscari
Dorsosuro 3246
30123 Venezia

Final Thesis

Investigation of the rising damp phenomenon in
historical Venetian buildings by a new multi-
analytical approach

Supervisor

Prof. Elisabetta Zendri

Assistant Supervisor

Dr. Laura Falchi

Graduand

Martina Corradini

Matriculation number 851769

Academic Year

2018/2019

Table of Contents

PURPOSES OF THE THESIS	5
1 INTRODUCTION	6
1.1 Venetian Lagoon	7
1.1.1 The high water events	9
1.1.2 Venetian buildings	12
1.1.2.1 Bricks structure and related deterioration	13
1.2 Mechanism of rising damp: physical and chemical features	14
1.2.1 Damages related to rising damp: salts effects	16
1.2.1.1 Salts solubility and distribution in masonry	18
1.2.2 Rising damp trend in Venetian masonries	20
1.3 Facing rising damp and high water in Venice: past, actual and future proposals	22
2 EXPERIMENTAL PART	26
2.1 SECTION 1 - Photos comparison	26
2.1.1 Archives of photos	26
2.1.2 Acquisition of current photographs and comparison	29
2.2 SECTION 2 - Case studies: analysis on six Venetian buildings	30
2.2.1 Buildings history	31
2.2.2 Non- invasive measurements and buildings sampling	34
2.2.2.1 Samples analysis	35
3 RESULTS AND DISCUSSION	40
3.1 SECTION 1 - Comparison of photographs	40
3.1.1 Sestiere Castello	42
3.1.2 Sestiere Dorsoduro	58
3.1.3 Sestiere San Marco	66
3.2 SECTION 2 - Venetian case studies	80
3.2.1 Ca' Foscari	81
3.2.2 Ca' Bottacin	85
3.2.3 Ex Slaughterhouse San Giobbe	89

3.2.4	Badoer Palace	92
3.2.5	Ca' Tron	95
3.2.6	Malipiero Palace	98
3.3	Six buildings results comparison	101
3.3.1	Weather and tidal situation during samplings	101
3.3.2	Moisture and salts distribution comparison among the six case studies	102
3.3.3	Anions distribution trend in Ca' Foscari, Ca' Bottacin and Ex Slaughtethouse San Giobbe	104
3.3.4	FT-IR analysis of the six Venetian buildings	106
4	CONCLUSIONS	109
	APPENDIX 1 – INSTRUMENTAL SPECIFICATIONS	111
	Bibliography and sitography	113

Purposes of the thesis

Rising damp is one of the most critical and complex mechanism affecting historic masonries and compromising the conservation of architectural heritage. Building materials, such as bricks, mortar and stones, are susceptible to degradation in relation to the environmental and exposure conditions. The unique context of Venice, both from environmental and constructive point of view, represents one of the main challenging case study for rising moisture investigation. The lagoon salty water is responsible of salts migration within masonry which produces physical damages on mortars and bricks. Considering the phenomenon entity throughout the city, its impact and periodical monitoring would be necessary. This Master thesis focuses therefore on the evaluation of rising damp effects over time and it is structured into two main sections:

1. Evaluation of the rising damp process trend over time by means of photographic sources comparison. Historical photos of Venice, selected from public and private archives, are compared with current ones of the same subjects. An evaluation system based on experts' elicitation and specifically calibrated for this research, allows to identify possible common trends among the investigation cases.
2. Analysis of actual conservation state of six historical buildings, considered prominent examples of rising damp effects. Ca' Foscari, Ca' Bottacin, Ex Slaughterhouse San Giobbe, Badoer Palace, Ca' Tron and Malipiero Palace are firstly analysed through non-invasive methods such as visual documentation and Infrared thermography. Samples are obtained by drilling previously selected walls at different heights and depths. Weighting methods are applied to determine moisture content, soluble salts and ions distribution. Moreover conductivity, Infrared Spectroscopy and Ion Chromatography give additional information on samples.

Both the thesis parts contribute to the implementation of the already existing dataset on moisture distribution in Venetian masonries and buildings. Indeed, crossing different research data could produce a general report and increasing awareness about the rising damp trend in Venice. The evaluation of the phenomenon through the time meets the future perspectives considering also the climate changes effects. This is one of the themes considered in the thesis, which is implemented in the larger framework of "Venezia 2021, Linea 5.3 Piano di adattamento al cambiamento climatico e implementazione di strategie di intervento per la salvaguardia del patrimonio architettonico" project leaded by CORILA in partnership with Ca' Foscari University.

1 Introduction

The architectural heritage conservation is fundamental in preventing cultural identity loss for future generations and assuring, as long as possible, buildings structural stability through continuous monitoring, restoration and maintenance.

All buildings, in particular the historical ones, need to be protected from harmful moisture, both outside and inside. Water infiltrations from the exterior, and uncontrolled humidity and condensation in the interiors, create serious structural damages and unhealthy internal environmental conditions. Moisture within masonries depends on different chemical-physical characteristics of the atmosphere and the several building materials applied in construction field [1]. All the water states (gas, liquid and solid) are involved in moisture entrance within materials [2]. In fact, water penetrates into porous building fabric in the vapour or liquid form. Depending on relative humidity (RH), water vapour condensation and hygroscopic absorption/desorption occur, while the liquid form is involved when the material is directly water exposed (e.g. infiltration, rainfall and rising damp) [1,3]. Finally, the solid state is reached through freeze-thaw cycles, which are dangerous for the materials integrity [3].

Generally, moisture in masonries is given by four primary sources: 1) the atmosphere (precipitations, condensed and absorbed water vapour); 2) water vapour deriving by exterior environments and interior activities; 3) liquid vapour from soil and 4) moisture in the building materials themselves [1,4]. The related moisture transport mechanisms are vapour diffusion and convection, liquid flow in macropores or cracks and liquid water capillarity suction [1,4]. This latter corresponds to the rising damp, a severe phenomenon of dampness which takes to wetness and decay of historical buildings [5-9]. The water sources, responsible of capillary rise, could be underground watercourse and aquifers, agricultural irrigation, obstacles in the drainage of rainfalls [6,10]. The rising damp is responsible of fungi and moulds growth, plaster and paint deterioration, salt stains and steel and iron rust. Additional effects are those related to the building occupants health, due to the possible development of respiratory illnesses or the danger of mortar and plaster fallings [5,6]. Considering all these negative consequences, the rising damp process is widely studied and it should be monitored over time.

Even if it is not possible to completely delete the phenomenon, it can be investigated and possible solutions developed in order to mitigate, or at least contain, the related damages on architectural heritage.

The Venice lagoon environment with its particular conditions for buildings and their materials represents the emblematic scenario for moisture and rising damp effects manifestation. This is obviously due to the direct contact between buildings, the lagoon and seawater and the periodical high tides throughout the city.

1.1 Venetian Lagoon

The Lagoon of Venice is the largest one in the Adriatic Sea [11] and it has the shape of an elongated arch (Figure 1a-b). Table 1 reports some numerical information concerning the Venice lagoon which is the result of a long and slow phase of environmental evolution started 17,000-20,000 years ago [12,13].

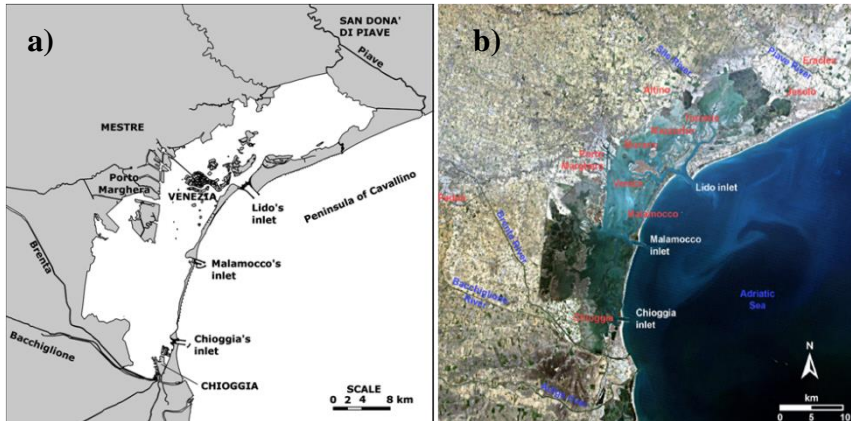


Figure 1 The Venetian Lagoon: a) map with nearest rivers and Lagoon's inlets of Chioggia, Malamocco and Lido [14]; b) Venice Lagoon view from the sky [13].

Length	51 km
Width	12 km
Perimeter	157 km
Total Surface	540 km ²
Canals and open water spaces	66 km ²
Slums (150- 40 depth)	243 km ²
Velme ¹	98 km ²
Sandbar ²	11 km ²
Fishing Valleys	92 km ²
Islands	29 km ²
Average depth	154 cm
Maximum depth ³	- 45 m
Salinity at Lagoon's inlets	36 PSU ⁴
Salinity near the mainland	27 PSU

Table 1 Information on the Venice lagoon [15]

After the glacial phases, the level of the Adriatic sea was 120 meters lower than today. Then it risen up reaching the actual value 6000 years ago. The primeval lagoon, smaller than the actual one, is the product of fluvial detritus accumulation moved against coast by waves. Water exchanges with the open sea are possible thanks to the main Lagoon's inlets that today are just three (Lido, Malamocco and Chioggia), against the eight of the past .

The abundant freshwater discharge has diminished [16] because of the deviation works (in 15th and 16th century) making rivers flowing directly into the Adriatic Sea [16,17]. In doing so, the lagoon changed progressively from a transitional to a marine environment [17]. Since 1800 deeper canals were dig and sea openings modified to enhanced industrial activities, accelerating erosion, producing changes in flora and fauna habitat and enhancing lagoon deepening. The actual lagoon's morphology shows salt marshes, channels network with shallow waters and tidal flats [18].

¹ Emerging Lagoon areas between 0.40 and 0.30 meters above sea level which are submerged during high tide phases.

² Emerging Lagoon areas lower than 0.30 meters, submerged by high tides.

³ At Malamocco Lagoon's inlet.

⁴ Practical Salinity Unit

Tides are periodic rising and falling of the sea level due to attraction of water bodies around all the Earth by Moon and Sun [19,20]. High and low tide are the two tidal phases oscillation and the difference among the two is called amplitude. Tides are classified into three groups: i) diurnal tides, (one high tide and low tide per day); ii) semi-diurnal tides (two high tides and two low tides every 24 hours) and iii) mixed tides (two high tides and two low tides but with a highly different amplitude among them) [19]. In the specific case, Venice is characterized by semi-diurnal tides with two maximum heights and two minimum heights every 24 hours [19, 21]. A tide is the sum of astronomical tide and meteorological surge (Figure 2) [19,20].

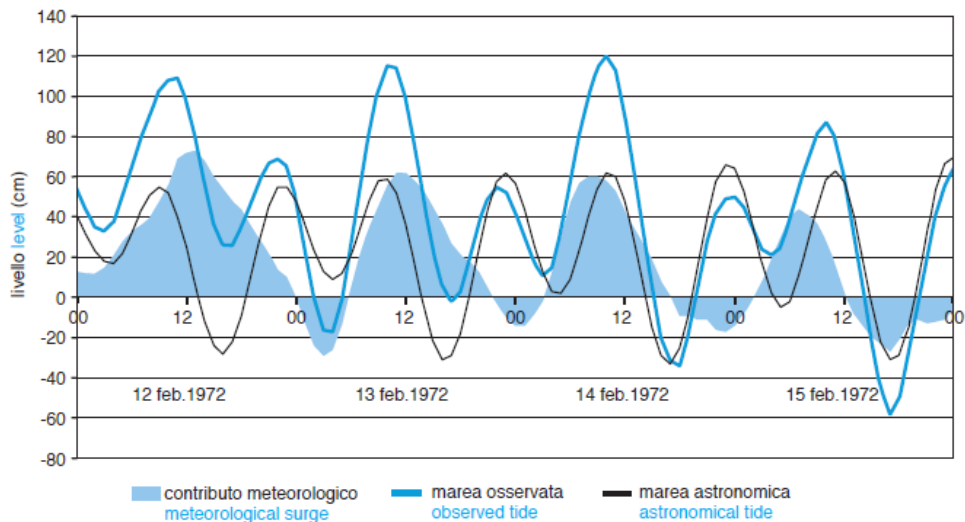


Figure 2 Example of tidal level observed in Venice. Astronomical tide and meteorological one registered between 12 and 15 February [20].

Usually, if no particular bad weather conditions are registered, the tide in Venice corresponds to the astronomical one. This latter can be altered by meteorological events [19], especially winds (Sirocco and Bora) and pressure variation. In the case of high water events a correspondence between the maximum of the astronomical tide and that of the meteorological one occurs. The Adriatic sea is a closed marine zone and characterized, in particular in the north area, by shallow water. For this reasons, if the winds are really strong, the water level can rise up even till one meter more. The pressure instead has an inversely proportional relationship with the water level: the higher the pressure, the lower the water lever and vice versa [19].

Since 1970s a centre for tides observation has been introduced in Venice by the municipality of the city [20]. This represents a service for the citizen thanks to an alarm system installation in order to warn in advance the high tide occurrence. Today an information improvement about tide changes in tides is given by the Centro Previsioni e Segnalazioni Maree (CPSM) [20].The increasingly frequency of high tide events is given by eustatism and subsidence [20] as described in the following paragraphs.

1.1.1 The high water events

The *acqua alta* phenomenon corresponds to a tide exceeding +80 cm on the mean sea level (m.s.l.), in comparison to the conventional zero which is the average sea level measured at Punta della Salute in 1897. While a +80 cm tide floods just the lowest parts of the city, a +110cm tide inundates the 12% of Venice. In exceptional cases, and so with a water level of +140 cm, the flooding of the city reaches the 59% and the 91% at +200 cm [20,22]. These events represent a disease for the inhabitants and a danger for the traditional buildings [23]. The municipality of Venice, through the Centro Maree established a tide classification (Table 2).

tide > +140 cm	Exceptional high tide
+ 110 ÷ +139 cm	Very high tide
+ 80 ÷ +109 cm	High tide
-50 ÷ +79 cm	Normal tide
-90 ÷ -51 cm	Low tide
tide < -90 cm	Exceptional low tide

Table 2 Thresholds of expected tides [20].

The mean water level in Venice, and consequently the flooding of the city, is affected by local land subsidence, both human and nature caused, and by the global eustatism due to climate changes [12,14,22,23]. In particular the sea level rising since the 19th century is about 1.8 ± 0.5 mm/year and the subsidence is given by the natural sediment compaction and human activity. Indeed till 1970s the industrial plant of Marghera was responsible of the aquifer depressurization induced by water pumping. Fortunately, this activity has been reduced through the years taking to a stabilization of the land subsidence, at least in Venice and the central part of the lagoon. On the contrary, the southern and northern parts of the lagoon are continuously affected by pumping for agricultural activities, peat oxidation and geochemical compaction due to the intrusion of saltwater [14]. According different studies through the years, the historical centre of Venice has sunk about 23-25 cm with respect to the mean sea level and the more exposed area of Venice is San Mark's square which is flooded 50 times a year [14,22]. Both subsidence and eustatism could take to the permanent submersion of the lower land portions (as small islands) of the lagoon. Indeed, due to the 25 cm relative sea level increase (RSLI) registered till the 20th century, the high water events have been more frequent in Venice [14]. *Acqua alta* is also characterized by seasonal variability with a maximum frequency mainly in November and secondly in December and October. Indeed, the two worst high water events occurred on the 4th November 1966 with a tide of 194 cm height and, the more recent one, on the 12th November 2019 with +187cm. Despite these events are considered isolated and exceptional, the city is constantly and increasingly exposed to flooding through the years as visible in Figure 3, 4 and 5. The high tides (> +110 cm) number per year are constantly increasing since the 60s while the low tides (<-50 cm) occurrence is decreasing over time. The mean sea level per year (red line in Figures 3 and 4), considered as the average of the maximum and minimum recorded values, progressively increased over years. The actual level is 31cm higher if

compared with that at the beginning of the last century. The period between 1930 and 1970 shows the maximum m.s.l. increase as eustatism and subsidence consequence. After a more constant trend between 1970 and 2008, m.s.l. highly increase in the last years [20].

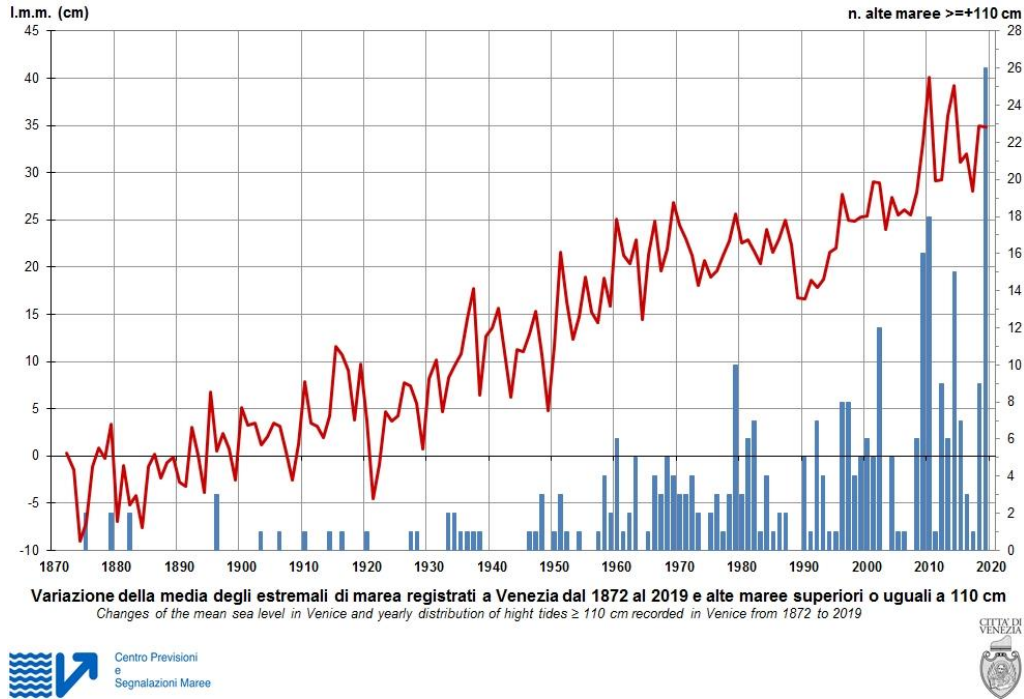


Figure 2 High tides ($> +110$ cm) distribution per year registered in Venice, from 1872 till 2019 [20].

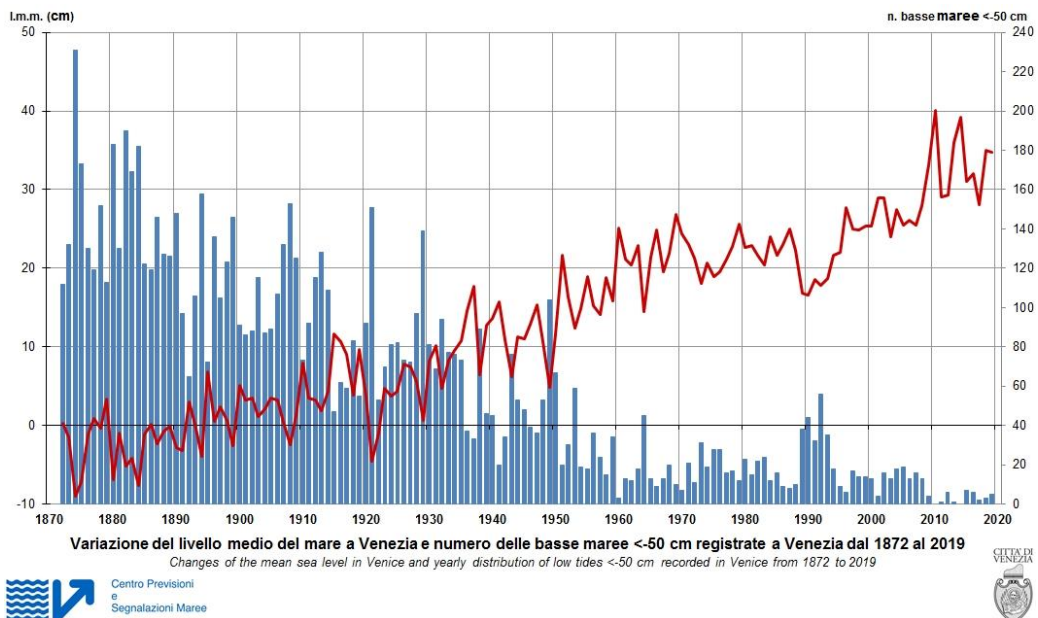


Figure 4 Low tides (< -50 cm) distribution per year registered in Venice and mean sea level changes, from 1872 till 2019 [20].

Tide values $\geq +140$ cm	date hour	value
16th of April 1936	21.35	147 cm
12th of November 1951	8.05	151 cm
15th of October 1960	7.55	145 cm
4th of November 1966	18.00	194 cm
3rd of November 1968	7.30	144 cm
17th of February 1979	1.15	140 cm
22nd of December 1979	9.10	166 cm
1st of February 1986	3.55	159 cm
8th of December 1992	10.10	142 cm
6th of November 2000	20.35	144 cm
16th of November 2002	9.45	147 cm
1st of December 2008	10.45	156 cm
23rd of December 2009	5.05	144 cm
25th of December 2009	3.55	145 cm
24th of December 2010	1.40	144 cm
1st of November 2012	1.40	143 cm
11th of November 2012	9.25	149 cm
12th of February 2013	0.05	143 cm
29th of October 2019	14.40	156 cm
29th of October 2019	20.35	148 cm
12th of November 2019	22:50	187 cm
13th of November 2019	9.30	144 cm
15th of November 2019	11.35	154 cm
17th of November 2019	13.10	150 cm

Figure 5 Data on tide values $> +140$ cm recorded in Venice from 1872 to 2019 [20].

Starting from the 12th November 2019 and for all the following days of the months, have been more or less severe. Indeed, 2019 represents the new high water events record for Venice. Statistically, considering the 1872-2019 range, this latter year has been interested by several flooding events (Table 3).

	Number of events in 2019	Previous record of events	Year
Tide $\geq +110$ cm	26	18	2010
$\geq +110$ cm in November	12	7	2012
$\geq +120$ cm	7	7	2010
$\geq +130$ cm	5	4	2009
$\geq +140$ cm	4	/	/
Tide $\geq +150$ cm	3	/	/

Table 3 Statistical data about high water events in Venice in 2019 [20].

The highest number of floods is registered in 2019, while the previous record was 2010 with 18 events. The major part of these were registered just in November 2019, according to the seasonality of the high water tendency, while in the past only the 2012 has been interested by 7 events in the same month [20]. As clearly visible in Table 5, the highest frequency and severity of floods regards mainly the last years, and in particular 2019.

1.1.2 Venetian buildings

The lagoon is a non-traditional place for constructions which therefore have specific structural requirements. Indeed the architecture of Venice does not follow the standard masonry mechanics but a specific one conceived for its environment [21]. Traditional building construction technologies took into consideration specific factors: brackish and sea water action during tides, soft soil basement and restricted space availability for constructions [21]. The limited space through the lagoon could be solved by multiple floor constructions but this, at the same time, could impose an excessive stress upon the soft soil base.

Considering all these implications, Venice has a specific and unique construction system. As well known, the city was build on soft, silt and clay based soil in which a wooden piles system was embedded till reaching the underlying harder soil (*caranto*) [24] (Figure 6).

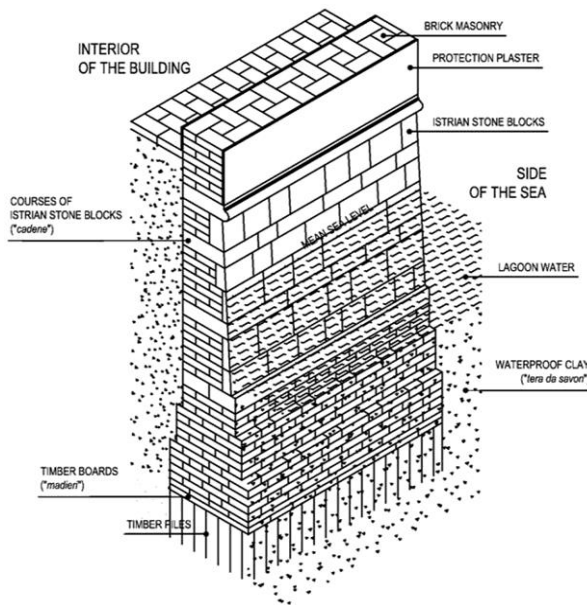


Figure 6 Schema of Venetian building foundations both interior and on the sea side [21].

The piles, since the 16th century had a maximum length between 2 and 3 meters while after the 16th century longer ones up to 6-7 m were installed [21,25]. They were inserted together as close as possible and on the upper surface two horizontal wooden layers constituted the base of the masonries. Then timber boards (*madien*), 10 cm thick, were put on the piles to create a flat and regular surface. The wooden strata allows a greater building weight distribution [21,25]. Above this, brick layers were put and covered with a waterproof clay (*tera da savon*) protecting them from the lagoon water [21].

All these elements constituted foundation itself. This latter corresponds to a plinth wall, with sloping walls and brick or Istria stone blocks [25]. Considering the wooden piles in water, normally these would have rotted in time. Nevertheless they were made in oak or larch, two wooden species highly water resistant but equally destined to rot over time. Since the wooden piles are underwater and so in an anaerobic environment, timber rot was thought to be impossible [21]. On the contrary, a study on the wooden foundations of Venice proved a slow timber rot in time [26] despite piles are additionally protected by the high amount of silt and silt clay sediment constantly driven by water and so absorbed by the wood increasing its hardness [21].

A protection against water were the vertical Istria stone layers on the building corners as well those continuous stone strata (*cadene*) whose position was above the middle sea level [21]. Finally, plasters

covered the buildings as external protection of masonries [21]. Today, all these prevention measures are no more sufficient because of the rising sea level due to climate changes and the increasingly frequent floods. Indeed the water level exceeds these Istria stone layers damaging the building wall fabrics [24].

The upper structure of buildings in Venice shows several weight-saving and space-saving elements. Indeed the majority constructions presents: perforations on as thin as possible walls, bricks widely used if compared to stones, columns widely employed, roof and floors usually wooden made and all the rooms disposed in order to exploit all the available space [21].

1.1.2.1 Bricks structure and related deterioration

The Venetian building wall foundations have been constructed in the marshy lagoon and the external constructions of the historical centre, are in direct contact with seawater and related wave motions [27]. Bricks are the main building components in Venice and therefore susceptible to degradation mechanisms linked to the lagoon environment. In particular, those below the sea level, directly in contact with sea water, are responsible of constructive static problems [28]. Always water is also part of the bricks manufacturing process itself, firstly present in the initial clay moulded (carbonate, silicates, oxides and aluminates based) then fired [21,29,30]. This lead to clay crystal destruction and *mullite* (crystalline aluminium-silicate) formation while potassium and sodium in the clay matrix determine its melting. The cooling process leads to formation of a non crystalline and hard silicate material. This latter, acting like a cement, fixes quartz crystals and *mullite* together creating a porous network. The porosity of Venetian bricks, and so water-soluble salts absorption, is mainly linked to the baking temperature of the handmade production process, as well as to the sand grain size [24,31]. The presence of crushed limestone lowers the melting point of clay minerals and the handmade bricks could present two kind of mistaken results: under burnt bricks (too soft) and over burnt bricks (too brittle) [31].

Depending on the firing temperature, a vitrification level is reached and the higher the temperature the stronger the brick. Indeed the well-fired ones are more resistant to the damages caused by repeated wetting-drying: the acid attack and leaking is favoured in the wetting phase and the pollutants crystallization is favoured in the drying one [27,29].

Another feature related to the firing temperature is the brick colour: the yellow bricks are fired at lower temperature while the red ones at higher ones. Moreover this is directly linked to iron oxides content, the red ones are richer in iron [29]. Venetian building masonries are visually characterized by bricks different both in colour and in production period. In particular in the past, before the 19th century, brick making process was responsible of very high void ratios which widely encourages water infiltrations. [21] This causes moisture content increasing which, if combined with sea salts, reduces compressive strength in bricks [21].

Bricks in a construction are affected by both external and internal stresses. The external ones are related to the environmental context and can cause damages both on a microscopic and macroscopic scale. In

particular, seasonal and daily temperature cycles lead to contraction of the building materials with the cold and their expansion with through heating [27]. Inner surfaces of the material undergo a greater stress with respect to the external ones, which are more sensible to temperature changes. This can cause deformation and cracks on bricks which progressively continue to open during time [29].

Among internal stresses in bricks, the most significant degradation phenomena are due to frost and salt crystallization. Both the processes cause a stress faced by the compression resistance of the brick material itself. In the case of frost, the pores with a size between 0.1 and 1 μm are interested by the greater stress [29]. When bricks are fired at low temperature they are more susceptible to salt attack and the consequently powdering and flaking. In addition also the pore structure and strength properties influence the brick resistance to salt crystallization [32,33].

1.2 Mechanism of rising damp: physical and chemical features

As already reported, considering the environmental and architectural features proper of the city, Venetian buildings structures are constantly wet by the lagoon water which penetrates into materials through rising damp processes. This latter is a vapour balance between evaporation, condensation and absorption and it occurs when the building base stands in close contact with groundwater and the moisture flow moves upward into the pores of a permeable masonry wall [7,10,30,34]. Material porosity and capillary structure influence the water transport inside the different building materials, their mechanical resistance to compression and bending, as like as the resistance against damages and degradation. Pores classification is based on their typology, geometry and size (Table 4), three fundamental factors in defining material properties and suitability in building construction field [3].

Typology				
Closed pores		Open pores		
<ul style="list-style-type: none"> • isolated • No water access • Affect mechanical and thermal properties 		<ul style="list-style-type: none"> • Connected with the external • Water entrance • Deterioration • Dead-end or interconnected pores 		
Geometry				
Spherical, cylindrical and elongated pores	Basic pores	Dissolution pores	Fracture pores	Shrinkage pores
Size				
<i>Micropores</i> Radius < 0.001 μm	<i>Mesopores</i> Radius between 0.001 and 0.025 μm		<i>Macropores</i> Radius > 0.025 μm	

Table 4 Pores classification according to their typology, geometry and size [3].

The sum of empty spaces, their shape and distribution influence the water transport inside the different materials which is based on the capillary action process [3,35]. This latter is spontaneously produced by electrochemical attraction of the hydrogen bonds of water molecules to mineral surfaces. Different forces are involved: cohesion of water molecules and their adhesion to the solid material [6,8,36]. When attraction force among water molecules and pores surface is stronger than that among water molecules themselves, water enters and moves horizontally and vertically, against gravitational force, inside pores of determined size [1,5,29]. All these relationships in rising damp process, are physically explained by the Jurin's Law (Equation 1) [37]. According to this one the capillary rise is related to the surface tension of the absorbed liquid and the dimensions of the capillaries involved. Moreover, the maximum water rise height is inversely proportional to the radius of the capillary pores [29,34] and so the narrower the capillary tube, the greater the water rise inside it [36].

$$H = \frac{2\gamma \cos\theta_0}{R\rho g} \quad (\text{Equation 1})$$

γ = surface tension of the liquid [N/m]
 ρ = liquid-to-air density difference [kg/m³]
 H = capillary rise [m]
 R = capillary inner radius [m]
 g = gravitational acceleration [m/s²]
 θ_0 = equilibrium contact angle specific of the liquid-solid surface coupling [°]

Despite Jurin's Law is the basic equation of capillary process, valid for hydrophilic ($\theta_0 < 90^\circ$) materials and $2R \ll H$ conditions, it has some limits, indeed it makes provisions in terms of infinite H and gravity force is not included [37]. Considering the specific case of water, its density is 1000 kg/m³, the surface tension corresponds to $72 \cdot 10^{-3}$ N/m and g value is 9,81 m/s². If a completely hydrophilic material is considered ($\theta = 0$), the maximum water height for the Eq.1 is $14,7 \cdot 10^{-6} / R$. For a porous material with $R=1\mu\text{m}$ (the mean radius of a brick, for example) the final water height within capillaries should be 14.7m. Considering real cases, the capillary radius is often between 0.1 and $1\mu\text{m}$ resulting in a water height $>14,7$ m. Jurin's Law represents just a theoretical approach while in real cases, the evaporation process lowers the maximum height reached by water within masonries [25]. Indeed, even in the worst cases, when the walls are in direct contact with water like in Venice, the maximum water height registered is around 3-4 m [38]. According other studies, generally it is between 0.5 and 4 m depending on the wall thickness, evaporation conditions and seasonal fluctuations influence [6].

Concerning salts, environmental parameters like temperature and relative humidity, as like as the presence of different saline species, influence their movement in materials [39]. In fact depending on the relative humidity, hygroscopic salts in masonry can absorb moisture till reaching the liquid state (deliquescence) [1,39]. For a specific temperature and salt, every saturated solution, inside the masonries, has a specific equilibrium relative humidity. Water evaporation from the saturated solution occurs when the environmental relative humidity is lower than the equilibrium one and this takes to supersaturated solution formation and

the successive crystals creation. Temperature and relative humidity cannot be controlled in external environments while in indoor conditions they can be monitored, avoiding serious damages of the internal surfaces and an improvement of the environmental conditions.

1.2.1 Damages related to rising damp: salts effects

In general water absorption within materials leads to chemical and physical reactions determining a more or less severe decay [3]. The chemical process is related to the aggressive pollutants and the physical one to mechanical stress deriving also from freeze-thaw cycles related to temperature changes [3,10]. The mechanical properties are compromised and the thermal conductivity and heat capacity change. If water is present in a large amount, it acts as the salts dissolution transport medium, which can solubilise and wash away some material components. Moreover water, is an essential substrate which facilitates the biological growth, highly encouraged by high temperature and high moisture content together [1,3,40]. Despite this, through all the cycles manifestation, those of salt solutions absorption and crystallization and that of water evaporation, salt deposition on and inside the masonries are the most damaging ones [29]. Salt-induced damage has both chemical and physical nature and an increasing salts amount determines a size reduction of pores and consequently an increase of the suction force [1]. When in a permeable surface, the moisture undergoes evaporation, salt accumulation occurs. Indeed salt precipitation from supersaturated solutions takes to deposits formation on the surface or inside it through two phenomena [8,10,24,31].

- *Subflorescence* if the salt crystallization takes place below the bricks surface and within the material pores causing internal pressures, cracks, defoliation, crumbling and spalling [21]. The process is favoured by the continuous changes in humidity inside the bricks due to high daily variation of water level [24]. Generally, subflorescence form in very dry and windy air which accelerates water evaporation, leading to an inner salt crystallizations [8,41].
- *Efflorescence* occurs in dry and calm air [41] due to the temperature difference between the internal and the external part of a building. The internal part is hotter (especially in winter) and this forces the moisture towards the external part of the masonries. Once the exterior wall is reached, the temperature change causes the moisture evaporation and consequently the salt crystals deposition. These in general are clearly visible as white masses on the bricks surface (Figure 7) often in the form of powder.



Figure 3 Efflorescence on Venetian masonries. Photos taken on the 25th November 2019 in Sestiere Castello.

Despite efflorescence is usually considered less harmful than subflorescence, the former indicates the presence of the latter and can affect the coherence, endurance of bricks and create spalling of their surfaces [21].

Prolonged and strong rains could be responsible of efflorescence disappearing, considering the high solubility of the main salts components. Usually, if the salts appear again after the rain, it means that the efflorescence is due to sea salts. Otherwise, if efflorescence salts disappear it means that the salt sources correspond to sodium sulphate possibly come from sulphate –contaminated bricks [41].

At low relative humidity, salts determine changes concerning the drying behaviour of building materials. In particular, some studies affirm that the drying rate of bricks saturated with a salt solution is lower if compare with the one of water saturated bricks [41,43].

In masonry, bedding mortar enhances mechanical cohesion among bricks, increasing the total wall resistance and the uniform distribution of the weight structure. Different binders have been applied through the time, firstly mortar but since XIX century also the Portland cement. As like as river sand was applied until XV-XVI century and then cocchiopesto was introduced in the masonry construction. At the same way also binder/aggregate ratio is variable [25]. A scarce bedding mortar- brick interaction enhances water penetration in voids of the surface contact between the two materials and material losses (Figure 8). In the worst cases, if bearing walls are involved, a reduced weight resistance of masonry is enhanced. In this way also the masonry resistance to freeze-thaw and crystallization cycles is compromised [44].

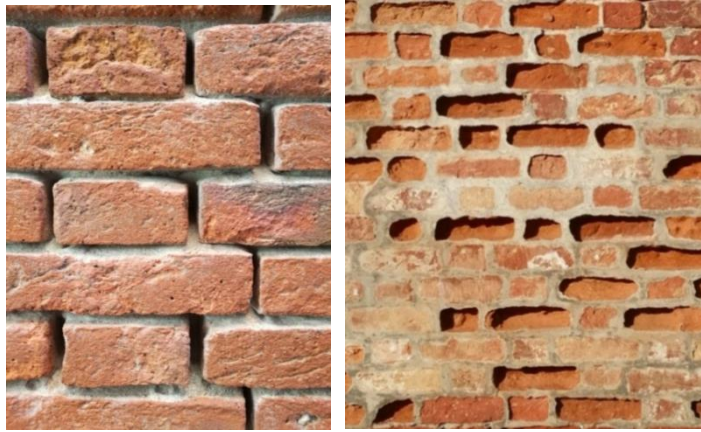


Figure 8 Examples of bricks and bedding mortar decays: a) bedding mortar loss and bricks quite undamaged; b) Advanced brick deterioration and losses, bedding mortar less damaged. Photos taken in Venice on the 25th November 2019 in Dorsoduro

1.2.1.1 Salts solubility and distribution in masonry

Salts with different solubility are contained in almost all masonries: chlorides, nitrates, sulphates and several kind of carbonates (potassium, sodium, calcium, ammonium and magnesium based) [3].

In particular, the main salts involved in rising moisture process are calcium and sodium sulphate, sodium chloride and carbonates. In the case of Venice a wide external salt contribution is given by the sea water rise rich especially in sodium chloride.

The different kind of salts and consequently the produced damages (Table 5), are proportional to their concentration and solubility. Three salts groups can be identified depending on the respective solubility degree [3]:

1. *Practically insoluble*: even if the reduced solubility takes to saturation within pores, no dangerous crystallizations are created.
2. *Slightly soluble*: the low solubility takes to crystallization below the external surface and this produces material losses. *Gypsum* ($\text{CaSO}_4 \cdot 2\text{H}_2\text{O}$) is part of this group and crystallizes also in humid environment.
3. *Highly soluble*: they reach high concentrations and many often they remain in solution in humid conditions, producing dark zones on masonries, while in dry conditions crystallization occurs creating efflorescence. In this group chlorides and nitrates and sodium carbonates included.

	Sulphates (SO ₄ ⁻)	Chlorides (Cl ⁻)	Nitrites and nitrates (NO ₂ ⁻ , NO ₃ ⁻)	Carbonates (CO ₃ ⁻)	Oxalates (C ₂ O ₄ ⁻)	Phosphates (PO ₄ ⁻)
<u>Sources</u>	Air pollution (SO ₂) contributing to acid rains (H ₂ SO ₄), sulphates in agricultural land, low quantity of magnesium sulphate in sea spray and metabolic products of micro-organisms	Sea spray, hydrochloric acid from industrial emission	Sewage water infiltration, burial sites proximity, fertilizers applied in agriculture, atmospheric pollution (HNO ₃)[1]	Calcareous stone and mortars (CaCO ₃ and the soluble ones NaCO ₃ [45]). The chemical reactions are enhanced by excessive CO ₂ concentration in air	Products secreted by micro-organisms as oxalic acid (H ₂ C ₂ O ₄) and chemical degradation of organic materials applied as superficial protection [46]	Fertilizers, bird excrements
<u>Chemical Reactions</u>	CaCO ₃ +H ₂ SO ₄ → CaSO ₄ ·2H ₂ O +CO ₂		CaCO ₃ +2HNO ₃ → Ca(NO ₃) ₂ + CO ₂ + H ₂ O	2CaCO ₃ + H ₂ O + CO ₂ ↔ Ca(HCO ₃) ₂		
Related deterioration processes						
	Corrosion Black crusts Efflorescences Pitting	Crusts Crumbling Steel corrosion	Corrosion General decayphenomena	Encrustations Concretions Disruptions	Chromatic modifications Yellow, brown, red patinas	Dark black deposits White patches Microbiological growth

Table 5 Classification of the salt species mainly present in masonry in form of anions. Their sources, chemical reactions and the respective derived deterioration phenomena are listed below [3].

Depending on their solubility, salts crystallize at different heights in masonry [39]. Since salts are present as mixed salts solution within masonry, equilibrium conditions of precipitation are different from those of each single pure salt solution. Consequently it is difficult to link a specific salt precipitation to a corresponding height. Although theoretical schemes link the salts distribution trend in masonries to their different solubility [33,39,47], real cases are more complicated. due to the lack of equilibrium conditions, the presence of different salts mixtures and the different environmental conditions [38]. Indeed, the solubility of the respective salts increases or decreases with respect to the presence of other salts. When salts with a common ion are present, such as NaCl and Na₂SO₄, the respective solubility decreases. On the contrary, when common ions are not present, the solubility of the less soluble salt increases. This is the case of gypsum solubility which increases in a solution NaCl based [33]. As previously underlined in this Master thesis introduction, porosity is a key factor for the salt deterioration and also the different porosity between the several building materials should be considered. Indeed, in a masonry, bricks undergo low or high deterioration degree considering the presence of Portland cement or mortar respectively. Mortars have higher porosity than bricks, while Portland cement has a lower one. For this reason, in a masonry, lime mortars (with well coarse pores) weather away before that bricks or stone. If masonries are restored using Portland cement mortars (less porous materials with a higher resistance), bricks deteriorate first [33].

1.2.2 Rising damp trend in Venetian masonries

Within masonries, the water rise level is an “equilibrium line” visible as an horizontal tide mark which separates the wet and darker part of the building from that whose moisture is in equilibrium with the environmental one [5,6]. Indeed when a porous construction material absorbs water, it appears more saturated in colour and so darker than its dry parts. Over time, the moisture level individuates a wet-drying zone characterised by a strong decrease of moisture gradient and a related salts crystals presence.

Rising damp phenomenon and its effects are closely related to the moisture amount inside masonry and its soluble salts content. The moisture content (MC%) is determined through normalized gravimetric methods applied on powder samples obtained by drilling walls at different heights and depths. On the other side, soluble salts distribution (SS%) is firstly measured starting from conductivity measurement on collected samples. Additional information on ionic species can be obtained through Ion Chromatography investigation.

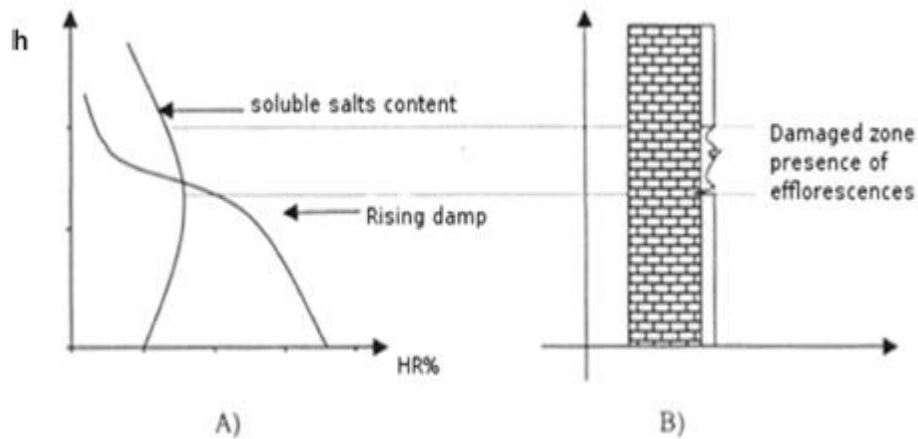


Figure 9 Empirical model proper of rising damp in Venetian walls: A) SS% and MC% curves distributions based on experimental measurements ;B) rising damp and salts damaging action on masonry [38].

MC% and SS% measurements and their relation defines the typical empirical model for rising damp in masonries as pointed out by studies specifically focused on Venetian buildings (Figure 9) [38].

At greater masonry heights, the decreasing moisture content and soluble salts distribution show an inversely proportional relationship related to evaporation area (Figure 9A) in fact a low moisture corresponds to a maximum salt content visible on masonry as efflorescence damaging the wall surface (Figure 9B).

At the same time, higher MC% values for the internal wall area are expected, which gradually decrease through external zones, since evaporation occurs on the wall surface.

Moisture and salt content distribution measurements are effective methods to investigate the rising damp phenomenon in Venice and, if they are performed on various buildings, it is possible to underline possible common trends among them. This is one of the purposes of this Master thesis since six Venetian buildings masonries were sampled and MC% and SS% determined. In this way, the knowledge on rising damp in Venice is enriched with novel data. These ones can be compared with future measurements performed on the same buildings with the aim of assessing moisture and soluble salts distribution changes over time also considering the increasing sea level effects related to climate changes effects.

1.3 Facing rising damp and high water in Venice: past, actual and future proposals

The attention on rising damp phenomenon in Venice raised after the city was flooded on the 4th November 1966. Indeed, exceptional event like this increase the collective awareness about the severity of the phenomenon and the need to take some preventive measures and elaborate solutions.

The common goal of all the interventions against rising damp is a significant decrease in moisture content within masonries. Indeed, the comparison between the wall moisture content, before and after the intervention, is the key factor to evaluate the efficiency of the intervention itself [48]. Table 6 shows an overview of the different methods to stop rising damp in masonries. In addition, in Venice also layers of paste of palygorskite (corresponding to attapulgite) are applied on one side of the wall. The other side is cleaned by water propelled at high speed. Moreover walls can be cleaned also in depth by adding some pipes into the walls. When bricks are highly damaged they are replaced with new ones according to the “scuci - cuci” technique [49,50]. Also deteriorated plaster are substituted by new macroporous ones to increase the resistance against water capillary [24]. Wall cut is an intervention widely present on Venetian masonries even if recently electromagnetic interventions are often applied.

The safeguard of Venice and its Lagoon as problem of national interest was established through the Law of the 16 April 1973, n171 according which State, regions and local authorities must preserve the lagoon environment from pollution and protect the city and its landscape, archaeological, historical and artistic environment [51,52]. This lead to specific plans elaboration by Venice municipality and other local authorities. Among these, CORILA [15] has an active role since years in safeguarding Venice through projects organized in different research lines. Another institution is Insula S.p.A. which was introduced by the municipality in 1997 and deals with urban maintenance, infrastructure and construction [20]. RAMSES⁵ project, a result of the collaboration between municipality and the implementation of Insula S.p.A., created for the first time a three-dimensional representation of the pavement of the historical city of Venice with centimeter accuracy. In particular the elevations of streets, embankments and squares are reported in detail. This helps in guaranteeing the circulation of pedestrians but also to predict the possible damages related to flooding by giving an estimation of the tide level threshold on buildings [53].

⁵ Rilievo Altimetrico, Modellazione Spaziale E Scansione 3D – Altimetric Survey, Spatial Modeling and 3D scan.

Methods to stop rising damp

	<u>Damp- proof course</u>	<u>Evaporation increase</u>	<u>Electrokinetic</u>
<u>Features</u>	<p>- low absorbance or impermeable barrier above the ground level</p> <p>1) Mechanical methods (lead, steel, plastic, glass, bitumenbased, PVC, polyethylene or polyesterbased slabs; stone impregnated with glue based on linseed oil and litharge; pvc foils and joints filled with resin based mortar (wedge method); drilling two overlapping rows of holes in the wall (Massari method); stainless steel slabs insertion)</p> <p>2) Chemical methods (drilling holes at wall base at different distances and from one or both side of the wall depending on its thickness, use of water or organic solvent)</p>	<p>- reduced rising damp height</p> <p>1) Knapen siphons Fired clay or perforated plastic or metal tubes placed in walls holes</p> <p>2) Drying stones Stones, similar to bricks, made of aero-dynamic holes placed at 30cm to damp walls</p> <p>3) Wall based ventilation Based on a hygro-regulable mechanical ventilation device. It increases evaporation</p> <p>4) Dehumidification plasters - high porosity (>45vol %), large amount of coarse pores - sacrificial layers</p>	<p>1) Electro-osmosis - electrical double layer at the aqueous electrolyte /solid interface and at pores surface - active osmosis (anode in walls and cathode in soil) - passive osmosis without electric current</p> <p>2) Other systems - based on electromagnetic waves, earth radiation and potentials</p>
<u>Limits</u>	<p>1) Mechanical methods -cracks formation due to walls cut - increased seismic vulnerability - not applicable for thick or irregular walls - high costs - plaster application below mechanical cut must be avoided - visible layers on masonry</p> <p>2) Chemical methods - irregular masonry - saturation degree of the wall treated - lower effectiveness in mortar than in bricks - silane/siloxane products works better than stearate and silicate/siliconate ones - organic solvents seems to work better than water ones - damages caused by high injection pressure</p>	<p>- faster salts accumulation</p> <p>1) Knapen siphons - low efficiency for unheated rooms, absence of solar radiation and thick materials - they take to higher dampness in walls if the outer relative humidity is high - clearly visible on walls</p> <p>2) Drying stones - efficiency influenced on temperature, relative humidity and air speed - clearly visible on walls</p> <p>3) Wall based ventilation - possible increase of salts - difficult to use in presence of adjacent buildings - only applicable if the groundwater is lower than wall base</p> <p>4) Dehumidification plasters lower effectiveness information</p>	<p>1) Electro-osmosis</p> <p>Active osmosis - pH materials affect results - higher moisture of clay soil than in masonry - possible loss of electrical continuity due to materials rigidity - electrodes corrosion - loss of electrical contact between electrode and masonry - salt migration</p> <p>Passive osmosis - ineffective method</p>

Table 1 Classification of the existing methods to stop the rising damp in masonries [24,48].

In 1987 Venice became part of the UNESCO World Heritage List and these increased the focus by international committees on the problem of salts in Venetian buildings masonries. Scientific researches focused also on the study of the historical centre subsoil characterized by a particular sedimentary structure [54]. UNESCO had always an active role in protective Venice and among the several scientific dissertations related to rising damp and climate changes an international meeting was held at Palazzo Zorzi, on 22-23 November 2010 in collaboration with ISMAR-CNR . The title was “From Global to Regional: Local Sea Level Rise Scenarios- Focus on the Mediterranean Sea and the Adriatic Sea” and the focus was on the extreme vulnerability of Venice to climate changes emergency and in detail to sea level increase [55]. The results reported a mean sea level increasing of 10 cm during summer months between 2007 and 2010. On the other hand, in winter months a 20 cm rise has been registered. These increase seems to be related to atmospheric pressure drop from 2020 to 2013 mbar during these 3 years. Adriatic sea and lagoon will experience the same water rise through the years and imagine a sea level rise of 80 cm means that the city will be flood twice a day according to the tidal oscillation. The most alarming previsions are those according which at the end of this century the sea level increase will range between 18-59 cm to 100 cm [55] . The first number is the result of a study which does not include and consider ice melting and steric changes. This means that the second increasing value, 100 cm should be the most reliable in the future [55].

Media and scientific community attention on climate changes and accelerated sea level rise in Venice is constantly increasing and recent researches are focused on these topics [56]. Among the projects whose aim is the protection of the city from flooding due to high tides, it figures the Mo.S.E. (Modulo Sperimentale Elettromeccanico i.e Experimental Electro- mechanic Module) with a mobile barriers system [12,23] . The safeguarding measure for the lagoon has been promoted by the Italian government through the Magistrato alle Acque, Venezia⁶ (MAV) and commissioned by Consorzio Venezia Nuova (CVN) [57]. This consists in mobile dams which allow the temporary isolation of the Lagoon from the Adriatic sea, before exceptional high tides of more than 110 cm occurs [14,22,23]. These four barriers are positioned at the three lagoon inlets of Lido, Malamocco and Chioggia [12,14]. The construction began in 2003, the total extension of the barriers is 1600 m and they are flap-gates made of steel which usually are full of water. According to the project, when tide exceeds normal threshold, compressed air is pumped inside them and so starts to empty and raised up to build a real barrier. These mobile dams are linked to the foundations thanks to hinge-connectors made in steel. The under structure of the barriers is made of caissons reinforced by concrete and it is buried into the ground. Initially, the expected efficiency of this high water defence structure is of 100 years but the steel corrosion and the cracking of materials through the time would shortening this time span [23]. Moreover, due to scandals and delays, the system is not yet in function and cannot protect the city from flooding occurrence, even if its commissioning is scheduled in 2021.

If the flood of the city in 1966 led to an increasingly awareness of the high water and salts building problems, the second most serious flood of 2019 will further concentrate forces and interest in facing the

⁶Until 2014, today it is called Provveditorato Interregionale alle Opere Pubbliche per Veneto, Trentino Alto Adige, Friuli Venezia Giulia

phenomenon. Considering the future of Venice strictly related to the climate changes emergency, the related effects should be mitigated by developing innovative and effective solutions.

2 Experimental Part

The research on investigation of the rising damp changes over time is structured into two sections:

1. Comparison of historical and actual photos of the same buildings to evaluate the rising damp trend changes over time in Venice. A private archive and a public one are considered to select the more representative photos. The private archive pages are photographed and scanned and all the collected photos are then reported together with the actual ones to evaluate the changes.
2. Analysis on brick powder samples of six Venetian buildings to quantitatively determine moisture content, soluble salts, ionic species and their related concentrations.

2.1 SECTION 1 - Photos comparison

2.1.1 Archives of photos

The archives considered for the photos selection and collection are: the private one by Giuseppe Pasqucci and the online public one of the Archivio Fotografico Urbanistica (AFU).

1. The private “Pasqucci” archive is composed by several photographic binders divided according to the Venetian Sestieri (Cannareggio, Castello, Dorsoduro, Santa Croce, San Marco and San Polo). It was created in a period of 15 years [58]. Each binder collects photos taken by the archive owner, those found in magazines and documents, newspaper articles and anecdotes about Venice and its streets, *calli*. Each binder is classified according to the civic numbers reported in each page with the name of the *campo*, *fondamenta*, *Rio* and a brief description of the respective photos and/or documents. An example of the page structure of the archive is shown in Figure 10.

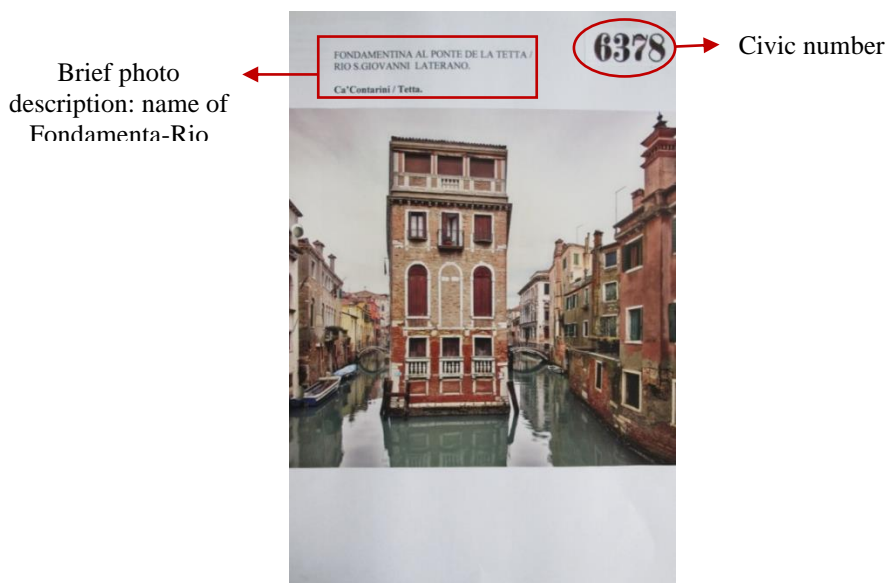


Figure 10 Example page of the archive. Street number and Fondamenta- Rio name are reported.

Castello, San Marco and Dorsoduro are the three Sestieri considered for the photo selection in this research, 69 locations in total. The information on the date of the shot was taken from the back of the photos. Unfortunately for most of the photos considered, the date is not shown even on the back. This is one of the limits of the photos collection from this archive. Table 7 lists location name of the selected photo, the civic number, the respective binders of each Sestiere. Originally, Sestiere Castello consists of 18 binders, Dorsoduro of 15 and San Marco is organized into 14 binders. Table 7 shows only the binders considered for this research (in Roman numbers) with the respective civic numbers of the analyzed locations.

Sestiere	Photos Binder	Civic Number	Location Name
Castello	I 1-269	69 98	Campo San Piero Altorilievo Rio delle Vergini. Resto di portale gotico ed iscrizioni
	II 270-999	485	Fondamenta San Gioachin. Iscrizione
	IV 1000-1643	1852	Rio de la Tana Arsenale- Canevo. Torre angolare col rio de San Daniel
	V 2161-2550	2426 2427 A 2466 2543	Campo San Martin Rio de le Gorne Campiello de la Grana. Cornice bizantina e patera Corte Rota presso Campo do Pozzi
	VI 2551-2830	2641 2654 2716 2784	Rio de San Martin(con ingresso in calle de l' Arco) Rio dei Scudi con ingresso in calle dei Scudi Ca' Venier. Portale ad acqua Calle Donà (San Termita) Campo de la Chiesa (San Francesco della Vigna) Simbolo religioso
	VIII 3171-3490	3405 3405 3471	Calle de la Madonna Rio dei Greci Ca' Zorzi Liassidi Rio dei Greci con ingresso in calle della Madonna a Ca' Zorzi Liassidi. Seconda porta acqua Rio de la Pietà. Due rilievi angolari
	XI 4198-4420	4313	Fondamenta Santa Apollonia (giù dal ponte) Edificio d' angolo su Rio di Palazzo o della Canonica
	XII 4421-4719	4425 4466	Rio di Santa Maria Formosa (con entrate in Ramo Venier 5269 A) Portale da acqua Corte Briani (a San Giovanni Nuovo) Porta da acqua con arco in mattoni
	XIII 4720-4999	4853 4907 4907 4979 A 4979 A	Rio di Santa Maria Fromosa. Portale da acqua Rio di S. Severo. Due porte da acqua Rio di San Severo (con ingresso in Calle dell' Arco detta Bon) Ca' Zorzi-Bon. Portale da acqua Calle del Diavolo Ca' Priuli Rio di San Provolo (con ingresso in Calle del Diavolo) Ca' Priuli. Portale da acqua
	XIV 5000-5263	5016 5152 5193	Campo San Severo Ex Carceri Rio de la Tetta o di San Giovanni Laterano. Ca' Gabrieli Rio di San Severo con ingresso da terra in Calle dei Olbi, Portale da acqua
	XV 5264-5645	5402	Fondamenta Papafava o Tasca- Papafava
	XVI 5646-6067	5745 5870 6036	Rio del mondo nuovo (con ingresso da terra in calle del Paradiso) Ca' Foscari Mocenigo Rio del Paradiso. Porta da acqua Rio del Malibràn con ingresso da calle della Scaleta. Vetrina
	XVII 6068-6395	6123 6282 6377 6378	Campo Santa Maria Formosa, Ca' Donà. Portale di terra Ponte dei Conzafelzi o ponte Storto o Pinelli. Ponte pubblico in ferro Ponte de l' Ospealeto (foto rivista) Fondamenta al ponte de la Tetta- Rio di San Giovanni in Laterano
	XVIII 6396-6828	6452	Corte Muazzo Ca' Muazzo
	Dorsoduro	XI 2615-2889	2635 2765 2824
XII 2900-3289		2927 2946 3228 3232-28 3246 3422 3423	Rio de Santa Margherita- Riva de acqua Rio di Santa Margherita- Sotoportego de l' uva quattro finestrelle Palazzo Giustinian Calle Giustinian dei Vescovi Calle Foscari- Ca' Foscari Corte del Fontego- Rio de Ca' Foscari. Palazzetto di testata Corte del Fontego Resti di porticato bizantino
XVI 3700-3984		3707 3859 A 3885 3900 3911	Campo San Pantalon Ca' Signolo- Loredan Rio de Ca' Foscari (con ingresso sa terra in Calle Larga Foscari) area demolita Ca' Renier Corte Marcona- Barbacani e porta di magazzino Calle del Remer- Canal Grande Fondazione Masieri Wright Crosera (San Pantalon)- Ca' della Frescada Corner

San Marco		3934 A	Rio de la Frescada (con ingresso da terra nel sottoportego di Calle Boldi) porta da acqua
	II 484-1036	556 A	Rio dei Bareteri (inglesi calle Erizzo)
	V 1810-1998	1906	Rio de la Verona
	VI 2000-2465	2307 2307 2432	Campielo Contarini- Ca' Contarini- Fasan Campielo Contarini Ca' Contarini Portale ad acqua (Rio de le Ostreghe)
	VII 2466- 2629	2513 2517 2557 2569 2598 A	Rio de San Maurizio- Ca' Malipieri. Porta ad acqua Rio Santa Maria del Giglio Portale murato A Fondamenta della Fenice, resti di finestra Rio de la Verona A Ponte dei Malvasia
	IX 2777-2888	2819 2840 2883	Sotoportego e ramo Ca' Pisani Ca' Benzon- Foscolo Ca' Barbaro Colonna antica Giustinian
	XI 3217-3464	3226 B 3319 3421 A	Chiesa di San Samuel Ca' Erizzo- Nani Mocenigo Rio de Ca' Garzoni
	XIII 3638-3956	3706	Rio de San Luca Riva da acqua
	XIV 3957- 4059	4013 A	Ca' Pisani- Revedin Riva da acqua

Table 7 List of the photo binders considered with the respective civic numbers and locations for the three Sestieri Castello, Dorsoduro and San Marco.

Each archive page was photographed with a Canon PowerShot G12 camera (*Appendix 1*) [59] and scanned to obtain photos at 300 dpi resolution and in TIFF format. The scanner used is the one of HP Laser Jet Pro M428fdw multifunction printer.

2. The Archivio Fotografico Urbanistica [60] (AFU) is an online photo archive and represents an heritage for the transformations of the municipal territory of Venice in over 50 years. It involves photos of implementation, maintenance and/or restoration of public works. It is organized in more than 20.000 digital catalogue cards with the images obtained through scanning of negatives and printed photos. The archive is continuously updated with historical material and with the most recent photographs [60].

In Table 8 are listed the four location for which the black and white photos have been requested to the AFU in TIFF format and so with a high resolution to enhance a better comparison with the actual ones.

Sestiere	Civic Number	Location Name
Castello	4419 4979 A 6122,6123	S. Zaccaria, Rio de la Canonica (o de Palazzo o de la Pagia), Palazzo Soranzo S. Zaccaria Fondamenta dell' Osmarin Palazzo Priuli S. Maria Formosa, campo di S. Maria Formosa, Palazzo Donà
San Marco	3957-3958	S.Luca, Palazzo Pesaro Fortuny (noto anche come Palazzo Pesaro degli Orfei), visto da Campo San Beneto

Table 2 The high resolution photos requested to the AFU in May 2019 and their Sestiere, civic number and location name

The exact position of considered buildings for the temporal comparison of rising damp level, was determined by Google Maps and Street View.

For each building the GPS coordinates have been obtained in order to build maps for each Sestiere (Castello, Dorsoduro, San Marco) through Google My Maps and Google Earth. Figure 11 shows the exact spatial position of the locations considered throughout the historic centre of Venice and the three Sestieri.

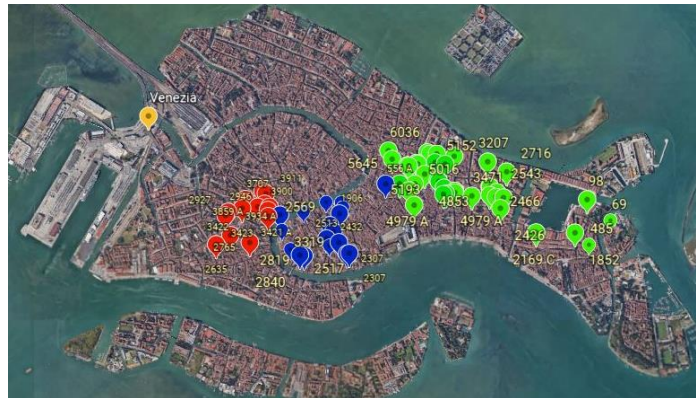


Figure 11 Locations of the considered buildings for the photos comparison throughout the three Sestieri: Castello (green), Dorsoduro (red) and San Marco (blue).

2.1.2 Acquisition of current photographs and comparison

In order to evaluate the rising damp trend and its changes over time, 166 photos were taken throughout the historical centre of Venice. The current photos were collected between the end of June and November 2019 using the Canon PowerShot 12 camera (*Appendix 1*). The photos were taken in automatic mode and particular attention was paid in taking them as similar as possible to those of the historical archives to facilitate their comparison.

Qualitative investigation

Old and current photos for each location were firstly qualitatively compared through an evaluation scale based on the investigation of any changes of five parameters:

- 1 Rising damp trend
- 2 Biological growth
- 3 Plaster loss
- 4 Efflorescence
- 5 Brick erosion

This system based on the elicitation of expert, allows to individuate a degree of increase (+, + +, + + +), decrease (-, - -, - - -) or unchanged situation (=) for the parameters. In this way worsening, improvement or absence of changes on conservation state can be assessed.

Semi- quantitative investigation

The only cases considered for the three Sestieri are those to whom all the five parameters were evaluable in a qualitative way (+,- or = scale). The number of cases and relative percentages about positive, negative or unchanged occurrence of the five parameters is stated. Finally a comparison between the obtained results for the three Sestieri is made, to find some possible correlations.

2.2 SECTION 2 - Case studies: analysis on six Venetian buildings

Ca' Foscari, Ca' Bottacin, Ex Slaughterhouse San Giobbe, Badoer Palace, Ca' Tron and Malipiero Palace are the six buildings considered, from which samples were taken in order to evaluate the current moisture and soluble salts content; their position in the historical centre of Venice is shown in Figure 12.

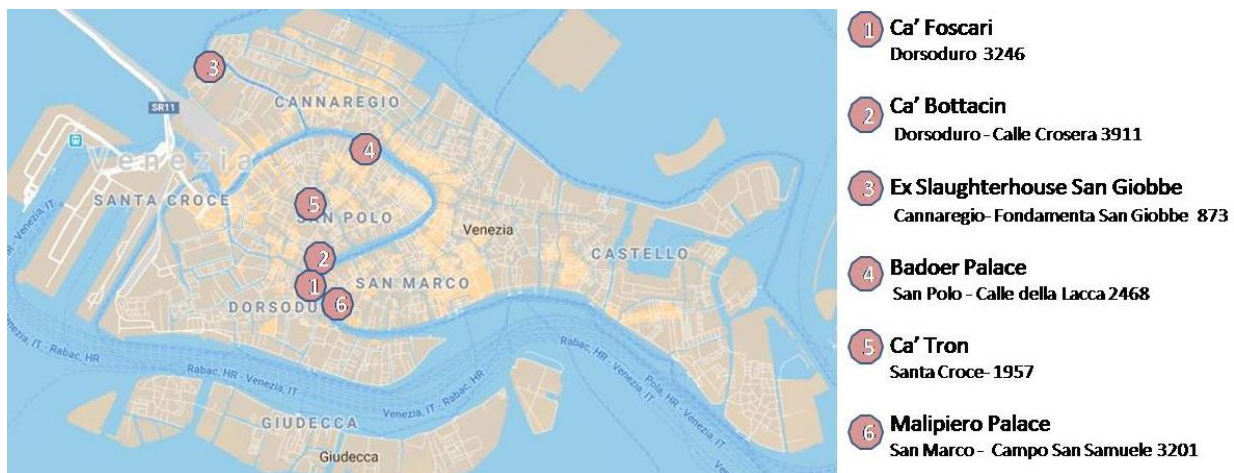


Figure 12 Location of the investigated buildings in the city of Venice. The Sestiere and civic numbers are listed.

For each one of the six buildings a site inspection was made few months before the sampling date in order to evaluate the best points and conditions to sample the selected walls. Ca' Foscari, Ca' Bottacin and Ex Slaughterhouse San Giobbe were inspected in February 2019 while Badoer Palace, Ca' Tron and Malipiero Palace in May 2019 .

A brief introduction for each building and its history is here proposed.

2.2.1 Buildings history

Ca' Foscari

Ca' Foscari is a Venetian Gothic palace of Sestiere Dorsoduro, facing the Canal Grande (Figure 13). It was built in 1453 on commission from the doge Francesco Foscari and today it is the seat of the homonymous University. Through the time the building has been restored, in particular two times in 1936 and 1956 by the guide of architect Carlo Scarpa. The first restoration on the entrance hall renovated the visual connection between the water entrance from the Canal Grande and the land one from the courtyard. The restoration works included also the hall at the first floor (over the total four floors) and the great hall. This latter was the object of the second restoration in 1956 to create classrooms for the University. A final restoration in 2006 included the creation of inner connections with the adjoining building Ca' Giustinian. This took to the discovery of fifteen-century frescoes and gilded ceilings at the second floor [61].



Figure 13 Ca' Foscari palace: view from the Canal Grande (left) and the internal facade (right) [61].

Ca' Bottacin

Ca' Bottacin, also known as Palazzo Corner della Frescada Loredan, is a XV century palace (Figure 14). The different names of the palace refer to its different owners in the history: the original ones were the Dalla Frescada, then the Corner, the Loredan (1567-1570), the Foscari and finally the Bottacin sisters. Since 1971 the palace is part of Ca' Foscari University and till 2015 it was the seat of the Department of Legal and Economic Sciences then transferred in San Giobbe Campus [61,62].

The palace was recently restored between 2016 and 2017 the restoration works concerned the roof and between 2018 and 2019 restoration works allow the structural seismic improvement intervention, construction of a cooling system and decorative intervention [63].



Figure 14 Ca' Bottacin, view from Rio de la Frescada [63] (left) and the inner yard (right) [62].

Ex Slaughterhouse San Giobbe

The building complex of San Giobbe stands on a peripheral zone with respect to the historic center of Venice, due to its former function of municipal slaughterhouse (Figure 15). It was built in the mid- 1800s and the activity continued till 1972 when the slaughterhouse was transferred in Mestre. From 1972 the area was decommissioned till 1977 when it was used by rowing companies. Finally, from 1991 the municipal administration granted the area on a ninety-year loan to Ca' Foscari University [64,65].



Figure 15 Ex Slaughtering San Giobbe entrance (left) [65] and its skyview (right).

Badoer Palace

Badoer Palace belonged to the homonymous family and was the home of the priory San Giovanni Evangelista (Figure 16). In 1350 a cemetery was created to bury the members of San Giovanni Evangelista and this reflects the building planimetry (similar to Z shape) indeed the cemetery is under the hall of the palace. Through the time some modification were made on the palace which from 1974 was bought by IUAV University and through restoration works started in 1978, it was adapted to Department of Architecture. Since 2008 the palace is seat of the Iuav School of Doctorate Studies [66].



Figure 16 The entrance of Badoer Palace (left) and the inner facade overlooking the garden [66].

Ca' Tron

Ca' Tron is a XVI century Gothic palace overlooking the Canal Grande (Figure 17). Its name come from the Procurator Andrea Tron who was an ambassador candidate to the Venetian Duchy (*Dogado*) [66]. During the 19th century the Tron family legacy ended and the palace was used for administration and as institute for judicial auctions and in 1972 became part of Iuav University and restored. This latter involved consolidation works, reorganisation of the spaces and their recovery. The current building planimetry involves two saloons at first and second floor [67].



Figure 17 Ca' Tron palace: the facade overlooking the Canal Grande (left) and the internal one on the garden (right) [67].

Malipiero Palace

Malipiero Palace is a Byzantine style fabric built between 10th and 11th century by the Soranzo family and facing the Canal Grande. The palace had different owners over time: the Cappello family in 1465 and finally the Malipiero in 1590. Some restoration works and enlargements were made first in 1622 and then in 1725 and these latter gave the actual shape to the palace. From 1778 onwards, due to the extinction of the Malipiero family, the palace started to deteriorate. This phase last till 1951 when, thanks to the Barnabò family, a new restoration allowed the building conservation [68]. Actually, Malipiero Palace is a seat of art exhibitions of Biennale di Venezia, and here the artists are hosted to live, work and expose their artworks [69]⁷. Malipiero Palace involves also a garden of the 17th century with an original structure (Figure 18) and rich of sculpture of the 19th century.

⁷<https://www.labiennale.org/it/bacheca/515>



Figure 18 Malipero Palace facade overlooking the Canal Grande (left) and its satellite imagery with the 18th century garden (right) [70].

2.2.2 Non- invasive measurements and buildings sampling

Photographic survey

The building walls were firstly documented with photographs both in Visible light and with an Infrared thermal imaging camera Flir One to obtain information on the moisture distribution in masonries. Indeed IR thermography allows the detection of damp zones due to their different temperature with respect to the dry areas [71]. In this way a first survey of the building masonries is possible in a non- invasive way. Since all objects with a temperature above absolute zero (-273°C) emits energy whose wavelength is proportional to surface temperature, this energy is then converted into thermal images thanks to infrared camera [72]. Infrared thermographic surveys in Cultural Heritage conservation is widely applied since 70s to localize superficial water damage and building defects [73-75]. This technique provides information on the moisture distribution in structures but doesn't allow its measure. This latter aim is reached through analysis on samples.

Sampling on masonries

All the six buildings were sampled in June 2019 only after the previous site inspections in February 2019 (Ca' Foscari, Ca' Bottacin and Ex Slaughterhouse San Giobbe) and in May 2019 (Badoer Palace, Ca' Tron and Malipiero Palace).

Samples were collected on the wall profiles by drilling bricks at various heights and depths [76]. Height and depths values slightly varied for the six historical buildings considered. The 10 mm drill bits were used and the obtained powders were put in previously weighted and then numbered empty glass tubes which, once sealed, were transported to the laboratory to be analyzed.

2.2.2.1 Samples analysis

Moisture Content

The moisture content in masonry at the moment of the sampling is evaluated through Moisture Content % (MC%) normalized measurement [76]. The overall 82 glass tubes containing the powder samples, were weighted, dried in oven at 60° C and then put in glass desiccators to prevent the moisture absorbance from the air. All the glass tubes with brick powders were weighted several times in a month till reaching a stable weight. The moisture content was calculated in w% for each sample from the Equation 2 where weight sample and dry weight refers to the powders, after the subtraction of glass tubes weight. Finally, the average MC% was defined for each sample.

$$MC = 100 * \frac{(\text{weight sample} - \text{dry weight})}{\text{dry weight}} \quad (\text{Equation 2})$$

Hygroscopic Moisture Content

Hygroscopic salts in masonries determine humidity absorption from the air. Indeed, if the relative humidity of the air exceeds the equilibrium one of the salts, the masonry MC will be influenced by air RH and hygroscopic salts themselves [71].

The moisture content due to the presence of hygroscopic salts is calculated through hygroscopic moisture content (HMC) measurements [77]. A weighted amount (about 1g) of each dry powder sample was put in plastic cap and these were stored in a box with about 2 litres of KCl saturated solution (solubility 330g/l) (Figure 19). The KCl solution was selected among other saturated aqueous solutions, reported by IUPAC⁸ [78] recommendation. This lists the main salts solutions used for calibration in the range 10 - 90% of RH. . Considering KCl, a temperature of 20°C corresponds to a RH of 85.11±0.29, while a RH of 84.34 ± 0.26 is related to a temperature of 25°C [78].

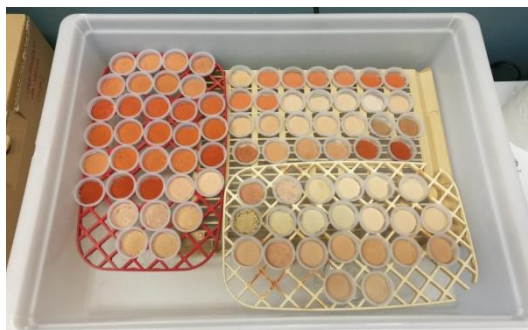


Figure 19 The 82 brick powder samples weighted and put into a box with the underlying saturated solution of KCl.

The box was closed and the samples weighted several times over more than a month, till a stable weight was reached.

A data logger was used in order to monitor RH and temperature values.

⁸International Union of Pure and Applied Chemistry

The HMC% is given by the difference between the dry sample and its weight after conditioning at temperature and RH values (Equation 3). The temperature and RH recorded for this research are 23.3°C and 85% respectively.

$$\text{HMC} = 100 * \frac{(\text{weight } 85 \% \text{ RH} - \text{dry weight})}{\text{dry weight}} \quad (\text{Equation } 3)$$

Once HMC% values were calculated for all the 82 samples, these were compared with the reference values (Table 9).

Material	RH=75%	RH=96%
Fired- clay brick	0.25	0.5-0.7
Calcium silicate brick	0.5-2	3-6
Gypsum	< 0.1	3.5
Cement plaster	0.5	2

If the HMC values are higher than the reference ones, soluble salts are present. Moreover the higher the salt content and the hygroscopicity of the salts, the higher the HMC values [71].

Table 9 Reference values of HMC % values for some materials at RH of 75% and 96% [71].

Electrical Conductivity and Soluble Salt content measurements

In addition to HMC%, also the conductivity normalized measurements are used to assess the salt content in all 82 samples [79]. For each sample, approximately 100 mg of powder were weighed and added in 100 ml of deionized water in plastic containers. The conductivity (σ) of the obtained solutions was measured for three consecutive days and the mean values calculated (Figure 20).

The conductometer used is the *Crison EC- Meter GLP31* with the *Crison 50 70* conductivity cell [80] (*Appendix 1*).



Figure 20 Sample solutions (left) and their conductivity measurements (right): conductometer and conductivity cell used.

In addition to the 82 solutions, also a blank (100 ml of deionized water) conductivity was measured and the following equation (Equation 4) applied at all samples:

$$\sigma = \frac{\text{sample conductivity} - \text{blank conductivity}}{\text{sample mass}} \times 100 \quad (\text{Equation } 4)$$

Starting from the conductivity values of the 82 samples, their soluble salt content (SS%) was calculated through the Equation 5:

$$SS\% = \frac{6.88 \cdot \sigma}{\text{sample mass (mg)}} \quad (\text{Equation 5})$$

Additional quantitative information on salts content, as type and amount of ions, was provided by Ion Chromatography.

Ion chromatography

A precise detection of the soluble ions salt content and their concentrations is possible through Ion Chromatography analysis.

Materials

The brick powder samples analyzed are 49 for the anionic detection and 32 for the cationic one, over the total 82.

The reagents used to prepare the mobile phases are Na₂CO₃ 64mM and NaHCO₃ 20mM H₂O for anions and HNO₃ 0.1 M [81] for cations. Both were diluted with water obtaining Na₂CO₃ 3.2 mM and NaHCO₃ 1mM solution for anions detection and HNO₃ 5mM for cations one.

The suppressor solution for the anion chromatograph was prepared with 2.7 mL H₂SO₄ in 1L of Milli- Q water. The standard solution are the Multielement Ion Chromatography Anion Standard Solution and the Multielement Ion Chromatography Cation Standard Solution by Sigma Aldrich [81].

Sample preparation

The sample solution analyzed were prepared by adding milliQ water to a weighted powder sample amount in 5 mL and 10mL flasks (Figure 21).

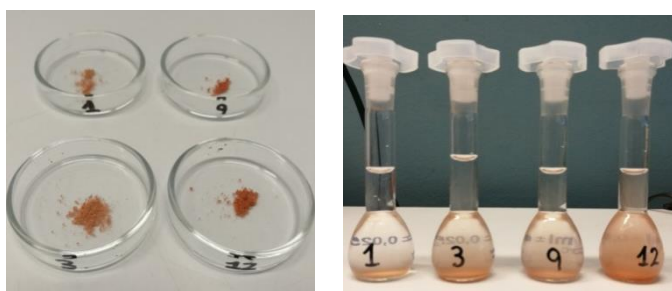


Figure 21 Preparation of the Ion Chromatography solutions: the powders were weighted (left) and brought up to volume with milliQ water in volumetric flasks

The amount of powder to be weighted for each sample solution was defined on the basis of the related conductivity values, previously measured. Powders were weighted with a high precision balance (Mettler TG50 M3).

The solutions were then taken with disposable syringes equipped with filters to avoid the presence of powder particles in the solutions ready to be injected into chromatographs.

Instrumentation

Ion Chromatography measurements were carried out with two 761 Compact IC Chromatographs by Metrohm (Appendix 1), one for the anions detection and one for that of cations (Appendix 1).

- Anions analysis

The 761 Compact IC Chromatographs by Metrohm has the suppressor module and the Metrosep A Supp 4 – 250/4.0 column was used for detection (Figure 22).

- Cations analysis

The 761 Compact IC Chromatographs by Metrohm has not the suppressor and the Metrosep C3 250/4.0 column was used for cations determination (Figure 22).



Figure 22 Chromatographs and column used for the anions (left) and cations (right) detection [82].

Analysis method

Before starting sample analysis, the anions and cations standard solutions were injected in order to know the exact retention times of each ion. Table 10 shows the retention time for each ion and the average total run time for each sample analysis are 23 minutes for anions and 24 min for cations.

Anion	Retention time (min)	Cation	Retention time (min)
F ⁻	4.6	Na ⁺	5.3
Cl ⁻	5.7	K ⁺	7.1
Br ⁻	8.1	Mg ²⁺	18.4
NO ₃ ²⁻	9.3	Ca ²⁺	21.8
SO ₄ ²⁻	21.4		

Table 30 Retention times of anions and cations analysis through Ion Chromatography.

During analysis pressure and conductivity values, given by the instrument detectors, were in average 7 MPa and 9.5 μ S/cm for anions investigation and 13 MPa and 969 μ S/cm for the cations one. Flow parameter for both anions and cations injections was 1mL/min.

Each sample was injected three times and the average of the peak areas values constitute the final values.

The calibration curves were obtained through the analysis of diluted anions and cations standards solutions at increasing concentrations. Starting from calibration curves equations, knowing the peak areas, the ions concentrations for each sample were determined and then divided by the concentrations of the initial solutions. Finally, anions and cations concentrations for 1 mg of brick powdered samples were determined relating obtained results to 1 mg of sample.

Infrared Spectroscopy

The Infrared Spectroscopy allows the qualitative determination of the species present in brick powder samples. In particular calcium sulphate bihydrated (*Gypsum*), nitrates, carbonates and silicates can be identified through this technique.

The measurements are performed on solid samples obtained mixing a sufficient amount of brick powder and KBr, previously dried in oven. The obtained mixtures, finely ground, are compressed using a manual hydraulic press in order to obtain KBr pellets ready to be analyzed. Using the *Nicolet Nexus 670* FT-IR spectrophotometer the infrared spectra were recorded in the 4000-400 cm^{-1} region for 32 scans with 4 cm^{-1} resolution.

Considering the high number of total samples obtained at the beginning, from the building samplings, just a reduced number of them, but particularly significant, was analyzed through IR spectroscopy. Indeed, for each sampling height of the six buildings, just the powders sampled at a depth of 1.5-5 cm are analyzed. Starting from the obtained IR spectra and thanks to the literature data, the main compound and species constituting the samples are identified.

3 Results and discussion

The results of the research work, their elaboration and discussion are treated in this section.

In order to evaluate possible changes over time in the intensity of the rising damp phenomenon on masonries, in the first part of this chapter, the comparison of conservation state by observation of old and current photographs of Venetian sites is qualitatively and semi-quantitatively evaluated.

The second part instead, regards the measurement via quantitative methods of moisture and salts content in six masonries of Venetian buildings (case studies introduced in section 2.2.1); the results obtained from samples analysis are discussed considering location and altimetry of the buildings.

3.1 SECTION 1 - Comparison of photographs

The old photos of Venetian masonries, collected from private and public archives described in section 2.1.1, and the respective current ones are separately treated according to the three Sestieri: Castello, Dorsoduro and San Marco. For each one of these, a map with the exact position of the subjects of the photos is provided. Subsequently the compared photos are listed according to decreasing exposure of the sites to the water canals of Venice (i.e. increasing altimetry) and not following the increasing order of their civic numbers. For each site the location name, altimetry, old photo, current photos and the comparison comments are reported. The altimetry of the buildings directly on the water canal was considered equal to 0 and so as the reference value of Punta della Salute. All the other altimetries were obtained from the Ramses database by Insula S.p.A [53]. For a wide number of locations, the current photos were taken after the flood of the 12th November 2019. The changes over time are assessed for the five parameters considered: rising damp trend, plaster loss, biological growth (algae level), efflorescence and bricks erosion. These 5 parameters changes are qualitatively evaluated according the following scale:

=	The situation is the same, there are not visible changes
+	Few changes are slightly visible
++	There are some differences between old and current photos
+++	The changes are clearly evident
-	There are few visible changes
--	Changes are noticed and the general conservation state is better
---	A lot of changes determine an improvement of the situation for the parameters considered
/	It is not possible to make a comparison for several reasons: <ul style="list-style-type: none">- Rising damp trend: a clear damp level is not visible or the quality or brightness of the past photo are low .- Biological growth: the water level exceeds the algae one and it is not possible to determine if the current biological growth is higher or lower than the past situation.- Plaster loss: the plaster is not present also in the old photo.- Brick erosion - efflorescence: the sunlight conditions and low zoom level make the comparison impossible.

The evaluation of algae belt changes, through photos comparison, is an effective tracer of the sea level changes in time. This approach has been recently applied in Venice comparing the actual algae front on water stairs of the palaces with the past one depicted on the paintings of Veronese, Canaletto and Bellotto. In this way a general estimate of sea level rise acceleration ($+0.0030 \pm 0.0004 \text{ mm year}^{-1}$) in Venice from 1350 to 2014 is provided [83].

The efflorescence decrease in photos can be associated with a rising damp increase. Indeed a more damp wall corresponds to less visible salts on its surface and this will be discussed at the end of this chapter considering the obtained results.

Limits and assumptions








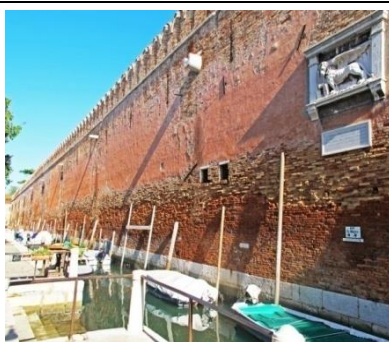
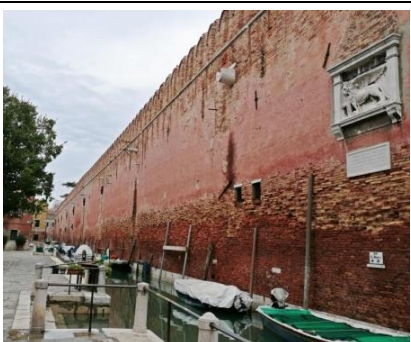
In order to facilitate the photos comparison, contrast and brightness parameters of the current photos were changed (by means of Photoshop) in order to be as similar as possible to the old ones. Moreover, when the old photos are in black and white, also the current ones are reported in the same format, to make the comparison possible. Despite this, several photo comparison cases are difficult to interpret due to the different cameras used in two different times and also for the different sunlight conditions of the photo acquisition. Indeed, when the building wall is hit by the sunlight, some details are difficult to see due to the high brightness and others are highlighted by the grazing light, as like as the lacking bricks. Although current photos were taken very carefully, it was not always possible to find exactly the same light and tide conditions of the original ones. Moreover the considered sites are many, and in particular for Castello for which photos were taken especially in November 2019. Since in 2019 the whole month was affected by exceptional high water events, it would not be possible anyway to find the same tide conditions of the old photos, that often don't show indication about the season in which they were taken.









3.1.1 Sestiere Castello







The Sestiere Castello presents the highest number of photos indeed 39 locations were considered and analyzed in order to evaluate the rising damp trend changes over time and the conservation state of building masonries. In Figure 23 the exact position of all locations studied is shown, while in Table 11 their photos are listed with the respective comments and evaluations.



Figure 23 Location and civic numbers of the considered building photos throughout Castello. Map created with Google Earth.

Location Name	Altimetry (cm on m.s.l.)	Old Photo	Current Photos		Comparison Scale /Comments
98 Rio delle Vergini. Resto di portale gotico ed iscrizioni	0	 <p data-bbox="584 584 694 608">Date: 2008</p>	 <p data-bbox="969 584 1144 608">Date: 16-11-2019</p>	 <p data-bbox="1391 584 1565 608">Date: 25-11-2019</p>	<p data-bbox="1731 363 2056 499">Rising damp trend (lower part): + Biological growth: / Plaster loss: / Efflorescence: / Brick erosion: /</p>
1852 Rio de la Tana Arsenale-Canevo. Torre angolare col rio de S. Daniel	0	 <p data-bbox="607 994 674 1018">Date: /</p>	 <p data-bbox="969 994 1144 1018">Date: 16-11-2019</p>	 <p data-bbox="1391 994 1565 1018">Date: 25-11-2019</p>	<p data-bbox="1731 735 2056 898">Rising damp trend (left part of the tower): = Biological growth: / Plaster loss: / Efflorescence: / Brick erosion: /</p>
2427 A Rio de le Gorne	0	 <p data-bbox="607 1393 674 1417">Date: /</p>	 <p data-bbox="969 1393 1144 1417">Date: 26-10-2019</p>	 <p data-bbox="1391 1393 1565 1417">Date: 16-11-2019</p>	<p data-bbox="1731 1153 2056 1289">Rising damp trend (lower part): - Biological growth: = Plaster loss: / Efflorescence: / Brick erosion: /</p>










<p>2641 Rio de S. Martin (con ingresso in Calle de l' Arco)</p>	<p>0</p>	 <p>Date: /</p>	 <p>Date: 26-10-2019</p>	 <p>Date: 16-11-2019</p>	<p>Rising damp trend: - Biological growth: + Plaster loss: + Efflorescence: - Brick erosion: +</p>
<p>2654 Rio dei Scudi con ingresso in calle dei Scudi Ca' Venier. Portale da acqua</p>	<p>0</p>	 <p>Date: /</p>	 <p>Date: 26-10-2019</p>	 <p>Date: 16-11-2019</p>	<p>Rising damp trend: = Biological growth: = Plaster loss: + Efflorescence: = Brick erosion: +</p>
<p>2716 Calle Donà (S.Ternita)</p>	<p>0</p>	 <p>Date: 21-08-2008</p>	 <p>Date: 26-10-2019</p>	 <p>Date: 16-11-2019</p>	<p>Rising damp trend: ++ Biological growth: = Plaster loss: ++ Efflorescence: - Brick erosion: +</p>

<p>2784 Campo de la chiesa (San Francesco della Vigna) Simbolo religioso</p>	<p>0</p>	 <p>Date: 21-08-2008</p>	 <p>Date: 26-10-2019</p>	 <p>Date: 16-11-2019</p>	<p>Rising damp trend: ++ Biological growth (visible on the religious symbol) : ++ Plaster loss: / Efflorescence: - Brick erosion: =</p>
<p>3207 Rio dei Scudi con ingresso da terra in ramo de le Gatte</p>	<p>0</p>	 <p>Date: /</p>	 <p>Date: 26-10-2019</p>	 <p>Date: 16-11-2019</p>	<p>Rising damp trend: / Biological growth: / Plaster loss: = Efflorescence: / Brick erosion: /</p>
<p>3405 Calle de la Madonna Rio dei Greci Ca' Zorzi Liassidi</p>	<p>0</p>	 <p>Date: /</p>	 <p>Date: 26-10-2019</p>	 <p>Date: 16-11-2019</p>	<p>Rising damp trend: ++ Biological growth: / Plaster loss: / Efflorescence: / Brick erosion: /</p>

	0	 <p>Date: /</p>	 <p>Date: 26-10-2019</p>	 <p>Date: 16-11-2019</p>	<p>In current photos the cut of the wall is visible. Despite this, the rising damp level is several bricks higher than wall cut.</p>
<p>3405 Rio dei Greci con ingresso in calle della Madonna a Ca' Zorzi Liassidi. Seconda porta da acqua</p>	0	 <p>Date: /</p>	 <p>Date: 16-11-2019</p>	 <p>Date: 25-11-2019</p>	<p>This is a detail of the previous building. In current photos the wall cut is visible: at the right of the door the rising damp level is limited while at the left of the door it exceeds the wall cut.</p> <p>Rising damp trend: + Biological growth: = Plaster loss: / Efflorescence: / Brick erosion: - (due to the restoration works and brick substitution)</p>
<p>3471 Rio de la Pietà. Due rilievi angolari</p>	0	 <p>Date: /</p>	 <p>Date: 16-11-2019</p>	 <p>Date: 25-11-2019</p>	<p>Rising damp trend: + Biological growth: = Plaster loss: + Efflorescence: - - Brick erosion: +</p>

<p>4313 Fondamenta S. Apollonia (giù dal ponte) Edificio d' angolo su rio di Palazzo o di Cornice</p>	<p>0</p>	 <p>Date: /</p>	 <p>Date: 16-11-2019</p>	 <p>Date: 25-11-2019</p>	<p>Rising damp trend: + + + Biological growth: = Plaster loss: + + Efflorescence: = Brick erosion: =</p>
<p>4419 Castello, S.Zaccaria, Rio de la Canonica (o de Palazzo o de la Pagia), Palazzo Soranzo (old photo taken from Archivio Fotografico Urbanistica)</p>	<p>0</p>	 <p>Date: /</p>	 <p>Date: 16-11-2019</p>	 <p>Date: 25-11-2019</p>	<p>Rising damp trend: + Biological growth: / Plaster loss: / Efflorescence: / Brick erosion: /</p>
<p>4425 Rio di S. Maria Formosa (con entrata in Ramo Venier 5269 A) Portale da acqua</p>	<p>0</p>	 <p>Date: /</p>	 <p>Date: 26-10-2019</p>	 <p>Date: 16-11-2019</p>	<p>Rising damp trend: + Biological growth: = Plaster loss: = Efflorescence: + (low- right area) Brick erosion: =</p>




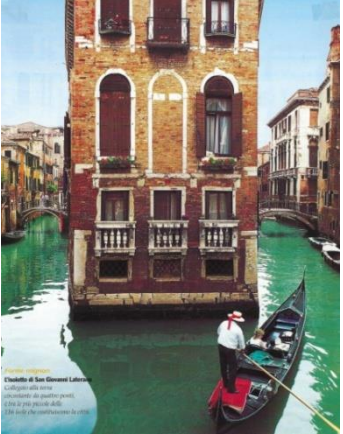





<p>4466 Corte Briani (a S. Giovanni Novo) Porta da acqua con arco in mattoni</p>	<p>0</p>	 <p>Date: /</p>	 <p>Date: 16-11-2019</p>	 <p>Date: 25-11-2019</p>	<p>Rising damp trend: = Biological growth: / Plaster loss: + Efflorescence: / Brick erosion: /</p>
<p>4853 Rio di Santa Maria Formosa Portale da acqua</p>	<p>0</p>	 <p>Date: /</p>	 <p>Date: 16-11-2019</p>	 <p>Date: 25-11-2019</p>	<p>Rising damp trend: + Biological growth: = Plaster loss: + Efflorescence: / Brick erosion: /</p>
<p>4907 Rio di S. Severo. Due porte da acqua</p>	<p>0</p>	 <p>Date: /</p>	 <p>Date: 26-10-2019</p>	 <p>Date: 16-11-2019</p>	<p>Rising damp trend: = Biological growth: = Plaster loss: = Efflorescence: + (low-left zone) Brick erosion: =</p> <p>A cleaning intervention has been made, looking the more whitish color of the Istrian stone parts of the door and of the terrace.</p>


<p>4907 Rio di S. Severo (con ingresso in Calle dell' Arco detta Bon) Ca' Zorzi – Bon. Portale da acqua</p>	<p>0</p>	 <p>Date: /</p>	 <p>Date: 26-10-2019</p>	 <p>Date: 16-11-2019</p>	<p>Rising damp trend: ++ (a little bit more on the high-left zone) Biological growth: = Plaster loss: = Efflorescence: - (probably due to the more wet wall of the current photos) Brick erosion: =</p>
<p>4979 A Calle del Diavolo Ca' Priuli</p>	<p>0</p>	 <p>Date: /</p>  <p>Date: /</p>	 <p>Date: 26-10-2019</p>  <p>Date: 26-10-2019</p>	 <p>Date: 16-11-2019</p>  <p>Date: 16-11-2019</p>	<p>Rising damp trend: +++ Biological growth: = Plaster loss: = Efflorescence: - (probably due to the more wet wall of the current photos) Brick erosion: =</p>

<p>4979 A Castello, S. Zaccaria Fondamenta dell' Osmarin Palazzo Priuli (old photo taken from the Archivio Fotografico Urbanistica)</p>		 <p>Date: 1966</p>	 <p>Date: 26-10-2019</p>	 <p>Data: 16-11-2019</p>	<p>Rising damp trend: + + + Biological growth: / Plaster loss: / Efflorescence: / Brick erosion: /</p>
<p>4979 A Rio di S. Provolo (con ingresso in Calle del Diavolo) Ca' Priuli Portale da acqua</p>	<p>0</p>	 <p>Date: /</p>	 <p>Date: 16-11-2019</p>	 <p>Date: 25-11-2019</p>	<p>Rising damp trend: + + (left zone) Biological growth: = Plaster loss: / Efflorescence: / Brick erosion: /</p>
<p>5152 Rio de la Tetta o di S. Giovanni Laterano.Ca' Gabrieli</p>	<p>0</p>	 <p>Date: 31-03-2009</p>	 <p>Date: 26-10-2019</p>	 <p>Date: 16-11-2019</p>	<p>Rising damp trend: = Biological growth: + (lower part) - (high-left zone) Plaster loss: + Efflorescence: - Brick erosion: =</p> <p>The wooden door has a worst conservation state in the current photo.</p>

<p>5193 Rio di S. Severo con ingresso da terra in Calle dei Olbi. Portale da acqua</p>	<p>0</p>	 <p>Date: /</p>	 <p>Date: 25-11-2019</p>	<p>Rising damp trend: + Biological growth: / Plaster loss: / Efflorescence: / Brick erosion: /</p>
<p>5402 Fondamenta Papafava o tasca-papafava</p>	<p>0</p>	 <p>Date: /</p>	 <p>Date: 18-11-2019</p>  <p>Date: 25-11-2019</p>	<p>Rising damp trend: = Biological growth: / Plaster loss: / Efflorescence: / Brick erosion: /</p>
<p>5745 Rio del mondo nuovo (con ingresso da terra in calle del Paradiso) Ca' Foscari Mocenigo</p>	<p>0</p>	 <p>Date: /</p>	 <p>Date: 16-11-2019</p>  <p>Date: 25-11-2019</p>	<p>Rising damp trend: + Biological growth: = Plaster loss: = Efflorescence: - - Brick erosion: +</p>

<p>5870 Rio del Paradiso. Porta da acqua</p>	<p>0</p>	 <p>Date: /</p>	 <p>Date: 16-11-2019</p>	 <p>Date: 25-11-2019</p>	<p>Rising damp trend: = Biological growth: + (right zone near the door) Plaster loss: / Efflorescence: / Brick erosion: +</p>
<p>6036 Rio del Malibran, con ingresso da calle Scaleta. Vetrina</p>	<p>0</p>	 <p>Date: /</p>	 <p>Date: 18-11-2019</p>	 <p>Date: 25-11-2019</p>	<p>Rising damp trend: ++ Biological growth: = Plaster loss: + Efflorescence: - Brick erosion: +</p> <p>Some changes have been made: three square metallic elements have been added, two in the upper part and one in the lower left area.</p>
<p>6282 Ponte dei Conzafelzi o ponte Storto o Pinelli. Ponte pubblico in ferro</p>	<p>0</p>	 <p>Date: 11-03-2009</p>	 <p>Date: 16-11-2019</p>	 <p>Date: 25-11-2019</p>	<p>Rising damp trend: + Biological growth: = Plaster loss: / Efflorescence: / Brick erosion: /</p>

<p>6377 Ponte de l' Ospealeto (foto rivista)</p>	<p>0</p>	 <p>Date: /</p>	 <p>Data: 26-10-2019</p>	 <p>Data: 16-11-2019</p>	<p>Rising damp trend: = Biological growth: + Plaster loss: - Efflorescence: / Brick erosion: /</p> <p>The whole wall has been covered with plaster.</p>
<p>6378 Fondamenta al ponte de la Tetta- Rio di S. Giovanni in Laterano</p>	<p>0</p>	 <p>Date: /</p>  <p>Date: /</p>	 <p>Date: 16-11-2019</p>  <p>Date: 16-11-2019</p>	 <p>Date: 25-11-2019</p>  <p>Date: 25-11-2019</p>	<p>Rising damp trend: + (in the middle-left part, near the window) Biological growth: = Plaster loss: / Efflorescence: / Brick erosion: /</p>

					
		Date: /	Date: 16-11-2019	Date: 25-11-2019	
6452 Corte Muazzo Ca' Muazzo	101-108				Rising damp trend: = Biological growth: - Plaster loss: + Efflorescence: = Brick erosion: +
		Date: 31-03-2009	Date: 16-11-2019	Date: 25-11-2019	
485 Fondamenta S. Gioachin. Iscrizione	113-118				Rising damp trend: + + + Biological growth: = Plaster loss: = Efflorescence: - Brick erosion: +
		Date: 2008	Date: 16-11-2019	Date: 25-11-2019	

<p>5016 Campo S. Severo.Ex Carceri</p>	<p>114-138</p>	 <p>Date: /</p>	 <p>Date: 26-10-2019</p>	 <p>Date: 16-11-2019</p>	<p>Rising damp trend: + Biological growth: = Plaster loss: = Efflorescence: - - Brick erosion: +</p>
<p>2426 Campo S. Martin</p>	<p>121-128</p>	 <p>Date: /</p>	 <p>Date: 16-11-2019</p>	 <p>Date: 25-11-2019</p>	<p>Rising damp trend: + Biological growth: = Plaster loss: / Efflorescence: - Brick erosion: =</p>
<p>2466 Campiello de la Grana. Cornice bizantina e patera</p>	<p>121-132</p>	 <p>Date: 2008</p>	 <p>Date: 16-10-2019</p>	 <p>Date: 25-11-2019</p>	<p>Rising damp trend: = Biological growth: = Plaster loss: = Efflorescence: - Brick erosion: + +</p>

<p>6122,6123 Castello, S. Maria Formosa, campo di S. Maria Formosa, Palazzo Donà (1962-06) (old photo taken from the Archivio Fotografico Urbanistica)</p>	<p>128-139</p>	 <p>Date: 06-1962</p>	 <p>Date: 16-11-2019</p>	 <p>Date: 25-11-2019</p>	<p>Rising damp trend: + Biological growth: / Plaster loss: - - - Efflorescence: / Brick erosion: -</p> <p>In the current photo the lower part of the building is no more covered by plaster.</p>
<p>6123 Campo S. Maria Formosa, Ca' Donà. Portale di terra</p>	<p>128-139</p>	 <p>Date: /</p>	 <p>Date: 26-10-2019</p>	 <p>Date: 16-11-2019</p>	<p>Rising damp trend: = Biological growth: / Plaster loss: / Efflorescence: - Brick erosion: +</p>
<p>2543 Corte Rota presso Campo do Pozzi</p>	<p>139-156</p>	 <p>Date: /</p>	 <p>Date: 26-10-2019</p>	 <p>Date: 16-11-2019</p>	<p>Rising damp trend: ++ Biological growth: = Plaster loss: = Efflorescence: - Brick erosion: +</p>

<p>69 Campo S. Piero Altorilievo</p>	<p>154-155</p>	 <p>Date: 2008</p>	 <p>Date: 16 -10-2019</p>	 <p>Date: 26-11-2019</p>	<p>Rising damp trend: + Biological growth: + Plaster loss: = Efflorescence: - Brick erosion: =</p>
---	----------------	---	---	---	--

Table 41 List of the considered sites in Castello. Location name, building altimetry, old photo, recent ones and the comparison comments are reported for each case.





3.1.2 Sestiere Dorsoduro

The building locations considered for the Sestiere Dorsoduro are 15. Their position is shown in Figure 24. Table 12 lists the respective old and current photos with related evaluation on their comparison. All current photos were taken in the month of November 2019 and in particular after the flooding of the 12th November 2019.



Figure 24 Locations and civic numbers of the building photos considered throughout Dorsoduro. Map created with Google Earth.

Location Name	Altimetry (cm on m.s.l.)	Old Photo	Current Photos		Comparison Scale/Comments
2635 Calle Lunga	0	 <p data-bbox="613 651 685 675">Date: /</p>	 <p data-bbox="1005 659 1178 683">Date: 18-11-2019</p> <p data-bbox="1467 659 1639 683">Date: 26-11-2019</p>		<p data-bbox="1839 400 2047 536">Rising damp trend: = Biological growth: / Plaster loss: / Efflorescence: / Brick erosion: /</p>
2765 Rio del Malpagà	0	 <p data-bbox="562 975 734 1026">Date: / Before restoration</p>  <p data-bbox="566 1369 730 1420">Date: / After restoration</p>	 <p data-bbox="1005 991 1178 1015">Date: 18-11-2019</p> <p data-bbox="1467 991 1639 1015">Date: 26-11-2019</p>  <p data-bbox="1005 1374 1178 1398">Date: 18-11-2019</p> <p data-bbox="1467 1374 1639 1398">Date: 26-11-2019</p>		<p data-bbox="1823 935 2054 1070">Rising damp trend: ++ Biological growth: / Plaster loss: / Efflorescence: / Brick erosion: /</p> <p data-bbox="1805 1102 2080 1177">The wall has been restored and the bricks replaced over time.</p>

<p>2927 Rio de Santa Margherita-Riva de acqua</p>	<p>0</p>	 <p>Date: /</p>	 <p>Date: 18-11-2019</p>	 <p>Date: 26-11-2019</p>	<p>Rising damp trend: = Biological growth: = Plaster loss: - Efflorescence: - - - Brick erosion: +</p> <p>Two ventilation grills and plaster have been added over time in the upper part but, as visible in current photos, it is already damaged and plaster losses are visible.</p>
<p>2946 Rio di Santa Margherita-Sotoportego de l' uva quattro finestrelle</p>	<p>0</p>	 <p>Date: /</p>	 <p>Date: 18-11-19</p>	 <p>Date: 26-11-2019</p>	<p>Rising damp trend: + + Biological growth: / Plaster loss: / Efflorescence: / Brick erosion: -</p> <p>The wall has been restored, bricks have been replaced and two metallic elements have been added in the upper part.</p>
<p>3228 Palazzo Giustinian</p>	<p>0</p>	 <p>Date: /</p>	 <p>Date: 25-11-2019</p>		<p>Rising damp trend: + Biological growth: + Plaster loss: / Efflorescence: / Brick erosion: /</p>

3232-28
Calle
Giustinian
Ca'
Giustinian dei
Vescovi



Date: /



Date: 25-11-2019

Rising damp trend: =
Biological growth: /
Plaster loss: /
Efflorescence: /
Brick erosion: /

3246
Calle Foscari-
Ca' Foscari

0



Date: /

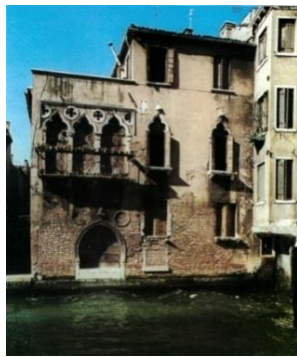


Date: 24-11-2019

Rising damp trend: =
Biological growth: /
Plaster loss: /
Efflorescence: /
Brick erosion: /

3422
Corte del
Fontego- Rio
de Ca'
Foscari.
Palazzetto di
testata

0



Date: /



Date: 18-11-2019



Date: 26-11-2019

The plaster has been
replaced over time but there
are visible losses in the
current one.



Date: /



Date: /



Date: 18-11-19



Date: 18-11-19



Date: 25-11-2019



Date: 26-11-2019

Rising damp trend: ++
 Biological growth: +
 Plaster loss: ++
 Efflorescence: =
 Brick erosion: +

The wooden poles have been modified or replaced over time.

3707
 Campo San
 Pantalon- Ca'
 Signolo-
 Loredan



Date: /



Date: 18-11-19



Date: 26-11-2019

Rising damp trend: =
 Biological growth: /
 Plaster loss: +
 Efflorescence: /
 Brick erosion: /

<p>3859 A Rio de Ca' Foscari (con ingresso da terra in Calle Larga Foscari) area demolita Ca' Renier</p>	<p>0</p>	 <p>Date: /</p>	 <p>Date: 18-11-2019 Date: 26-11-2019</p>	<p>Rising damp trend: = Biological growth: + Plaster loss: = Efflorescence: - Brick erosion: +</p>
<p>3900 Calle del Remer- Canal Grande Fondazione Masieri Wright</p>	<p>0</p>	 <p>Date: /</p>	 <p>Date: 26-11-2019</p>	<p>Rising damp trend: = Biological growth: / Plaster loss: / Efflorescence: / Brick erosion: /</p>
<p>3911 Crosera (S.Pantalon)- Ca' della Frescada- Corner</p>	<p>0</p>	 <p>Date: /</p>	 <p>Date: 26-11-2019</p>	<p>Rising damp trend: = Biological growth: / Plaster loss: / Efflorescence: / Brick erosion: /</p> <p>Probably the building has been cleaned over time, indeed the black incrustations (under the window and in the upper zone) are no more visible in the current photo.</p>

				
<p>3934A Rio de la Frescada (con ingresso da terra nel sotoportego di Calle Boldù) porta da acqua.</p>	<p>0</p>			 <p>Rising damp trend: = Biological growth: = Plaster loss: + Efflorescence: - Brick erosion: +</p> <p>Plaster has been added near the left upper angle. Interventions over time are visible by the zones with different bricks color, especially in the right area of the door.</p>
<p>2824 Fondamenta Gherardini- Ca'Soranzo</p>	<p>103-108</p>			 <p>Rising damp trend: = Biological growth: = Plaster loss: = Efflorescence: - Brick erosion: +</p> <p>The red plaster has been added in the lower area near the door.</p>







<p>3885 Corte Marcona- Barbacani e porta di magazzino</p>	<p>119-124</p>	 <p>Date: 23-03-2005</p>	 <p>Date: 18-11-2019</p>	 <p>Date: 26-11-2019</p>	<p>Rising damp trend: + Biological growth: - Plaster loss: = Efflorescence: - Brick erosion: +</p> <p>The wall has been restored, bricks replaced and the wooden edges of the door, which in the old photo are white painted, lost the colour.</p>
<p>3423 Corte del Fontego Resti di porticato bizantino</p>	<p>137-141</p>	 <p>Date: /</p>	 <p>Date: 18-11-2019</p>	 <p>Date: 26-11-2019</p>	<p>Rising damp trend: + Biological growth: - Plaster loss: - Efflorescence: - Brick erosion: +</p> <p>The wall has been restored and bricks replaced, especially in the lower part. A cleaning intervention is clearly visible in the upper part of the masonry. A hole in the right area of the wall is present in the current photos.</p>

Table 12 List of the considered sites in Dorsoduro. Location name, building altimetry, old photo, recent ones and the comparison comments are reported for each case

3.1.3 Sestiere San Marco

For San Marco 19 building locations are analyzed and their position on the map is shown in Figure 25, while photo comparison and respective evaluation comments are listed in Table 13.

It is important to specify that a wide part of San Marco current photos was taken between the end of June and the beginning of July 2019 so a different situation is expected from photos taken in November 2019. This is important also when San Marco situation will be compared with the ones of Castello and Dorsoduro to whom the major part of the photos was taken in autumn and not in summer 2019.



Figure 25 Locations and civic numbers of the building photos considered throughout San Marco. Map created with Google Earth.

Location Name	Altimetry (cm on m.s.l.)	Old Photo	Current Photos		Comparison Scale/Comments
556 A Rio dei Bareteri (inglesi calle Erizzo)	0	 <p data-bbox="651 646 723 670">Date: /</p>	 <p data-bbox="983 651 1160 675">Date: 26-06-2019</p>	 <p data-bbox="1361 651 1538 675">Date: 16-11-2019</p>	<p data-bbox="1711 284 1939 419">Rising damp trend: ++ Biological growth: = Plaster loss: ++ Efflorescence: -- Brick erosion: =</p> <p data-bbox="1666 451 1984 587">The plaster loss of the upper left wall area is visible in current photos. Moreover plaster loss increased in just ten days (the two current photos).</p>
1906 Rio de la Verona	0	 <p data-bbox="636 962 707 986">Date: /</p>	 <p data-bbox="983 970 1160 994">Date: 26-06-2019</p>	 <p data-bbox="1368 970 1545 994">Date: 17-11-2019</p>	<p data-bbox="1720 770 1926 906">Rising damp trend: + Biological growth: + Plaster loss: +++ Efflorescence: - Brick erosion: +</p>
2307 Campiello Contarin- Ca' Contarini- Fasan	0	 <p data-bbox="640 1398 712 1422">Date: /</p>	 <p data-bbox="983 1398 1160 1422">Date: 26-06-2019</p>	 <p data-bbox="1368 1398 1545 1422">Date: 25-11-2019</p>	<p data-bbox="1720 1074 1926 1209">Rising damp trend: + Biological growth: + Plaster loss: / Efflorescence: / Brick erosion: +</p> <p data-bbox="1666 1241 1984 1345">Changes are visible in windows and probably the building undergone a cleaning intervention.</p>



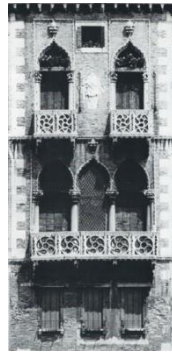
Date: 2007



Date: 26-06-2019



Date: 26-11-2019



Date: 1985



Date: 26-06-2019



Date: 26-11-2019



Date: /




Date: 26-06-2019





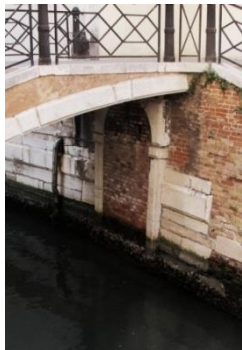





Date: 25-11-2019










Rising damp trend: +
 Biological growth: =
 Plaster loss: /
 Efflorescence: -
 Brick erosion: +







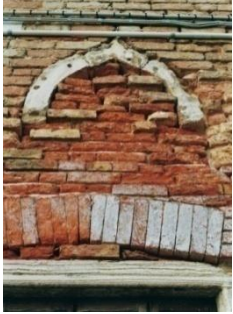


Several changes are visible from the black and white photo of 1985. Indeed window are different, especially the lower ones and those in the middle of the façade.

<p>2307 Campiello Contarini Ca' Contarini</p>	<p>0</p>	 <p>Date: /</p>  <p>Date: /</p>	 <p>Date: 26-06-2019</p>  <p>Date: 26-06-2019</p>	 <p>Date: 26-11-2019</p>  <p>Data: 26-11-2019</p>	<p>Rising damp trend: = Biological growth: = Plaster loss: = Efflorescence: - Brick erosion: +</p> <p>The comparison is quite difficult due to the high distance from the building. However the rising damp level seems to be the same between the old photo and the current ones.</p>
<p>2432 Portale ad acqua (Rio de le Ostreghe)</p>	<p>0</p>	 <p>Date: 2007</p>	 <p>Date: 26-06-2019</p>	 <p>Date: 26-11-2019</p>	<p>Rising damp trend: + Biological growth: = Plaster loss: / Efflorescence: - Brick erosion: +</p> <p>In the current photo of June a wide round zone in the left part of the wall is visibile. The same area is found in the photo of November despite the evidently wetter wall.</p>

<p>2513 Rio de San Maurizio- Ca' Malipieri Porta ad acqua</p>	<p>0</p>	 <p>Date: /</p>	 <p>Date: 03-07-2019</p>	 <p>Date: 26-11-2019</p>	<p>Rising damp trend: + Biological growth: = Plaster loss: ++ Efflorescence: + Brick erosion: +</p> <p>The comparison is not so easy due to the boat covering the lower zone. Also the different light conditions between the two current photos make more difficult an obvious comparison.</p>
<p>2517 Rio Santa Maria del Giglio Portale murato</p>	<p>0</p>	 <p>Date: /</p>	 <p>Data: 03-07-2019</p>	 <p>Date: 26-11-2019</p>	<p>Rising damp trend: + Biological growth: + Plaster loss: / Efflorescence: - - - Brick erosion: +</p>
<p>2569 Rio de la Verona</p>	<p>0</p>	 <p>Date:</p>	 <p>Date: 03-07-2019</p>	 <p>Date: 26-11-2019</p>	<p>Rising damp trend: + Biological growth: + Plaster loss: = Efflorescence: - Brick erosion: +</p>

<p>2598A Ponte dei Malvasia</p>	<p>0</p>	 <p>Date: 2007</p>	 <p>Date: 03-07-2019</p>	 <p>Date: 26-11-2019</p>	<p>Rising damp trend: + Biological growth: = Plaster loss: + Efflorescence: - Brick erosion: +</p> <p>A comparison of the right wall part is not possible because it is covered.</p>
<p>2819 Sotoportego e ramo Ca' Pisani Ca' Benzon- Foscolo</p>	<p>0</p>	 <p>Date: /</p>	 <p>Date: 03-07-2019</p>	 <p>Date: 26-11-2019</p>	<p>Rising damp trend: + Biological growth: = Plaster loss: ++ Efflorescence: + Brick erosion: +</p>
<p>2840 Ca'Barbaro</p>	<p>0</p>	 <p>Date: /</p>	 <p>Date: 03-07-2019</p>	 <p>Date: 26-11-2019</p>	<p>Rising damp trend: +++ Biological growth: = Plaster loss: = Efflorescence: - Brick erosion: +</p>

<p>3319 Ca' Erizzo- Nani Mocenigo</p>	<p>0</p>	 <p>Date: /</p>	 <p>Date: 03-07-2019</p>	 <p>Date: 26-11-2019</p>	<p>Rising damp trend: + Biological growth: / Plaster loss: / Efflorescence: ++ Brick erosion: +</p>
<p>3421 A Rio de Ca' Garzoni</p>	<p>0</p>	 <p>Date: 2007</p>	 <p>Date: 03-07-2019</p>	 <p>Date: 26-11-2019</p>	<p>Rising damp trend: = Biological growth: + Plaster loss: + Efflorescence: + Brick erosion: +</p> <p>The comparison is difficult due to the different sunlight exposition of the building walls.</p>
<p>3706 Rio de San Luca Riva da acqua</p>	<p>0</p>	 <p>Date: /</p>	 <p>Date: 03-07-2019</p>	 <p>Date: 26-11-2019</p>	<p>Rising damp trend: + Biological growth: + Plaster loss: + Efflorescence: - Brick erosion: +</p>

<p>4013 A Ca' Pisani- Revedin Riva da acqua</p>	<p>0</p>	 <p>Date: 2007</p>  <p>Date: 2007</p>	 <p>Date: 03-07-2019</p>  <p>Date: 03-07-2019</p>	 <p>Date: 26-11-2019</p>  <p>Date: 26-11-2019</p>	<p>Rising damp trend: + Biological growth: - Plaster loss: + Efflorescence: = Brick erosion: +</p> <p>The wall cut is present.</p>
<p>2557 A Fondament a della Fenice, resti di finestra</p>	<p>92-102</p>	 <p>Date: 2007</p>	 <p>Date: 03-07-2019</p>	 <p>Date: 26-11-2019</p>	<p>Rising damp trend: + Biological growth: / Plaster loss: / Efflorescence: - - Brick erosion: +</p>

<p>3957-3958 S.Luca, visto da campo san Beneto Palazzo Pesaro- Fortuny (o palazzo pesaro degli Orfei) (old photo from the AFU)</p>	<p>92-106</p>	 <p>Date: 20-11-1968</p>	 <p>Date:03-07-2019</p>	 <p>Date: 26-11-2019</p>	<p>Rising damp trend: = Biological growth: / Plaster loss: / Efflorescence: / Brick erosion: +</p> <p>The darkness of the lower area of the building is not due to the rising damp level but to the different colour of the bricks, a deep red. The building wall has been cleaned over time, as visible in the middle zone.</p>
<p>2883 Colonna antica Giustinian</p>	<p>122-128</p>	 <p>Date: /</p>	 <p>Data: 03-07-2019</p>	 <p>Date: 26-11-2019</p>	<p>Rising damp trend: = Biological growth: = Plaster loss: / Efflorescence: - Brick erosion: =</p> <p>The column and the wall were cleaned over time. Indeed the writing on the right part of has been removed from the wall.</p>
<p>3226B Chiesa di S. Samuel</p>	<p>132-135</p>	 <p>Date: 2005</p>	 <p>Date: 03-07-2019</p>	 <p>Date: 26-11 2019</p>	<p>Rising damp trend: + Biological growth: +++ Plaster loss: ++ Efflorescence: = Brick erosion: ++</p>

Table 13 List of the considered sites in San Marco. Location name, building altimetry, old photo, recent ones and the comparison comments are reported for each case.

Photos and degradation parameters: a semi- quantitative interpretation

The photos comparison in Tables 11,12 and 13 is just qualitative, in order to make a semi-quantitative one, only comparable cases were considered, and so those for which all the five degradation parameters (rising damp trend, biological growth, plaster loss, efflorescence and brick erosion) were evaluable. In doing so, for each Sestiere (Castello, Dorsoduro, San Marco), the positive (+, + +, + + +) and negative (-, - -, - - -) changes occurrence of the parameters is quantified over the total amount of considered cases. Also the unchanged situations (=) are included. Based on these results, possible correlations between the three Sestieri are pointed out.

Sestiere Castello

Among the 17 comparable cases considered for the Sestiere of Castello (Table 14), just the last four have an altimetry on m.s.l. greater than zero and their values are reported in brackets:

2614 Rio de S. Martin (con ingresso in Calle de l'Arco)	4979 A Calle del Diavolo Ca' Priuli
2654 Rio dei Scudi con ingresso in calle dei Scudi Ca' Venier.	5152 Rio de la Tetta o di S. Giovanni Laterano. Ca' Gabrieli
2716 Calle Donà (S. Ternita)	5745 Rio del mondo nuovo (con ingresso in calle delParadiso) Ca' Foscari Mocenigo
2784 Campo de la chiesa (San Francesco della Vigna) Simbolo religioso	6036 Rio del Malibràn, con ingresso da calle Scaleta. Vetrina
3471 Rio de la Pietà. Due rilievi angolari	485 Fondamenta S. Gioachin. Iscrizione (113-118 cm)
4313 Fondamenta S. Apollonia (giù dal ponte) Edificio d'angolo su rio di Palazzo o di Cornice	5016 Campo S. Severo. Ex carceri (114-138 cm)
4425 Rio di S. Maria Formosa (con entrate in Ramo Venier)	2466 Campiello de la Grana. Cornice bizantina e patera (121-132 cm)
4907 Rio di S. Severo. Due porte da acqua	69 Campo S. Piero. Altorelievo (154-155 cm)
4907 Rio di S. Severo (con ingresso in Calle dell'Arco detta Bon) Ca' Zorzi-Bon. Porta da acqua	

<i>Parameters</i>	<i>Improvement</i>			<i>Unchanged situation</i>	<i>Worsening</i>		
	<i>- - -</i>	<i>- -</i>	<i>-</i>		<i>=</i>	<i>+</i>	<i>++</i>
Rising damp trend			1/17 (5.9%)	4/17 (23.5%)	5/17 (29.4%)	4/17 (23.5%)	3/17 (17.7%)
Biological growth				12/17 (70.6%)	4/17 (23.5%)	1/17 (5.9%)	
Plaster loss				10/17 (58.8%)	5/17 (29.4%)	2/17 (11.8%)	
Efflorescence		3/17 (17.6%)	10/17 (58.8%)	2/17 (11.8%)	2/17 (11.8%)		
Brick erosion				8/17 (47.0%)	8/17 (47.0%)	1/17 (5.9%)	

Table 14 Number of better, equal or worst cases for each one of the five parameters over the 17 considered cases in Castello. Percentages are reported in brackets.

Generally an increase of the rising damp trend can be noticed in 12 cases over 17, in 4 cases the situation has not changed and for just one case it seems decreased (Table 14). The rising damp level increasing could be related to the exceptional high water event of the 12th November 2019 since a wide part of the comparison photos was taken after this date. Indeed masonry could appear more saturated in colour and so more damp considering high water and rainfall events, more frequent in autumn. The other four parameters (biological growth, plaster loss, efflorescence and brick erosion) are better with respect to rising damp. In particular, efflorescence decreased in 13 cases over 17 but this can be again related to washout action of rainfall and high water during the month of November 2019. Damper is the wall, and less visible are efflorescence on masonries.

Sestiere Dorsoduro

The comparable cases for the Sestiere of Dorsoduro are 7 (Table 15), among them just the last 3 have an altimetry higher than zero on the m.s.l.:

- 2927 Rio de Santa Margherita- Riva de acqua
- 3422 Corte del Fontego –Rio de Ca’ Foscari. Palazzetto di testata
- 3859 A Rio de Ca’ Foscari (con ingresso da terra in Calle Larga Foscari) area demolita Ca’ Renier
- 3924 A Rio de la Frescada (con ingresso da terra nel sottoportego di Calle Baldo) porta da acqua
- 2824 Fondamenta Gherardini- Ca’ Soranzo (103-108 cm)
- 3885 Corte Marcona- Barbacani e porta di magazzino (119-124 cm)
- 3423 Corte del Fontego. Resti di porticato bizantino (137-141 cm)

<i>Parameters</i>	<i>Improvement</i>			<i>Unchanged situation</i>	<i>Worsening</i>		
	---	--	-		=	+	++
Rising damp trend				4/7 (57.1%)	2/7 (28.6%)	1/7 (14.3%)	
Biological growth			2/7 (28.6%)	3/7 (42.6%)	2/7 (28.6%)		
Plaster loss			2/7 (28.6%)	3/7 (42.6%)	1/7 (14.3%)	1/7 (14.3%)	
Efflorescence	1/7 (14.3%)		5/7 (71.4%)	1/7 (14.3%)			
Brick erosion					7/7 (100%)		

Table 15 Number of better, equal and worst cases over the 7 considered for Dorsoduro. Percentages are reported in brackets.

The rising damp level for 3 cases over 7 in Dorsoduro increased (Table 15) and so at the same time, efflorescence seem to be less when comparing old photos with current ones. Comparing Castello and Dorsoduro, this latter has a lower percentage of plaster loss but at the same time all the 7 considered cases show in general a greater brick erosion.

Sestiere San Marco

Among the collected photos for San Marco, the selected cases for the numerical comparison are 12 (Table 16). Just one of them has altimetry greater than zero which is 132-135 cm on the m.s.l. The considered locations are :

556 A Rio dei Bareteri (inglesi in calle Erizzo)
 1906 Rio de la Verona
 2307 Campiello Contarini Ca' Contarini
 2513 Rio de San Maurizio- Ca' Malipieri. Porta ad acqua
 2569 Rio de la Verona
 2598 A Ponte dei Malvasia
 2819 Sotoportego e ramo Ca' Pisani Ca' Benzon- Foscolo
 2840 Ca' Barbaro
 3421 A Rio de Ca' Garzoni
 3706 Rio de San Luca. Riva da acqua
 4013 A Ca' Pisani- Revedin Riva da acqua
 3226 B Chiesa di S. Samuel (132-135 cm)

<i>Parameters</i>	<i>Improvement</i>			<i>Unchanged situation</i>	<i>Worsening</i>		
	---	--	-	=	+	++	+++
Rising damp trend				2/12 (16.7%)	8/12 (66.7%)	1/12 (8.3%)	1/12 (8.3%)
Biological growth			1/12 (8.3%)	6/12 (50.0%)	4/12 (33.3%)		1/12 (8.3%)
Plaster loss				3/12 (25.0%)	4/12 (33.3%)	4/12 (33.3%)	1/12 (8.3%)
Efflorescence		1/12 (8.3%)	6/12 (50.0%)	2/12 (16.7%)	3/12 (25.0%)		
Brick erosion				1/12 (8.3%)	11/12 (91.7%)		

Table 16 Number of better, equal or worst cases over the 12 considered for San Marco. Percentages are reported in brackets.

San Marco shows a general worsening among the considered cases and parameters, this can be linked to its lower altimetry with respect to Dorsoduro and Castello. Moreover, quite all the considered cases for San Marco are building directly in contact with the water canals so a higher degree of damage is expected .

Results are graphically presented considering each parameter and the percentages in Tables 14,15 and 16, for each Sestiere (Figures 26-30).

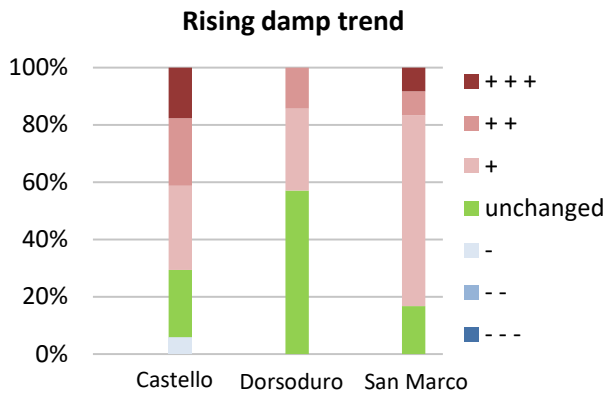


Figure 26 Rising damp changes percentages for the three Sestieri.

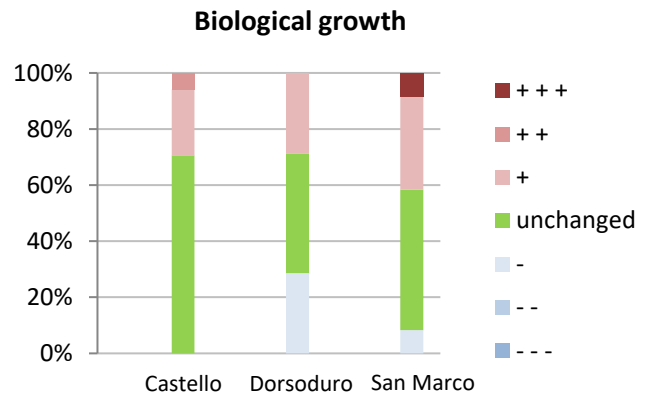


Figure 27 Biological growth changes percentages for the three Sestieri.

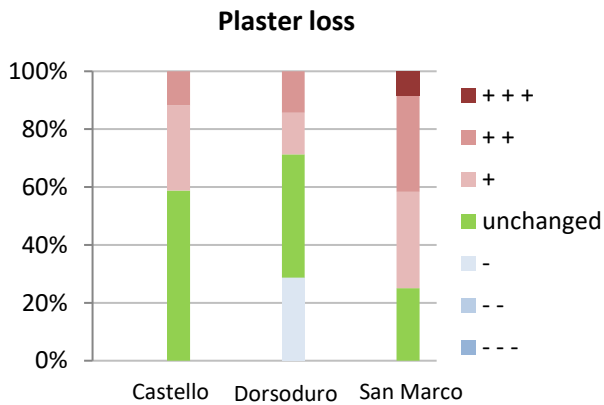


Figure 48 Plaster loss changes percentage for the three Sestieri.

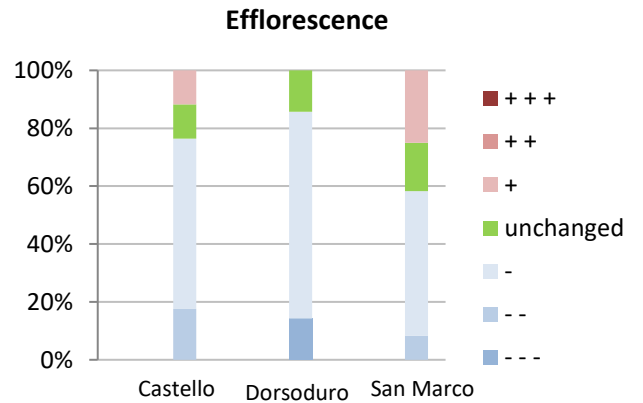


Figure 29 Efflorescence changes percentages for the three Sestieri.

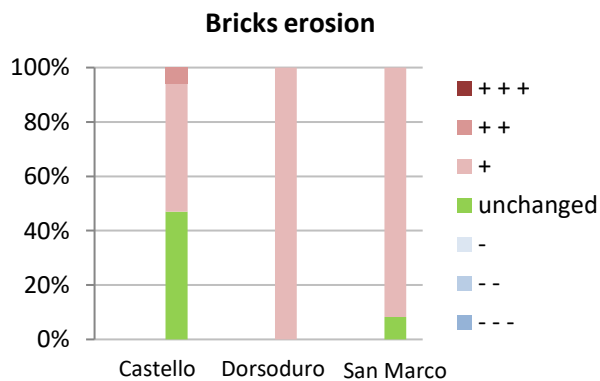


Figure 30 Brick erosion changes percentages for the three Sestieri.

An increase in rising damp trend is registered throughout all the three considered Sestieri but with different intensity (Figure 26). Indeed, Dorsoduro shows lower increase if compared with Castello and San Marco. This latter is characterised by the greater percentage of worsening of the rising damp parameter probably linked to the lower altimetry of the Sestiere itself if compared with the other two. The locations with altimetry greater than zero in Castello and Dorsoduro show a quite unchanged situation or slightly changes on rising damp trend. By contrast in San Marco, the only considered site not directly on water canal shows a general worsening of all the five parameters considered.

Biological growth is quite unchanged, indeed the algae level on considered locations is the same for the major part of the cases in the three Sestieri (Figure 27). Just in few cases, especially in San Marco, a higher algae level is visible. At the same time, San Marco is the most affected also by plaster loss, while in Castello the situation seems quite unchanged and in Dorsoduro some new plaster was added in time, defining an improvement of the parameter itself (Figure 28).

In the major part of the current photos of Castello, Dorsoduro and San Marco efflorescence are less visible but this is strictly related to the damp level of the masonry considered (Figure 29). Indeed if the wall has a high moisture percentage, like when rainfall events occurred, salts deposits are less visible from the photos comparison.

Finally, bricks erosion generally increased over time, especially for Dorsoduro and San Marco (Figure 30). This is probably a consequence of both rising damp phenomenon and unavoidable ageing of the brick itself.

All the evaluated changes regard a period of around 10 years and this research is a way to a non-invasive monitoring of the general conservation state of masonries in Venice through images comparison over time. Naked eye observation should not be underestimated since it allows a first examination of the considered surface, also in any restoration intervention. It is however essential that the observation is conducted by trainee personnel and that the definition and evaluation of semi-quantitative parameters came from expert's elicitation.

Despite a purely visual approach provides information on conservation and degradation phenomena on external masonry parts, it should be integrated with scientific analyses obtaining information on the real situation. Only the combination of both approaches provides a complete knowledge on masonries conservation state. In the present work, the extended visual observation and semi-quantitative identification of effects related to rising damp is additional to the in depth analysis of six Venetian buildings presented in the following section.

3.2 SECTION 2 - Venetian case studies

The real case studies of this research are the six Venetian buildings previously described in section 2.2.1.

In this chapter, the six buildings are individually treated considering wall photos observations in visible light and implemented by the Infrared thermography

Aside from information obtained from non-invasive techniques of documentation, Moisture Content (MC%) results, conductivity values and respective salt content (SS %) also from the point of view of the hygroscopic ones (HMC%), are reported.

The general climatic situation during masonries sampling is then considered. Finally, the characterization of salts and their amount provided by Ion Chromatography and FT-IR Spectroscopy are discussed. Despite Ion Chromatography allows a more specific idea about salt species through their distribution quantification, it has not been yet performed on Badoer Palace and Ca' Tron masonries. This represents a future perspective in this study even if conductivity, SS% and HMC% give a general idea on salt content in these two walls.

3.2.1 Ca' Foscari

The site was inspected on the 18th February 2019 and the main hall of the building chosen as the sampling site. In particular the wall from which samples were taken is the one in front of the door facing the Canal Grande (*Porta da Mar*). The building altimetry on the m.s.l. was obtained from Ramses system by Insula S.p.A. and it corresponds to +130 cm.

Powder samples were taken from the wall by drilling it at different heights and depths (Figure 31).

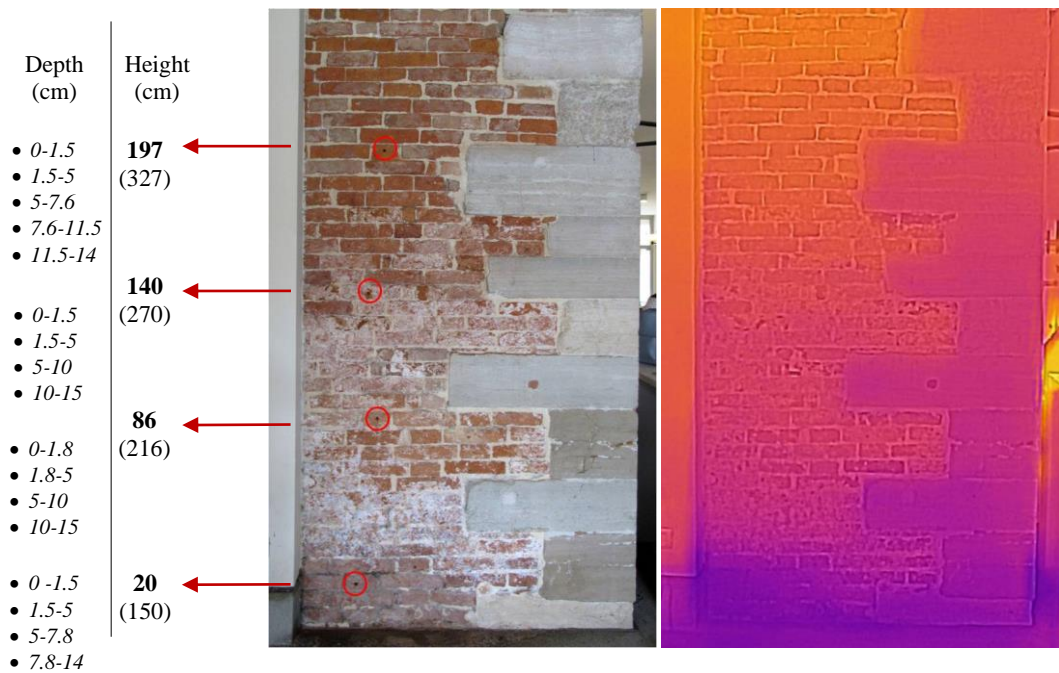


Figure 31 Ca' Foscari wall photos in visible light and by IR thermographic analysis. Heights and depths of the samplings are listed. The heights on the mean sea level (m.s.l.) are reported in brackets. The scale of the colours for the IR thermografy photo is 21.2°C (blue) and 36.4°C (red).

The masonry in visible light appears more saturated in colour in the upper part (above 140 cm in Figure 31) maybe because it is not covered by white efflorescence mainly present at lower zone, especially between 20 and 86 cm. The upper bricks appear slightly different in colour, some have an intense red colour while others are more brownish.

Infrared thermography gives additional information with respect to visible light indeed at wall base a temperature of 21.2 °C is registered (blue parts) which gradually increases with wall height, till reaching the highest temperature (around 36°C) for the red areas. Probably the lower zone (below 20 cm) is most humid and the area above 197 cm is the drier one.

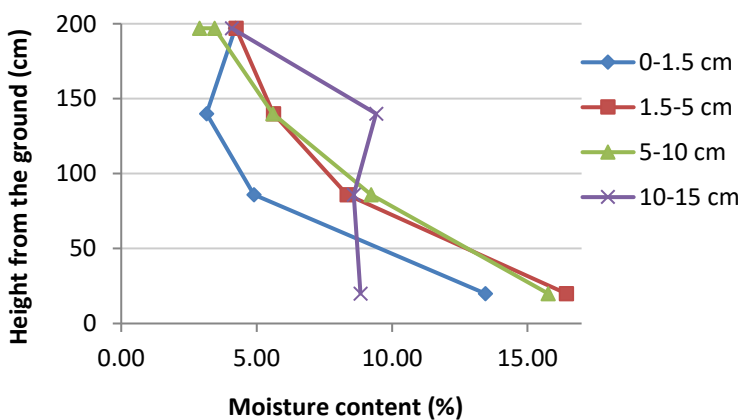
Moisture content, conductivity and soluble salts measurements

The moisture content values (MC%) obtained for the Ca' Foscari wall, through normalized [76] weight method, are listed in Table 17, as like as conductivity and soluble salts ones. As for all masonries, a higher moisture content is expected at lower heights and grater depths (section 1.2.2).

Sampling height from the ground (cm)	Depth (cm)	MC%	Conductivity (μS/cm)	SS%	HMC%
20	0-1.5	13.44	187.93	12.50	10.59
	1.5-5	16.43	113.94	7.69	10.51
	5-7.8	15.76	101.30	6.71	10.18
	7.8-14	8.84	95.13	6.49	7.22
86	0-1.8	4.90	172.99	12.03	18.17
	1.8-5	8.34	197.27	13.16	13.87
	5-10	9.22	131.58	8.90	18.78
	10-15	8.58	111.07	7.61	11.94
140	0-1.5	3.15	890.78	63.57	118.85
	1.5-5	5.62	110.18	7.48	15.51
	5-10	5.60	101.17	6.71	9.31
	10-15	9.41	120.74	8.22	17.28
197	0-1.5	4.21	209.08	14.23	30.47
	1.5-5	4.24	138.84	9.54	17.53
	5-7.6	3.44	172.17	11.67	25.47
	7.6-11.5	2.89	206.07	14.06	39.47
	11.5-14	4.08	235.81	15.57	32.51

Table 57 Moisture content, conductivity and soluble salts values obtained from Ca' Foscari measurements. In addition also hygroscopic moisture content results are listed.

The moisture content trend recorded through Infrared thermography (Figure 31) for the external part of the masonry reflects on average the quantitative MC% data (Table 17). As visible in Figure 32, the humidity trend in the upper area of the wall (197 cm) is clearly lower, around 3-4%.



Moreover the decreasing trend is the same at all depths except for the 10-15 cm one (purple line in Figure 32). In fact at this depth and at 140 cm the MC% is higher than that measured at the lower height of 20 cm.

Figure 32 Moisture content % trend with respect to height and depth of Ca' Foscari wall

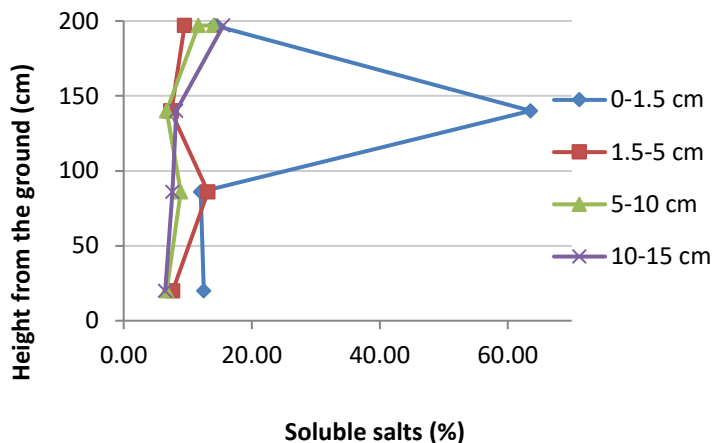


Figure 33 Soluble salt content % trend with respect to height and depth of Ca' Foscari wall.

The soluble salts content trend (Figure 33) decreases at increasing depths and no significant variations with the height are measured (Table 17). The samples taken directly on the wall surface (0-1.5 cm) are the ones interested the most by salt efflorescence, this is the case of the sample at 140 cm height (blue line). A huge amount of salts is registered here (63.57 %) (Table 17).

This sample shows also an HMC value of 118.85 %. During the HMC% measurements, the powder sample, leaved with the other 81 samples in a closed box with a KCl saturated solution, exhibited a water layer above the powder. It has been weighted and placed again inside the box and after one month, salt crystallization occurred (Figure 34).



Figure 34 The formation of the water layer and subsequently of the salt crystals for the sample at 140 cm height and 0-

This occurred just for two samples over the total 82, the one in Figure 34 and the other sample coming from Ca' Bottacin building (next section 3.2.2). Probably this can be due to a wide presence of hygroscopic salts responsible of deliquescence. Despite this, all the Ca' Foscari samples show a HMC% higher than the reference value for the fired- clay bricks which is 0.25 at 75% of relative humidity and between 0.5-0.7 at 96% of relative humidity [71]. In fact among all the samples analyzed for this building the lower HMC% value is 7.22 %. This means that a huge amount of hygroscopic salts is present [71].

Ion chromatography analysis

Considering the results showed in Table 18, it is clear that fluorides and bromides are present in traces in all the samples, never reaching 1 mg/L concentration. Nitrates in general are present at lower amounts but increasingly with the wall height, considered their high solubility. On the contrary, sulphates are slightly present at greater heights.

Height from the ground (cm)	Depth (cm)	Anions and cations concentration (mg/L) for 1mg of powder brick sample								
		[F ⁻]	[Cl ⁻]	[Br ⁻]	[NO ₃ ⁻]	[SO ₄ ²⁻]	[Na ⁺]	[K ⁺]	[Mg ²⁺]	[Ca ²⁺]
20	0-1,5	/	16.77	/	0.11	25.92	11.44	15.20	2.48	82.22
	1,5-5	0.11	17.61	/	0.12	1.61	12.25	21.80	3.08	40.64
	5-7,8	0.12	17.39	0.08	0.17	1.59	11.87	15.50	3.08	54.42
	7,8-14	0.10	10.96	/	0.44	4.65	8.92	15.14	1.78	35.75
86	0-1,8	0.63	31.16	0.35	5.26	2.68	3.11	4.79	0.23	8.05
	1,8-5	0.12	25.45	0.14	2.30	1.07	2.13	4.21	0.19	8.61
	5-10	0.10	19.64	0.11	14.06	0.14	10.48	11.79	0.88	19.40
	10-15	0.15	17.86	0.09	1.99	2.55	5.58	13.85	0.57	29.74
140	0-1,5	/	159.70	/	1.96	3.85	11.15	5.65	/	3.32
	1,5-5	0.10	5.41	0.05	0.35	/	3.23	5.62	/	6.94
	5-10	/	18.31	0.12	1.13	0.29	8.64	15.50	0.90	1.11
	10-15	0.12	27.58	0.12	1.28	0.69	8.56	11.36	/	10.29
197	0-1,5	0.20	131.87	0.30	9.41	0.23	71.77	66.93	4.21	59.11
	1,5-5	0.12	25.33	0.17	5.98	0.19	7.81	32.02	1.17	26.60
	5-7,6	0.11	41.17	0.17	5.90	0.28	19.14	33.79	2.97	36.68
	7,6-11,5	0.11	57.09	0.12	3.26	0.92	31.46	17.35	0.39	14.42
	11,5-14	0.22	52.07	0.13	2.63	0.18	28.40	22.20	0.18	24.61

Table 18 Moisture content, conductivity, soluble salts and hygroscopic values for Ca' Foscarini considered heights and depths.

Chlorides are the most abundant anions with a maximum concentration of 159.70 mg/L at 140 cm height and 0-1.5 cm depth. This is in accordance with the extremely high values previously discussed for conductivity, soluble salts and hygroscopic moisture (Figure 34). Concerning the cations, calcium has the higher concentrations, especially at lower and higher wall heights and they are inversely proportional to the sampling depths. Indeed at increasing depths a lower calcium concentrations are registered but just at the height of 20 and 197 cm. On the contrary, for the two heights in the middle (86 and 140 cm) the greater the depth, the higher the calcium concentration. The greater potassium concentrations are registered at the maximum sampling height of 197 cm as like as for the sodium ones. Although a specific speciation of the ion is extremely difficult in such complex systems, the high relative presence of sodium and sulphates suggests the possible presence of Na₂SO₄ at lower height, a salt that highly damages the masonries.

3.2.2 Ca' Bottacin

The building site inspection was carried out on the 18th February 2019 to have a general overview of the conservation site of masonries and individuate the best sampling point. This is a masonry pillar at ground floor, in a room at low height, which connects the main building entrance to the internal garden. The building altimetry is around +155 cm on m.s.l. at the conventional zero at Punta della Salute, a greater value with respect to Ca' Foscari (+130 cm on m.s.l.). At first sight, the pillar appears as extremely wet. Indeed as visible in Figure 35 bricks have a saturated red colour.

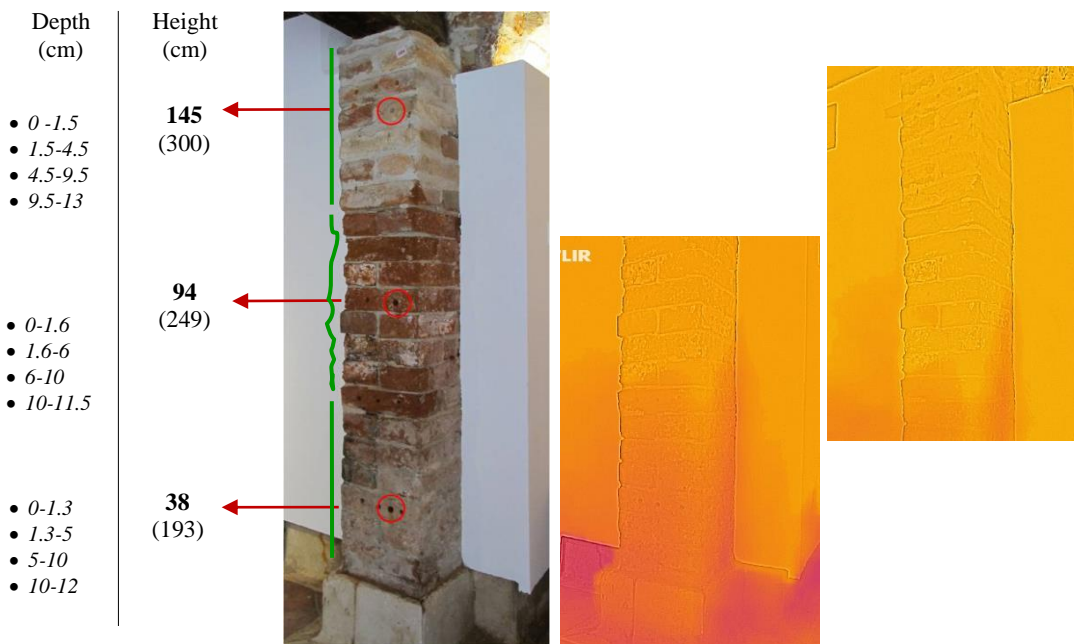


Figure 35 Visible light and infrared photos of the masonry pillar in Ca' Bottacin. Depths and heights of samplings are specified as also the height on m.s.l. in brackets. The green lines show the damaged bricks with an irregular profile in the middle area. The temperature scale of colours for IR thermography photos is between 20.8 °C (purple) and 25.2 °C (yellow)

The presence of salt efflorescence is slightly visible on some bricks at middle height and in the lower ones. Bricks in the middle area clearly appear more damaged with jagged edges due to material losses as consequence of rising damp phenomenon (green profiles in Figure 35). Despite this damaged zone seems humid in visible light, the infrared images registered lower temperature (20.8 °C) below the first sampled height of 38 cm and this probably indicates a lower moisture content. Concerning the upper part of the pillar (right- upper infrared photo) the temperature is around 25°C and this may suggest a lower moisture content.

Moisture content, conductivity and soluble salts measurements

The humidity and salt content in Ca' Bottacin pillar are listed in Table 19. The upper area of the pillar (145 cm) was almost dry considering that MC values were not exceeding the 1.30%. The lower one (38 cm) has the higher moisture percentage around 20% while mean values regard the height of 94 cm.

Sampling height from the ground (cm)	Depth (cm)	MC%	Conductivity ($\mu\text{S}/\text{cm}$)	SS%	HMC%
38	0-1,3	20.85	200.22	14.26	5.48
	1,3-5	24.51	81.32	5.35	7.43
	5-10	22.84	79.75	5.57	6.45
	10-12	22.69	52.22	3.49	4.58
94	0-1,6	9.25	396.14	26.18	79.13
	1,6-6	13.76	193.25	13.16	35.36
	6-10	14.34	223.46	14.96	34.25
	10-11,5	14.38	188.83	12.82	30.01
145	0-1,5	0.71	56.94	3.91	2.03
	1,5-4,5	1.29	64.54	4.45	3.82
	4,5-9,5	0.52	53.80	3.61	1.55
	9,5-13	0.43	52.87	3.61	1.76

Table 19 Moisture content, conductivity, soluble salts and hygroscopic moisture content values. Heights and depths for the Ca' Bottacin pillar are indicated.

As noticeable from visible light photo (Figure 35), the masonry pillar is characterized by salt efflorescence at lower heights and this is proved by greater conductivity values, SS and HMC percentages. These latter are lower at greater heights. Moreover, high presence of salts regards the middle pillar area, for which conductivity values are the highest (around 200 $\mu\text{S}/\text{cm}$) as like HMC % ones. In this masonry part (94 cm height), the more superficial sample at 0-1.6 cm depth has a conductivity of 396.14 $\mu\text{S}/\text{cm}$, almost double in comparison of the others taken at the same height but in depth. This is often observed as results of the typical moisture and salts distribution in masonries (section 1.2.2). Indeed, water strata formed on the powder sample during the HMC% measurements at RH of 85 % (Figure 36).



Figure 36 Formation of the water layer on powder sample 23 (left) and subsequently salts formation (right). The crystal salts are lesser visible with respect to the Ca' Foscari case in Figure 34.

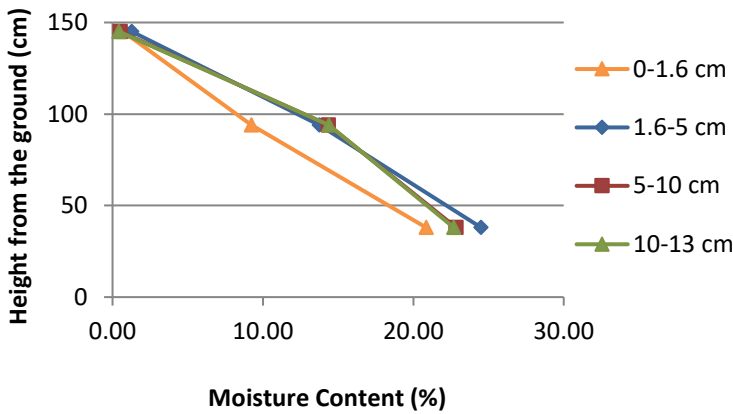


Figure 37 MC % trend with respect to height and depth for Ca' Bottacin wall

The moisture content trend in Figure 37 is the same at all depth, the only exception is the more superficial layer between 0-1.6 cm. Indeed here, a lower percentage of humidity was measured, especially at the height of 94 cm.

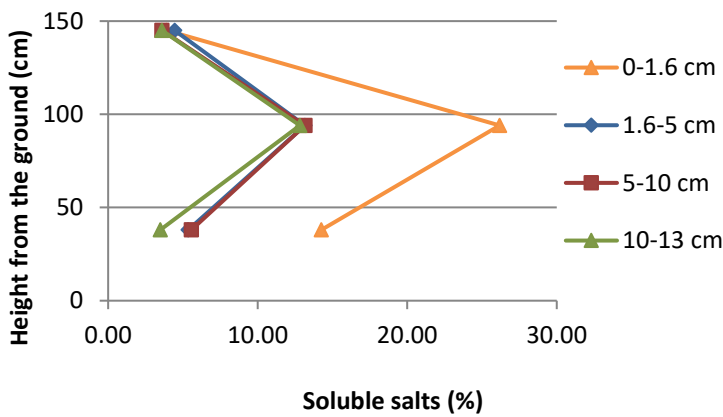


Figure 38 Soluble salts % with respect to samples height and depth for Ca' Bottacin wall.

As like as in Figure 37 for MC, the SS trend (Figure 38) of the samples at 0-1.6 cm depth is different from the other ones. As expected, a greater salt content is measured in the evaporation zone at decreasing MC values.

In addition, a greater SS% values at all depths was registered at the same height which is 94 cm (Figure 38). Moisture and salts distribution in Ca' Bottacin, reflects the empirical model for rising damp in Venice present in literature studies [38] (section 1.2.2) (Figure 39).

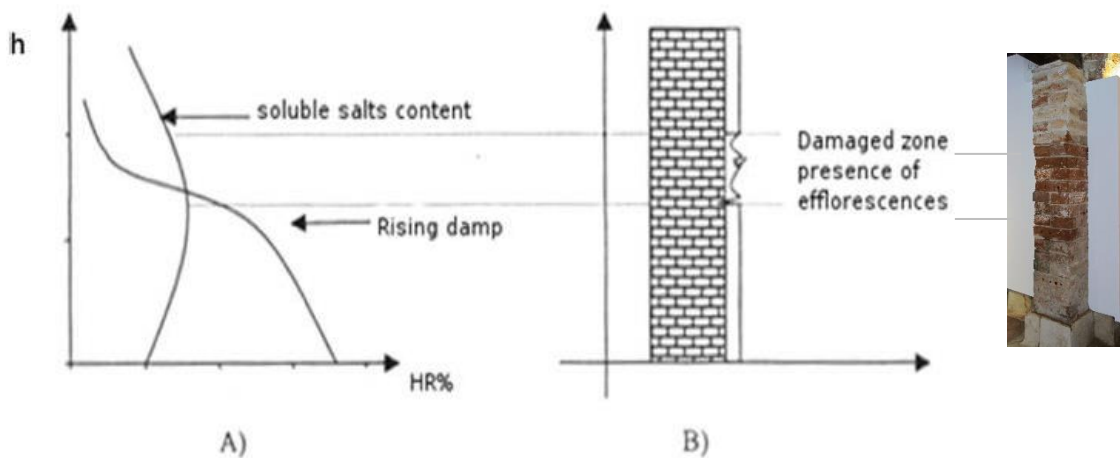


Figure 39 Relationship between Ca' Bottacin pillar and empirical model for rising damp in Venice. The evaporation area corresponds to the maximum salt concentration and so maximum damage on masonry [38]

Considering the moisture and salts distribution as in Figure 38, when the two patterns cross each other, the maximum salts precipitation occurs during evaporation in relation to a moisture decreasing. In Ca' Bottacin case, measured MC and SS data and their distribution curves are particularly in accordance with the empirical models, as shown in Figure 38.

Ion Chromatography analysis

The ion concentration on samples was determined by means of Ion Chromatography, completely for anions and partially for cations (Table 20). As already pointed out for Ca' Foscari (section 3.2.1), fluorides and bromides concentrations are very low as confirm of their presence only as traces.

Height from the ground (cm)	Depth (cm)	Anions and cations concentration (mg/L) for 1mg of powder brick sample								
		[F ⁻]	[Cl ⁻]	[Br ⁻]	[NO ₃ ⁻]	[SO ₄ ²⁻]	[Na ⁺]	[K ⁺]	[Mg ²⁺]	[Ca ²⁺]
38	0-1.3	0.20	6.31	0.07	0.16	0.18	4.10	10.15	0.28	55.05
	1.3-5	0.19	8.39	0.08	0.03	1.50	5.39	7.36	/	12.75
	5-10	0.21	8.62	0.08	0.04	1.36	8.22	12.43	/	13.01
	10-12	0.20	5.11	0.06	0.08	0.88				
94	0-1.6	0.48	218.32	0.35	4.92	4.23				
	1.6-6	0.22	55.82	0.19	1.41	0.79	32.61	11.57	1.13	16.99
	6-10	0.30	52.07	0.20	1.24	3.56	31.55	11.35	1.31	15.55
	10-11.5	0.20	20.46	0.18	0.71	0.44				
145	0-1.5	0.22	2.61	0	0.99	0.12				
	1.5-4.5	0.22	4.29	0.15	2.89	0.11				
	4.5-9.5	0.21	1.96	0	0.81	0.41				
	9.5-13	0.22	2.27	0	0.93	0.05				

Table 20 Ion concentrations for the samples analyzed from Ca' Bottacin wall. Some data are missing for cation determination.

The greater chloride concentrations characterize the sampling points at 94 cm and their values decrease at decreasing depth. The quantitative result for chlorides at 94 cm and 0-1.6 cm depth (218.32 mg/L) is four times higher than the two successive depths (around 50 mg/L), in accordance with the extremely high SS% and HMC% values previously discussed. Nitrates and sulphates concentrations are low in general even if for these latter, values around 3-4 mg/L are found at 94 cm height.

Among available data for cations, potassium concentrations are higher with respect to the sodium ones at 38 cm while at 94 cm it is the inverse. The highest sodium concentration should be expected for the sample with 218.32 mg/L of chlorides, since the sea water is widely rich in NaCl. A wide quantity of calcium is measured at lowest height and depth.

3.2.3 Ex Slaughterhouse San Giobbe

The buildings complex was inspected on the 18th February 2019, as like as Ca' Foscari and Ca' Bottacin. This allowed to identify the better sampling site from which the brick powders were taken at different height and depth on the 13th of June 2019. The building altimetry is around +125 cm on m.s.l. with respect to the conventional zero at Punta della Salute. In particular, the considered external masonry faces the lagoon and it is partially covered by white plaster whose manufacturing process resembles fake ashlar (Figure 40).



Figure 40 Ex Slaughterhouse San Giobbe masonry in visible and infrared light. The infrared colour scale covers the temperature range between 20-25 °C. Infrared image is shifted with respect to the other one in order to facilitate the comparison by aligning the respective masonry morphological details.

The observation in visible light does not allow to differentiate masonry areas according various humidity levels. As a matter of fact bricks uncovered by plaster show two different colours: a lower saturated red area and an upper yellow one. This is attributable to the technique of “scuci-cuci”, widely diffused in Venice, aiming at replace the damaged bricks with new ones. Indeed yellow bricks present a greater erosion degree while the surface of red ones (probably the newest ones) is better preserved despite showing salt efflorescence. Moreover in the middle right area, behind the red gate, a further third type of brick is present, perhaps the most recent one with an intermediate colour between yellow and red.

The infrared thermography gives additional information on colder areas (20°C) usually more humid and mainly found in the lower left masonry zone. The bluish colder spots corresponds to the lighter spots on plaster and brick areas recognizable in visible light photo, these spots showed the presence of efflorescences and probably are colder due to hygroscopic moisture retention. Further colder spots are found at upper height till the middle of the red bricks band. Above this threshold the masonry heats up till maximum temperature of 25°C.

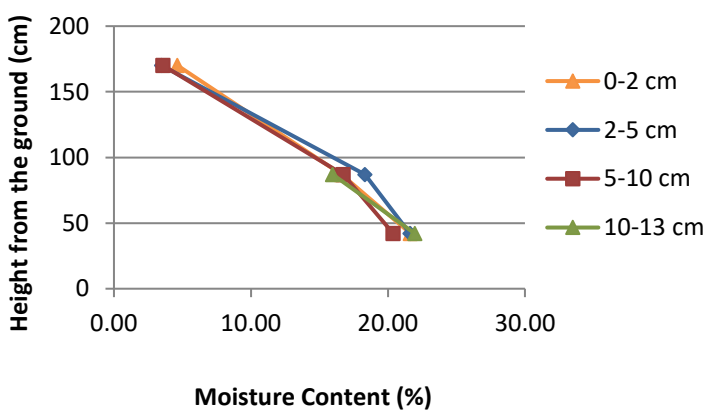
Moisture content, conductivity and soluble salts measurements

The humidity of Ex slaughterhouse San Giobbe considered masonry decreases with increasing sampling height (Table 21).

Height from the ground (cm)	Depth (cm)	MC %	Conductivity (μS/cm)	SS %	HMC %
42	0-2	21.65	110.84	7.57	10.16
	2-5	21.61	87.78	5.88	7.53
	5-10	20.39	90.56	6.22	6.88
	10-13	21.97	69.22	4.58	3.53
87	0-2	16.63	99.11	6.63	4.22
	2-6	18.33	74.79	4.97	4.88
	6-10	16.73	70.62	4.86	4.42
	10-13	15.97	69.44	4.75	3.47
170	0-3	4.64	120.11	8.17	12.72
	3-5	3.48	96.06	6.53	8.74
	5-10.2	3.58	101.77	6.93	9.75
	10.2-11	4.26	104.26	7.25	10.26

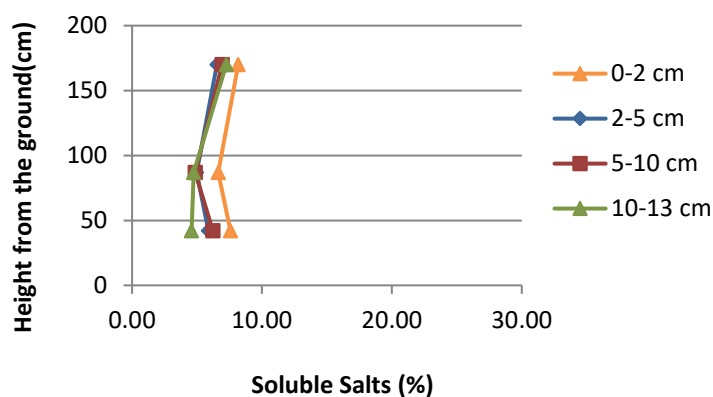
Table 21 Moisture content, conductivity, soluble salts and hygroscopic moisture values obtained for the Ex Slaughterhouse San Giobbe masonry.

On the contrary, no wide differences are measured for conductivity, SS% and HMC% considering the different heights of the wall. Hygroscopic salts (10.16 %) are found at the lower and external masonry area and similar values characterizes the maximum sampling height of 170 cm, especially on the surface and at maximum depth (10.2-11 cm). The HMC percentage values, if compared with those of Ca' Foscari and Ca' Bottacin previously discussed, are really lower.



MC% trend for San Giobbe is homogeneous at all masonry depths. Values around 20-22% characterize the lower part of the wall (42 cm height); 16-18 % range was found at middle height (87cm) and 3-4% corresponds to the highest wall area (Figure 41)

Figure 41 MC% trend according to height and depth of the Ex Slaughterhouse San Giobbe.



The graphical homogeneity for MC% at all depths is found also for SS% (Figure 42). The only exception is the external wall surface (0-2 cm depth) for which the highest salt content is measured (8.17%). On the contrary, the lower SS% is around 5% at 87 cm height.

Figure 42 Soluble salts trend according height and depth for the Ex Slaughterhouse San Giobbe masonry.

Ion Chromatography analysis

The Ex Slaughterhouse San Giobbe masonry, according Ion Chromatography analysis, shows fluorides and bromides presence in traces (Table 22). Low nitrates concentration is measured, slightly higher at 170 cm on the wall. Sulphates are present in a greater amount with respect to the values previously discussed for Ca' Foscari and Ca' Bottacin (section 3.2.1 and 3.2.2).

Height from the ground (cm)	Depth (cm)	Anions and cations concentration (mg/L) for 1mg of powder brick sample								
		[F ⁻]	[Cl ⁻]	[Br ⁻]	[NO ₃ ⁻]	[SO ₄ ²⁻]	[Na ⁺]	[K ⁺]	[Mg ²⁺]	[Ca ²⁺]
42	0-2	1.30	11.72	0	1.75	6.80	10.62	24.86	1.17	182.25
	2-5	0.21	8.45	0	0.19	6.07				
	5-10	1.12	7.48	0	1.97	1.84	8.53	21.81	0	172.35
	10-13	0.22	5.19	0.07	0.02	1.57				
87	0-2	0.20	6.18	0.07	0.16	12.65				
	2-6	0.22	6.85	0.07	0.15	3.58				
	6-10	0.21	6.02	0.08	0.06	1.72				
	10-13	0.20	6.18	0	0.05	2.55	4.25	11.46	0.04	38.59
170	0-3	0.13	23.44	0.09	2.07	5.19	8.92	29.53	0.68	33.64
	3-5	0.19	12.72	0.10	1.81	1.06				
	5-10.2	0.19	15.52	0.09	2.32	0.84	6.93	26.53	0.35	24.15
	10.2-11	0.21	10.45	0.09	1.62	10.44	5.40	22.70	0.79	49.73

Table 22 Ion concentrations for the analyzed samples in San Giobbe site. The available data for cations analysis are reported.

The available concentration data for the cations underline an extremely high calcium concentration in comparison with those found in Ca' Foscari (maximum of 82.22 mg/L) and Ca' Bottacin masonries (maximum of 55.05 mg/L). The higher presence of sulphates and calcium may be linked to the presence of gypsum in plaster which previously covered the bricks as visible in Figure 40. However this hypothesis is not sufficient in justifying a so high calcium concentration (maximum of 182.25 mg/L) which is probably related to a high carbonates presence (see section 3.3.4 for FTIR results). Despite this, additional investigation on anions are required in order to have a more precise interpretation.

3.2.4 Badoer Palace

The building inspection was conducted during the month of May, specifically on the 20th and samples taken on the 18th June 2019. Together with masonry considered for Ex Slaughterhouse San Giobbe, these two are the only cases in which an external masonry has been chosen for the samplings even if they show different exposition to environmental factors (Figure 43).



Badoer Palace wall is located in *Sotoportego de la Laca* and so quite protected from rainfall and wind, the same cannot be said for San Giobbe masonry without any protection and so directly exposed to weathering. The Badoer Palace sampling site has an altimetry of +102 cm on m.s.l. with respect to Punta della Salute.

Figure 43 Sotoportego de la Laca with the sampled masonry on the left. The wall is protected by the upper structure. Image taken from Stretview by Google.

The masonry considered shows bricks quite damaged, in an advanced decay state with eroded surfaces and material losses (Figure 44).

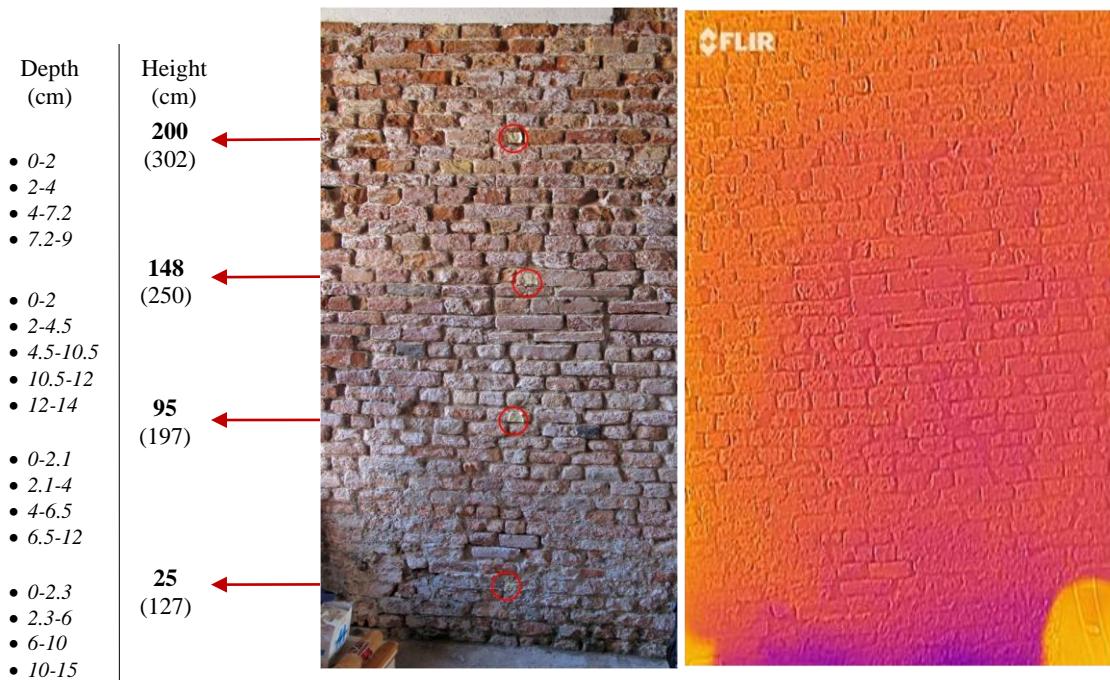


Figure 44 The external masonry of Badoer Palace in visible light with the chosen sampling points. Height and depth of the samplings are specified, as like as their height on the m.s.l. in brackets. The colour scale for the infrared photo is comprised between 19.4-22.9 °C

The whole masonry is covered by salt efflorescence, in particular the area below 95 cm of height. Bricks have different colours, more red near 200 cm and yellow throughout the masonry. The former appears less damaged than the latter and in general quite all bricks have an irregular shape perhaps due to their erosion. The wall, being covered by the portico is not subject to direct rain and consequently to washout of salts. Among the bricks two are almost black and this probably depends on the extremely high firing temperature during their manufacturing process which give them a brittle nature [84]. The lowest masonry band is characterized by biological growth favoured by humidity presence, also confirmed by the blue area in infrared photo (19.4° C). The masonry temperature gradually increases with the height, especially in the left part. This latter, even if not directly hit by the sun-light since it is a covered wall, it is probably slightly more exposed to the weak amount of light which enters from the left into the portico. This perhaps is the reason of the higher temperature of this wall area which may have a lower humidity content.

Moisture content, conductivity and soluble salts measurements

Moisture content values and the hygroscopic moisture ones are high, apart from the greater height considered (Table 23).

Height from the ground (cm)	Depth (cm)	MC%	Conductivity (µS/cm)	SS%	HMC%
25	0-2.3	21.42	194.91	13.10	15.17
	2.3-6	27.44	124.42	8.25	12.32
	6-10	28.80	101.86	6.91	8.63
	10-15	26.93	83.27	5.58	5.58
95	0-2.1	15.64	216.00	14.46	20.40
	2.1-4	20.12	213.15	14.33	28.06
	4-6.5	18.02	167.82	11.24	20.66
148	0-2	22.75	320.90	21.75	46.57
	2-4.5	19.87	237.27	15.74	38.96
	4.5-10,5	18.03	253.07	17.05	37.93
	10.5-12	14.72	202.25	13.93	26.42
	12-14	13.58	201.01	13.30	24.87
200	0-2	1.85	90.37	6.18	16.62
	2-4	1.53	72.14	4.78	5.15
	4-7.2	1.32	71.31	4.86	5.60
	7.2-9	1.01	69.36	4.72	4.13

Table 23 Measured values for moisture and soluble salt content, conductivity and hygroscopic moisture content. At the height of 95 cm and 6.5-12 cm depth mortar was found during sampling activity. For this reason the related values are not reported.

According conductivity and SS% measurements, the salts are concentrated mainly at 148 cm height and show an hygroscopic nature since this values at this height are the greater ones.

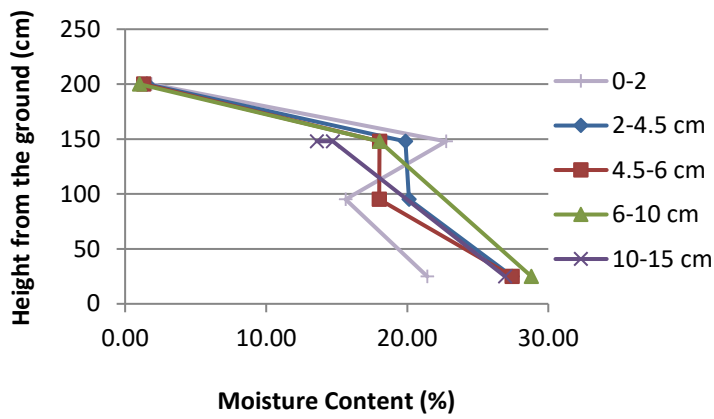


Figure 44 Moisture Content % at each height and depth for Badoer Palace masonry.

The wall is more humid at lower height, while the external surface (0-2 cm depth) is drier than the inner one. The 0-2 cm depth has the most irregular path since at 148 cm height the MC (22.75 %) is higher than that at 20cm (21.42%). The highest MC registered is 28.80 % at 25 cm height and 6-10 cm depth (Figure 44).

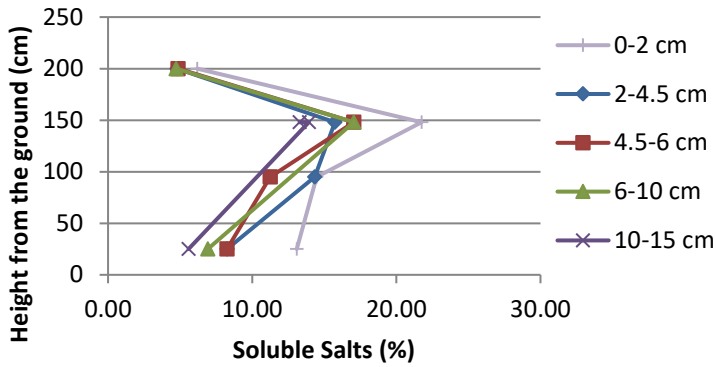


Figure 45 Soluble salt distribution for each sampling depth and depth at Badoer Palace.

The highest SS content is found at the height of 148 cm at all depths. The more superficial zone of the wall (0-2 cm depth) has the highest SS value of 21.75 %. This is in accordance with the empirical models of rising damp phenomenon (Figure 45).

The measured trends for MC and SS, especially for the external part, are probably influenced by the particular location of the masonry since it is under a portico and so not exposed to rainfall but partially to environmental parameters action.

3.2.5 Ca' Tron

Ca' Tron building was investigated on the 20th of May and the masonry successively sampled on the 18th of June 2019. The internal wall considered is located on the right with respect to the door facing the canal (*Porta da Mar*). The altimetry of the building, near the sampled masonry, is about +104 cm on m.s.l. if compared to the reference value at Punta della Salute.

Ca' Tron masonry was sampled at three heights and different depths (Figure 46) .

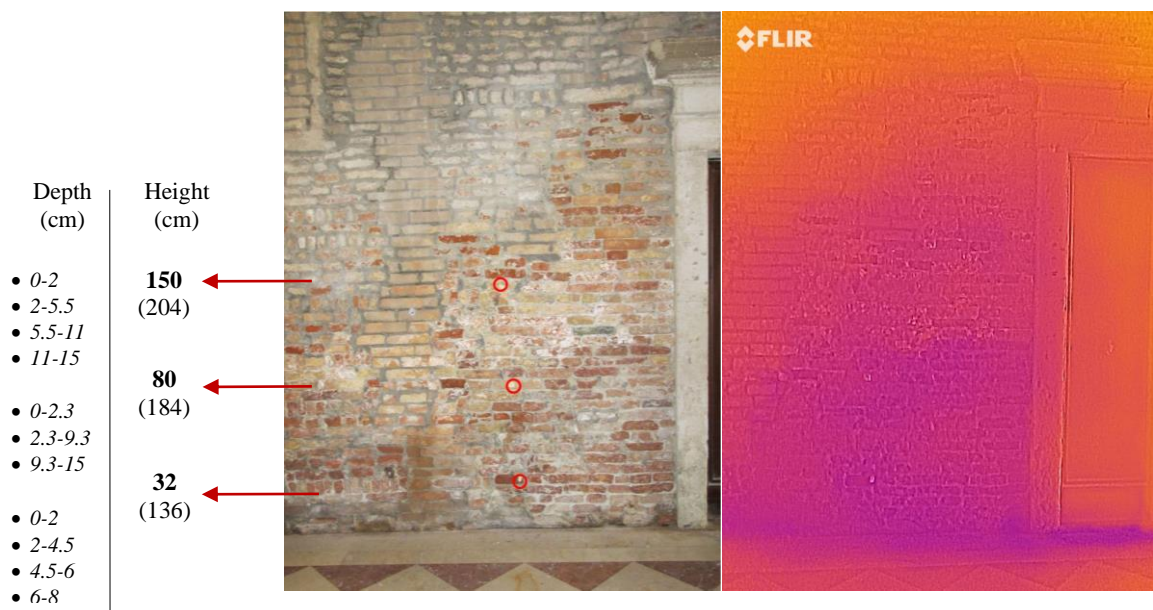


Figure 46 Ca' Tron masonry in visible light and in infrared thermography. The sampling points, with related height and depth are indicated. The infrared photo covers the degree range between 20.6 and 23.4. Heights on m.s.l. are reported in brackets.

The masonry appears clearly humid till above 150 cm, in particular on the right, where the moisture level seems to reach the door height. Some bricks, probably damaged, may have been replaced through “scucucuci” intervention since a wide variety of bricks, different also in colour, constitutes the wall. A saturated red spots appear due probably by the humidity, since bricks of this colour are noticed just in correspondence of the damp area. White encrustations (probably efflorescence or plaster/mortar residuals) are visible between 80 and 150 cm where a slightly higher humidity is confirmed by the Infrared thermography photo. The lower temperature (20.6 °C) particularly regards the base of the wall till the middle of the door. The masonry gradually heats up till reaching the greater temperature (23.4 °C) on the upper area, especially in the upper left corner. Concerning the conservation state of bricks, these appeared almost fragile during sampling activity since they tended to lose material in the form of powder if touched. This may be a consequence of rising damp or other degradation phenomena, like freeze-thaw cycles, which if summed up with the unavoidable aging of ceramic materials lead to damages especially on oldest bricks.

Moisture content, conductivity and soluble salts measurements

As already stated through observations in visible and infrared light, the masonry is most humid at lower height (Table 24). Despite this, high MC% values were expected also at 80 and 150 cm, since also this area appeared saturated in Figure 46.

Height from the ground (cm)	Depth (cm)	MC%	Conductivity (µS/cm)	SS%	HMC%
32	0-2	15.43	180.19	11.99	25.24
	2-4,5	19.15	232.92	15.99	33.70
	4,5-6	14.23	205.18	13.75	21.37
	6-8	17.37	207.51	14.26	18.43
80	0-2,3	6.54	103.17	6.85	11.13
	2,3-9,3	6.05	72.64	5.02	5.32
	2,3-9,3	5.70	88.12	5.93	6.44
	9,3-15	10.14	71.17	4.92	2.09
150	0-2	1.01	71.09	4.80	2.61
	2-5,5	1.17	76.03	5.22	5.76
	5,5-11	0.74	55.94	3.84	2.41
	11-15	0.66	52.64	3.59	2.36

Table 24 Moisture content, conductivity , soluble salts and hygroscopic moisture content values . Depth and height of Ca' Tron samples are specified.

Likewise, the highest conductivity and soluble salt values are always found at lowest height that is 32 cm. Moreover salts at this height are found to be highly hygroscopic, considering the high HMC% measured values. Hygroscopic salts, depending on the species, tend to absorb and retain a variable amount of humidity. This, and the several “scuci-cuci” intervention, justify that the highest values, both of MC% and HMC%, measured at the height of 32 cm.

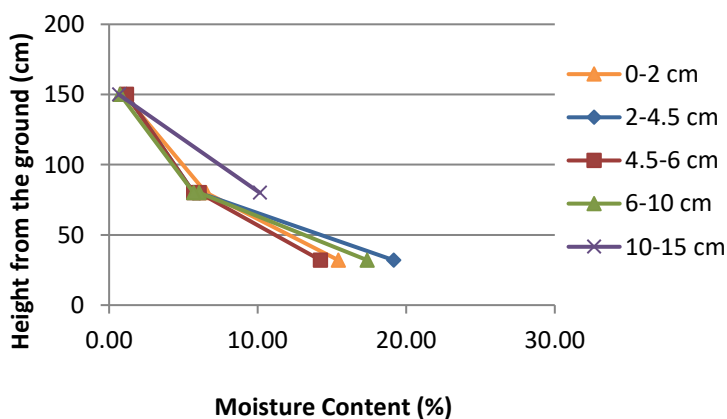


Figure 47 MC % distribution according height and depth in the Ca' Tron wall.

The MC trend (Figure 47) is homogeneous at all heights, the exception is the last depth (10-15 cm) which at a 80 cm height seems to have a higher moisture content. It has been not possible to have data for the same depth at the lower point of 32 cm height due to mortar presence.

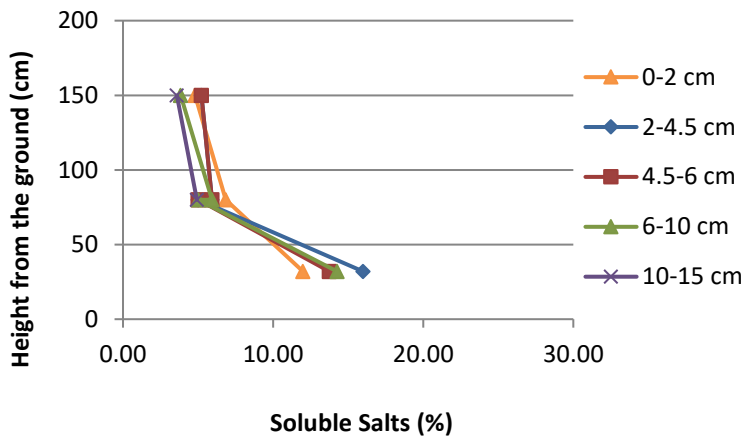


Figure 48 SS content distribution according heights and depths of Ca' Tron wall.

As like as the MC distribution in Figure 34, the SS content is homogeneous at all depths. Comparing Figure 34 and 35 the MC and SS trend are the same, this is different from the results of the other buildings for which the respective trend were opposed each other (Figure 48).

3.2.6 Malipiero Palace

The last investigated building among the total six is Malipiero Palace whose site was inspected on 23th May 2019 and its masonry subsequently sampled on the 20th June 2019. This building has an altimetry of + 90 cm on m.s.l. with respect Punta della Salute and it represents the lowest sampling site considered in this research. In particular, Malipiero Palace masonry is located near the door facing the Canal Grande (*Porta da Mar*), specifically on its left. For this reason and for the low altimetry of the building (+ 90 cm) its masonry is easily flooded during high water events (Figure 49).

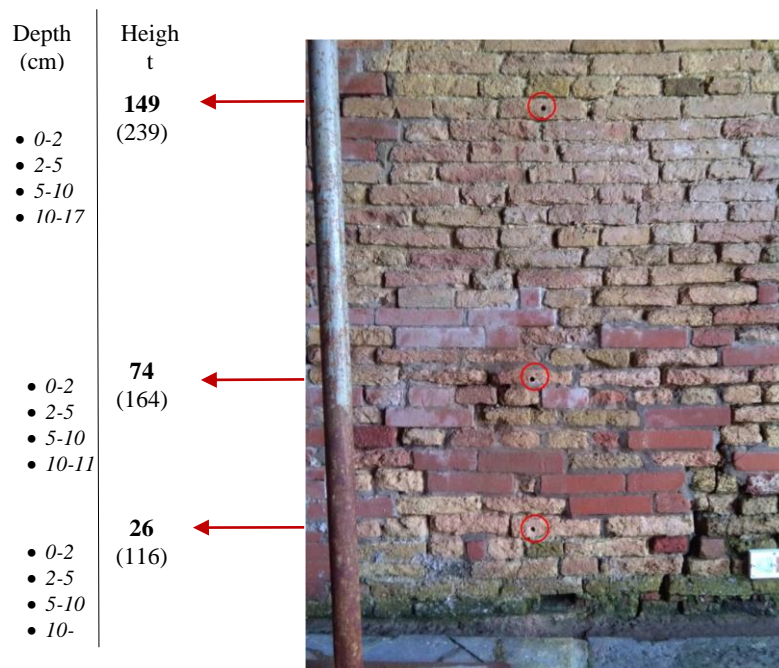


Figure 49 Malipiero Palace masonry in visible light. Height and depth of samplings point are specified, as like as their height on m.s.l. in brackets.

As visible in Figure 49, several damaged bricks were replaced with new ones according the “scuci-cuci” technique, in order to assure the structural stability of masonry. The different kind of bricks are clearly recognizable from shape and colour, in fact the new ones appear saturated red and with more intact and regular edges. On the contrary, the older and yellow ones are highly damaged, characterized by an high erosion degree both at edges and on surfaces. This could be firstly linked to different raw materials in manufacturing process and maybe secondly to its firing temperature, indeed yellow bricks are under burnt and so they possess low strength [84]. The wall appears wet at lower heights and covered by a biological patina, especially for base bricks. The red bricks are covered by white salt efflorescence, mostly visible in the middle left masonry area. The bedding mortar is missing in some areas: near the sampling point at 74 cm height and in the right part, especially at low heights.

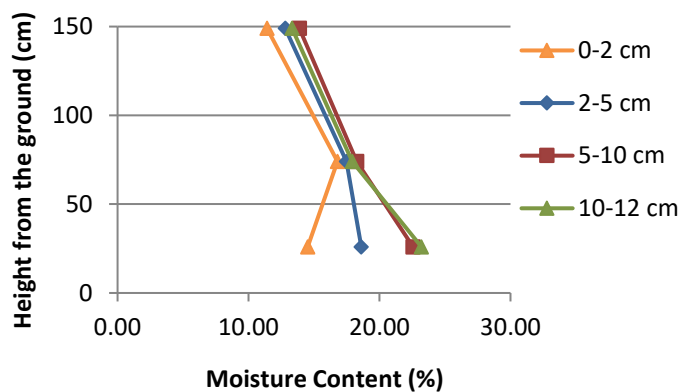
Moisture content, conductivity and soluble salts measurements

Moisture content values are in general quite constant and similar among the three height analyzed (Table 25).

Height from the ground (cm)	Depth (cm)	MC%	Conductivity ($\mu\text{S}/\text{cm}$)	SS%	HMC%
26	0-2	14.51	211.17	14.51	14.99
	2-5	18.61	129.35	8.61	13.12
	5-10	22.56	105.46	7.18	20.51
	10-12	23.20	101.42	6.85	9.26
74	0-2	16.79	213.17	14.29	20.49
	2-5	17.48	193.39	12.91	20.56
	5-10	18.25	160.70	10.90	16.49
	10-11	17.91	118.96	7.94	13.29
149	0-2	11.41	163.92	11.24	22.48
	2-5	12.80	164.71	11.20	26.16
	5-10	13.88	202.02	14.15	31.48
	10-17	13.32	176.56	11.73	24.37

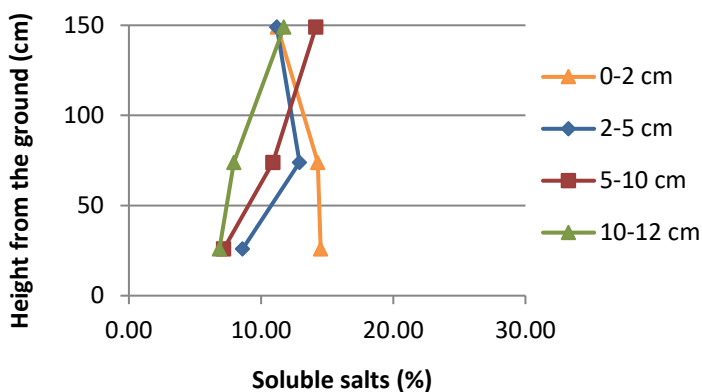
Table 25 Moisture Content, Hygroscopic Moisture, conductivity and Soluble Salts data with the corresponding heights and depths.

The measured MC values do not decrease significantly with height, in the same way as SS and HMC ones. The conductivity and soluble salts values decrease at increasing depths with the only exception of the height at 149 cm for which they are more or less similar and constant at all depths. Different HMC% and SS% are found for the same conductivity levels. This means that a greater content of hygroscopic salts is present in these samples.



Despite not so high MC% differences were measured, the highest values are those of the middle zone (74 cm) and the lower one (26 cm). Here MC values increase at increasing depths. At the 149 cm MC is around 11-13%, the lowest registered percentages (Figure 50).

Figure 50 Moisture content distribution according heights and depths considered for the Malipiero Palace masonry.



The wall salt content is higher at 149 cm height (11-14%), especially at 5-10 cm depth. At the lower height of 26 cm and 0-2 cm depth has a higher salt content than the other considered depths (Figure 51).

Figure 51 Soluble salts content with respect heights and depths considered for Malipero Palace masonry

Ion Chromatography analysis

As like as stated for the other considered five buildings, fluorides and bromides are found in traces.

Considering the available data on ion concentrations, chlorides are mainly present at 149 cm masonry height (Table 26).

Height from the ground (cm)	Depth (cm)	Anions and cations concentration (mg/L) for 1mg of sample								
		[F ⁻]	[Cl ⁻]	[Br ⁻]	[NO ₃ ⁻]	[SO ₄ ²⁻]	[Na ⁺]	[K ⁺]	[Mg ²⁺]	[Ca ²⁺]
26	0-2	0.21	20.16	0	0.06	47.34	16.50	8.91	1.55	102.25
	2-5	0.12	10.36	0.07	0.19	8.38				
	5-10	0.12	14.62	0	1.01	4.09	12.45	11.60	0.37	20.45
	10-12									
74	0-2	0.10	26.91	0.13	4.85	31.88				
	2-5	0.13	25.42	0.10	0.33	16.32				
	5-10	0.14	23.51	0.09	0.32	5.46				
	10-11									
149	0-2	0	35.64	0	0.17	1.49	22.09	15.50	1.59	38.79
	2-5									
	5-10	0	50.12	0.25	0.48	0.86	30.25	20.88	1.46	23.71
	10-17									

Table 26 Ion concentrations for the analyzed Malipero Palace samples.

Nitrates content is very low, the same cannot be said for sulphates which at low heights show quite high concentrations which almost disappear at higher ones. Magnesium has lower concentrations while those of potassium exceed 8 mg/L among the available data and are greater at higher heights.

Calcium is widely present at lower height and the maximum concentration found is 102.25 mg/L for the more superficial area at 26 cm height. At the same way at 149 cm its concentration tends to decrease at increasing depth. A high amount of sulphates is generally found and it decreases at increasing heights. This suggests the possible presence of Na₂SO₄ salt, considering also the consistent sodium concentrations.

3.3 Six buildings results comparison

3.3.1 Weather and tidal situation during samplings

The awareness of the environmental parameters values previously and at the moment of the building samplings is fundamental considering that external temperature, humidity, amount of precipitations and direct contact with water due to high tides' floodings influence the moisture content and the masonries appearance. Information on environmental parameters before and during samplings are useful for future studies too. In this way a comparison between past and new data can be pointed out also considering the future changes on temperature, relative humidity, rainfall and high tides occurrence.

The six buildings were sampled between the 11th and the 20th of June 2019, a period of time with less rainfall if compared with the previous month of May, according data recorded at Cavalli Palace control station [20] (Figure 52). Indeed two main rainfall peaks, around 17-20th and 26-29th May were registered.

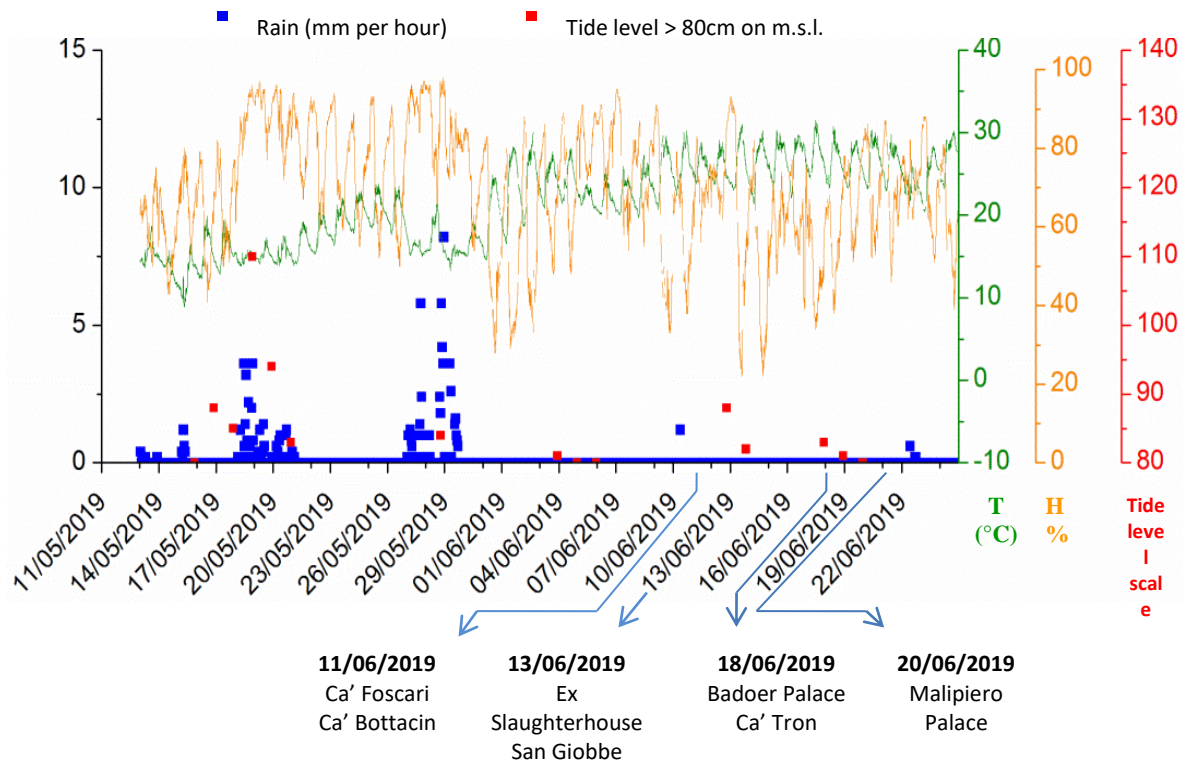


Figure 52 Weather and tidal information obtained from the Control Station at Cavalli Palace between 11th May and 22th June 2019 [20]. Temperature (T, °C), humidity (H%), rain and tide level with its scale are reported. The sampling date for the six analyzed buildings are specified.

Tidal events < 100 cm on m.s.l. (except +110 cm on the 19th of May) occurred before and during the sampling period. The six considered buildings have different altimetries on m.s.l., so only Badoer Palace, Ca' Tron and Malipiero Palace were flooded with a +110 cm tide, indeed they have an altimetry of + 104 cm, +102 cm and 90 cm respectively. On the contrary Ca' Foscari, Ca' Bottacin and Ex Slaughterhouse San Giobbe with greater ones (+130 cm, +155 cm and +125 cm), have not been in direct contact with sea water during high water events for the considered period of time.

As visible in Figure 52 the air humidity was higher (exceeding 90%) till the end of May while it was in general lower, with the exception of the 13th of June which is the day of Ex Slaughterhouse San Giobbe sampling. In addition an increase of the temperature is visible at the beginning of June. The brick material itself absorbs a variable amount of humidity from the air depending on environmental relative humidity and temperature but also to its, porosity, chemical composition and firing temperature [85]. According literatures data, the equilibrium moisture content of bricks fired at 850°C is between 25-52 kg/m³ while for those fired at 1050 °C a lower absorption of 1.3-6.5 kg/m³ was measured. Despite this wide variability of hygrometric properties of bricks, it is sure that the ceramic materials itself absorbs humidity alone and this values than increases due to hygroscopic salts in solution [85].

All the environmental parameters here discussed could contribute to increase or decrease the masonry moisture content and its evaporation rate influencing also the salts presence. These values are related to seasonal variation since a sampling in autumn would correspond to a greater moisture content if compared with summer season for which rainfall occurrence and temperature changes are generally lower.

3.3.2 Moisture and salts distribution comparison among the six case studies

The six Venetian buildings have different ranges of moisture and soluble salts content since their altimetry, sea water exposure and sampling heights differ for each single case. Despite this, two masonries over the six considered are in complete accordance with the empirical model of rising damp for Venetian masonries with MC gradually decreasing with height . This is the case of Ca' Bottacin and Badoer Palace whose maximum salts content is for both registered at + 250 cm on mean sea level. In particular, Badoer Palace generally shows the highest conductivity values among all the case studies.

Ex Slaughterhouse San Giobbe is the unique external masonry considered in this research and this could be the reason of the different soluble salts trend with the lowest amount at middle height. Indeed, this deviation from the empirical model could be due to the washout action of rain determining a general decrease in salts content since rainfall was registered two days before San Giobbe sampling as visible in Figure 52.

Malipero Palace (with the lowest +90 cm altimetry) has a SS% and humidity trend quite constant if compared with the other five buildings for which the MC% at low heights differs most from those at greater ones. This constant trend determines a difference with respect to the empirical MC curve resulting rather in a vertical line.

Partial deviation with respect to empirical model are found also for Ca' Foscari moisture content and Ca' Tron for which both MC and SS at middle heights have an inverse trend with respect to the theoretical one.

Figure 53 shows the different MC values measured for the six buildings with respect to their sampling depths and height on mean sea level.

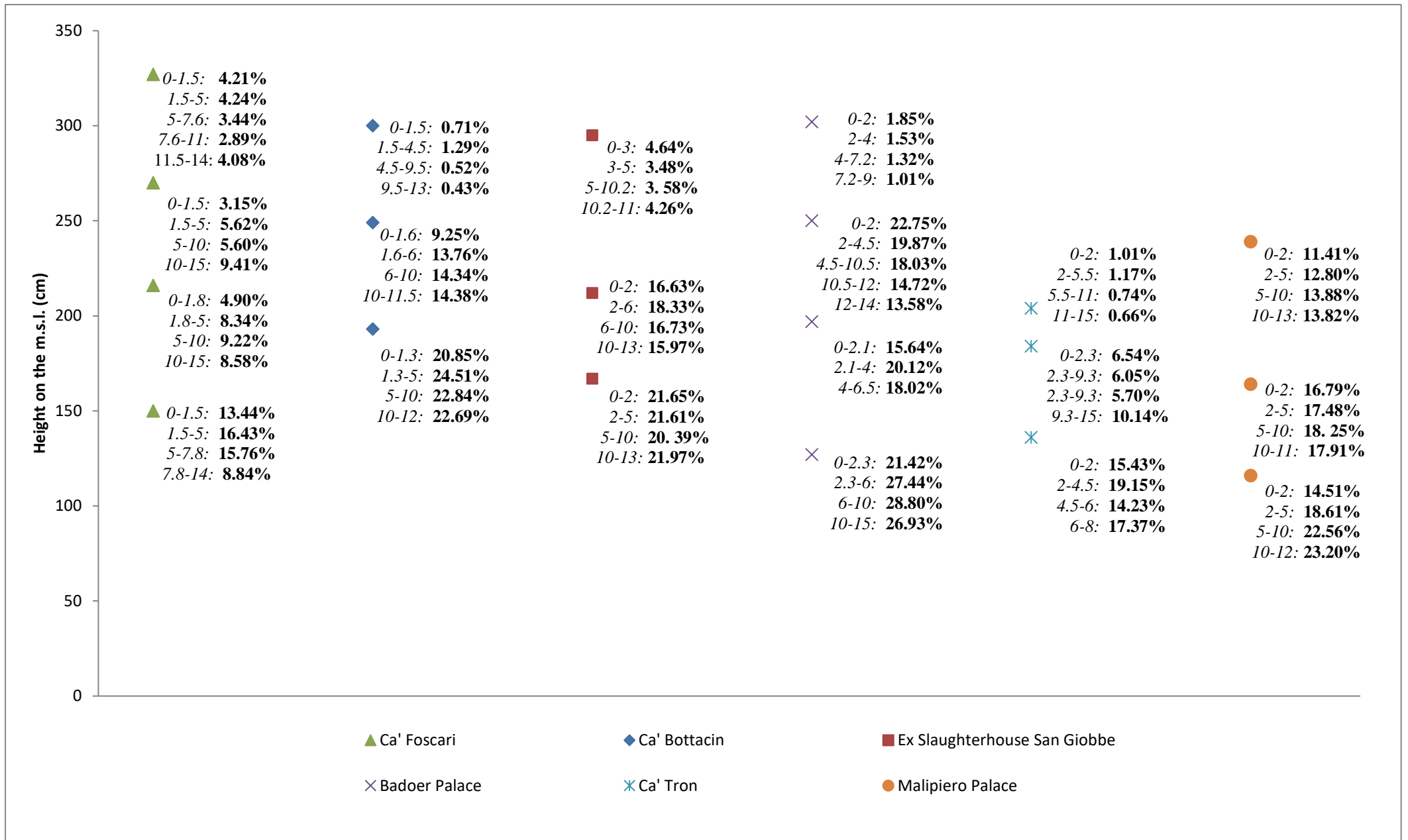


Figure 53 Comparison of Moisture Content percentage values for the six buildings, considering their height on m.s.l. and the respective samplings depths (all values are intended in cm).

3.3.3 Anions distribution trend in Ca' Foscari, Ca' Bottacin and Ex Slaughtethouse San Giobbe

In this chapter only three buildings are considered since a complete information about their anions concentration is available. These are Ca' Foscari, Ca' Bottacin and Ex Slaughterhouse San Giobbe which have different heights on m.s.l., +130 cm, +155 cm and +125 cm respectively. These heights and the anions concentration at each sampling depth are graphically plotted for the main anionic species chlorides, nitrates and sulphates (Table 27). These are the anions mostly present in soluble efflorescence and responsible of deterioration linked to the crystallization pressure of their salts like NaCl, KCl, Na₂SO₄, Ca(NO₃)₂ [86]. Ca' Bottacin presents the highest chlorides content at each depth and at middle height of 250 cm on m.s.l (Table 27). The only exception is the last depth (10-15 cm) for which Ca' Foscari chloride concentration exceeds that of Ca' Bottacin, reaching the maximum value at 327 cm height. In general, San Giobbe shows the lowest chlorides content at all depths but at the same time it has the highest content in sulphates. The low presence of chlorides on Ex Slaughterhouse San Giobbe walls can be related to the rainfall and salt washout since this is an external exposed site while the other two building masonries are internal. At the same time the highest sulphates concentration with the lowest one in chlorides for San Giobbe site, may be an indication of the absence of efflorescence (NaCl based) and a presence of subflorescence. The presence of sulphates may be also related to the presence of plaster on the sampled masonry.

Ca' Foscari has the highest nitrates concentration especially at 216 cm height and 5-10 cm depth. These are highly soluble salts and so their presence is expected at greater heights.

Although Ca' Bottacin has the highest altimetry (+155 cm on m.s.l.), and so is flooded only with exceptional high water, it has the maximum concentrations of chlorides. This latter, and those of nitrates and sulphates are stated at the same height of 250 cm, corresponding to the middle zone of the sampled masonry pillar and visually damaged by the salts.

Among the three buildings considered, the Ex Slaughterhouse San Giobbe masonry is the only one exposed to atmospheric agents (rain, winds, temperature excursions) and with the lower altimetry (+ 125 cm on m.s.l.) so more easily accessible to sea water. Ca' Foscari has a similar altimetry (+ 130 cm on m.s.l.) but, since it is not directly exposed to rain action, it has a higher chlorides content at greater heights and depths. Comparing the anions data with those available for cations, it is evident that calcium concentrations are extremely high with respect to those of sulphates, especially for Ex Slaughterhouse San Giobbe (Table 27). This suggest that additional anions (probably CO₃²⁻), not investigated in this research work, are present at important concentrations, since calcite is widely found on samples through FTIR (see next section 3.3.4). On the contrary, sodium and chlorides concentrations, on average more similar each other, can be considered compatible with sodium chloride presence, Additional analysis are required in order to obtain a more complete information on the further anions species and their relative concentrations.

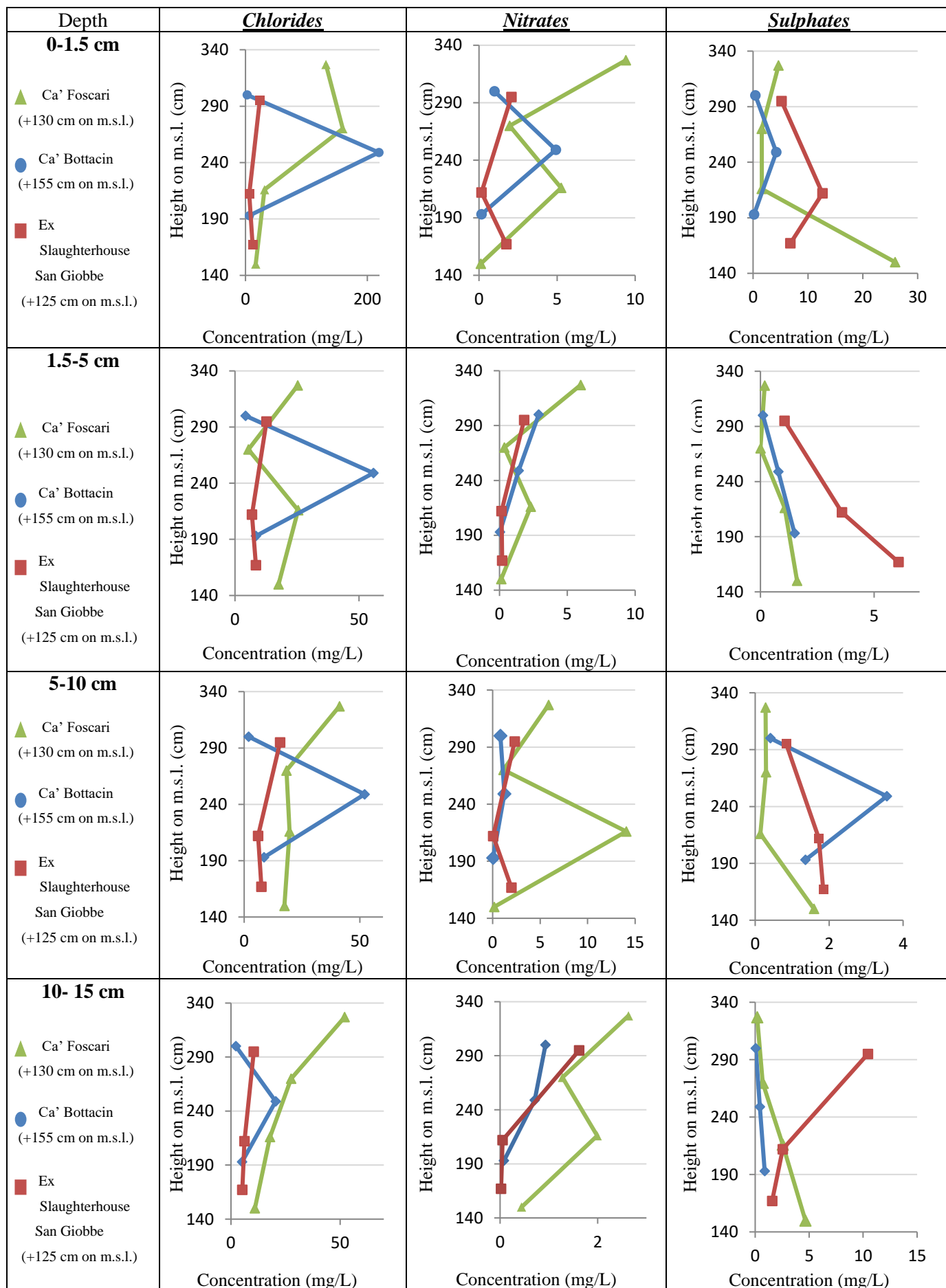


Table 67 Anions concentration trend for Ca' Foscari, Ca' Bottacin and Ex Slaughterhouse San giobbe with respect to the height on m.s.l. and sampling depths. Buildings altimetries are reported in brackets.

3.3.4 FT-IR analysis of the six Venetian buildings

The powder samples collected from the six Venetian case studies masonries were analyzed through FT-IR Spectroscopy (Table 28). Since the samples were 82 in total, only a specific depth range was investigated, one at each height considered. In doing so, the 20 samples analyzed are those at 1.5-5 cm depth. As expected, all infrared spectra show in general a similar profile, especially for the region between 3500 and 1600 cm^{-1} , while some differences regard the rest of the spectral range. A broad band is always centred between 3429-3467 cm^{-1} and it is attributable to hydroxyl group stretching vibrations of water typical of ceramic materials structure [87-89]. As reported in literature, this band is usually accompanied by another one around 1640 cm^{-1} corresponding to H-O-H bending of structural water of clays [87-90] and found experimentally between 1633 and 1638 cm^{-1} . Carbonate minerals are found according the weak signals around 1790 cm^{-1} attributable to calcite and registered only in four spectra (42 cm height San Giobbe; 25 and 95 cm Badoer Palace and 80 cm Ca' Tron) [91]. Moreover the 1500-1400 cm^{-1} spectral range is characterized by signals of carbonate bands of calcite related to C-O asymmetric stretching/bending [87,88,90]. These are registered in all the 20 samples analyzed.

The presence of potassium nitrate is linked to the sharp band at 1380 cm^{-1} [92] which Malipiero Palace in is slightly present (Figure 54). Moreover the signal intensity increases with the sampling height for Ca' Foscari, Ca' Bottacin and San Giobbe, in accordance with the increasing nitrates concentrations measured through Ion Chromatography (Figure 55). The same general trend regards also Badoer Palace while Ca' Tron does not show the presence of nitrates at middle height.

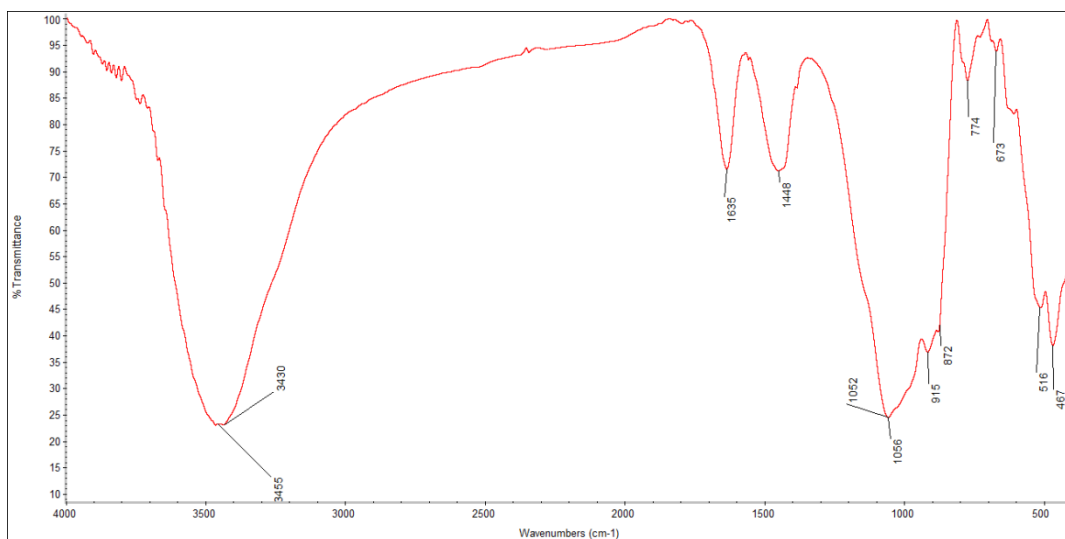


Figure 54 Infrared spectra of Ca' Foscari sample taken at 197 cm height from the ground (327 cm on m.s.l.) and 1.5-5 cm depth. The strong and narrow nitrates peak is clearly recognizable at 1380 cm^{-1} .

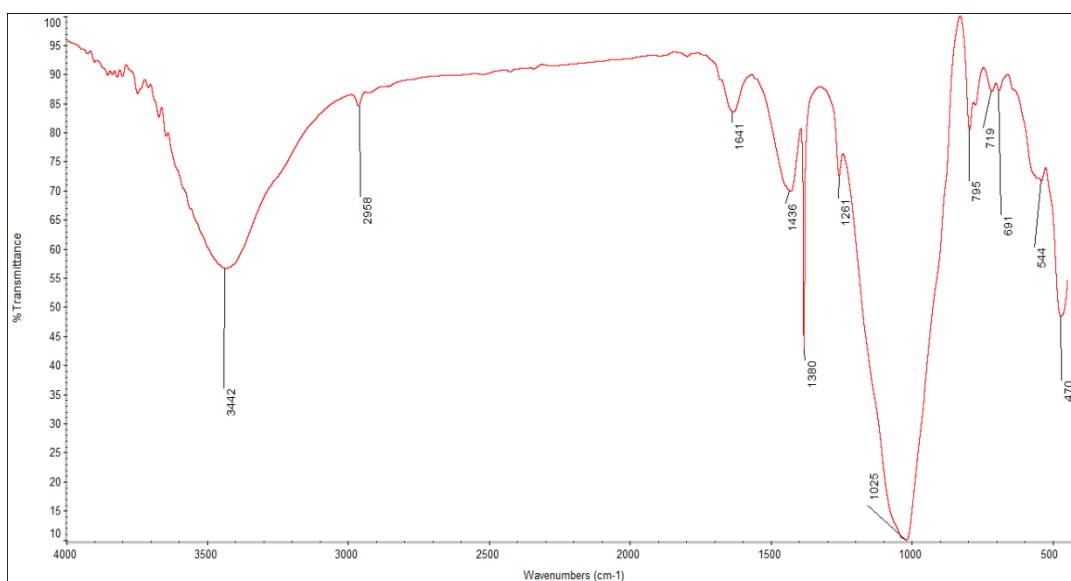


Figure 55 Infrared spectra of Malipero Palace sample taken at 149 cm height from the ground (239 cm on m.s.l.) and 2-5 cm depth. The nitrate peak is slightly visible.

The 1200-850 spectral range shows the signals proper of silica oxides. In this region, between 1000-1066 cm^{-1} a broad band was registered in all 20 analyzed samples and it is probably due to the overlapping of the signals of clay minerals bands. Literature confirms between 1100-1000 cm^{-1} the asymmetric Si-O stretching band for silicates [87,93].

The signals at around 875 cm^{-1} may be due to C-O stretching/bending proper of aluminasilicate phase and the same signals are related to calcite [90]. The successive ones between 800-770 cm^{-1} are linked to the Si-O-Si stretching of quartz [88,89].

At lower wavelengths, below 600 cm^{-1} are found the signals of iron oxides, in particular Fe-O vibration of hematite [87,88] and those of Si-O-Si bending [88,89].

Building Name	Height from the ground (cm)	Carbonatic minerals (Calcite)		Nitrates		Silicates	Silicates	Calcite (bending out of plane)	Quartz	Calcite (bending in plane)	Silicates	Iron oxides	Quartz
		1790 cm ⁻¹	1440 cm ⁻¹	1380 cm ⁻¹	1260 cm ⁻¹	1100-1000 cm ⁻¹ (broad band)	930-900 cm ⁻¹	870-78 cm ⁻¹	800-770 cm ⁻¹	721-710 cm ⁻¹	690 cm ⁻¹	579-530 cm ⁻¹	470-454 cm ⁻¹
Ca' Foscari (1.5-5 cm depth)	20		X		X	X	X	X	X	X		X	X
	86		X	X		X		X	X				X
	140		X	X	X	X			X	X		X	X
	197		X	X	X	X			X			X	X
Ca' Bottacin (1.5-5 cm depth)	38		X	X	X	X			X	X	X	X	X
	94		X	X	X	X			X		X	X	X
	145		X	X	X	X	X	X	X			X	X
Ex Slaughterhouse San Giobbe (2-5 cm depth)	42	X	X		X	X	X	X	X	X		X	X
	87		X	X	X	X		X	X		X	X	X
	140		X	X		X		X	X		X	X	X
Badoer Palace (2-5 cm depth)	25	X	X	X		X		X	X	X		X	X
	95	X	X	X		X	X	X	X	X			X
	148		X	X		X	X					X	X
	200		X	X		X	X		X			X	X
Ca' Tron (2-5 cm depth)	32		X	X	X	X	X	X	X				X
	80	X	X			X	X	X	X	X		X	X
	150	X	X	X	X	X	X	X	X	X			X
Malipiero Palace (2-5 cm depth)	26	X	X			X	X	X		X		X	X
	74	X	X			X	X	X	X	X			X
	149		X			x	X	X	X			X	X

Table 28 Results on FT-IR analysis performed on samples at 1.5-5 cm depth at each sampling height for the six Venetian buildings.

4 Conclusions

The aim of the present research is to widen the knowledge of rising damp phenomenon in Venetian masonries. The topic is of particular importance for the conservation of the architectural assets of the city in the present century, considering also the global climate change and its effects on Venetian Lagoon, e.g. the recent flooding in November 2019. The research involves two complementary approaches: the visual comparison of masonries photos over time and expert elicitation by considering specific decay parameters and the analytical determination of moisture and salts distribution within six Venetian buildings masonries.

Qualitative and semi-quantitative comparison of past and actual photos throughout the three Sestieri Castello, Dorsoduro and San Marco pointed out the main changes on conservation state of masonries over about 10 years. Among the total 36 considered locations, those of San Marco show a general worsening of the five evaluated parameters i.e. rising damp trend, plaster loss, biological growth, efflorescence and brick erosion. The observed greater changes could be probably related to Sestiere altimetry since San Marco is the lowest one among the three investigated.

This first research part is based on a visual approach that allow to observe superficial changes on masonry conservation state but at the same time should be integrated with further analytical investigation. This latter is exemplified by the second section of this research, based on quantitative determination of moisture and salts content within masonries of six Venetian buildings: Ca' Foscari, Ca' Bottacin, Ex Slaughterhouse San Giobbe, Badoer Palace, Ca' Tron and Malipiero Palace. Each one of these is differently exposed to sea water and weathering, based on their altimetries on mean sea level and their external or internal position. Efflorescence and deterioration on masonries surfaces are clearly distinguishable through visible light observation then integrated with the ones in Infrared Thermography. Moisture and salt content determination at each masonry height and depth, including the hygroscopic contribution, reveals in general higher moisture contents for the two external masonries analysed, of Badoer Palace and Ex Slaughterhouse San Giobbe and a higher salt content for Ca' Bottacin. This latter and Badoer Palace, both with maximum salts content at + 250 cm on m.s.l., are the closest one to the empirical model for moisture and salts distribution in Venetian masonries found in literature.

The comparison of chlorides, nitrates and sulphates quantification is performed on Ca' Foscari, Ca' Bottacin and Ex Slaughterhouse San Giobbe masonries. This latter has lower ionic concentrations since it is an external wall and so weathering exposed while the other two masonries are characterized by a high, sea water derived, chloride content and nitrates at greater heights are mainly found in Ca' Foscari wall. Nitrates presence is confirmed in all masonries, except Malipiero Palace one, also by FTIR Spectroscopy and the related peak intensity increases with height.

In both research sections, the first of photo comparison and the second of six case studies investigation, buildings exposure to sea water and their altimetry on m. s. l. constitute discriminating factors in evaluating a rising damp worsening or improvement over time and the current conservation state of masonries.

This study represents a contribution to rising damp investigation in Venice and its possible future perspective are the photo comparison extension to further archives and also to the Sestieri Santa Croce, San Polo and Cannaregio, covering the entire historic centre of Venice and the completion of Ion Chromatography analysis for Badoer Palace, Ca' Tron and Malipero Palace. In particular further anions investigation is necessary, since the pointed out discrepancies between anions and cations concentrations, especially concerning sulphates and calcium. Moreover, all the analysis performed on the six masonries, included the registered environmental parameters during their samplings, can be considered a starting point in assessing effectiveness of possible future interventions against rising damp if performed on the same six building masonries.

APPENDIX 1 – Instrumental specifications

Canon PowerShot G12 camera

CCD optical sensor with a 10.0 Megapixel resolution and 1/1.7" size (14.9 mm)
 28mm wide, 5x zoom lens, Hybrid IS
 7.0 cm (2.8") Vari-Angle LCD, Electronic Level, OVF
 ISO capabilities from 100-12,800, with expansion
 Front Dial, Full Manual control & Multi-Control Dial
 Lens from 6.1-30.5mm
 RAW shooting
 HD movies, HDMI
 High Dynamic Range mode
 Smart Auto mode
 Multi- Aspect Shooting
 Extensive accessory system, including FA-DC58B lens filter adapter

EC- Meter GLP 31 Conductivity meter

<p>Measured parameters</p> <table style="width: 100%; border-collapse: collapse;"> <tr> <td style="width: 20%;">Conductivity</td> <td style="width: 40%;">0.001* μS...1000 ** mS/cm</td> <td style="width: 40%;"></td> </tr> <tr> <td>Salinity</td> <td>5.85 mg/l... 311.1 g/l NaCl</td> <td></td> </tr> <tr> <td>T.D.S.</td> <td>0 mg/l ...500 g/L</td> <td></td> </tr> <tr> <td>Temperature</td> <td>-20.0 ... 150.0 °C (-4 ... 302 °F)</td> <td></td> </tr> </table> <table style="width: 100%; border-collapse: collapse;"> <tr> <td style="width: 20%;"></td> <td style="width: 40%;">Measurement error</td> <td style="width: 40%;">Reproducibility</td> </tr> <tr> <td>Conductivity</td> <td>$\leq 0.5\%$</td> <td>$\pm 0.1\%$</td> </tr> <tr> <td>Salinity and T.D.S.</td> <td>$\leq 0.5\%$</td> <td>$\pm 0.1\%$</td> </tr> <tr> <td>Temperature</td> <td>≤ 0.2 °C (0.36 °F)</td> <td>± 0.1°C(0.18)°F</td> </tr> </table> <p>Automatic temperature compensation</p> <p>CT (temperature coefficient) Linear, 0.00 ... 5.00% /°C Non linear for natural waters (UNE EN 27888).</p> <p>TR (reference temperature) 20°C (68°F), 25°C (77°F) or values between 0...99°C (0...210°F).</p> <p>EC Calibration (conductivity) Standards: 147 μS/cm, 1413 μS/cm ,12.88 mS/cm and 111.8 mS/cm With 1,2 or 3 standards inside the range. Special calibration at any EC, salinity or TDS value. Manual introduction of cell constant. Programmable calibration validity from 0 to 99 days</p> <p>TDS conversion factor Values between 0.4 ... 1. Standard 0-64.</p> <p>Temperature readjustment Correction of the temperature probe deviation (A.T.C.) at 25°C (77°F) and 85°C (185 °F)</p>	Conductivity	0.001* μ S...1000 ** mS/cm		Salinity	5.85 mg/l... 311.1 g/l NaCl		T.D.S.	0 mg/l ...500 g/L		Temperature	-20.0 ... 150.0 °C (-4 ... 302 °F)			Measurement error	Reproducibility	Conductivity	$\leq 0.5\%$	$\pm 0.1\%$	Salinity and T.D.S.	$\leq 0.5\%$	$\pm 0.1\%$	Temperature	≤ 0.2 °C (0.36 °F)	± 0.1 °C(0.18)°F	<p>Data Logger. Storage capacity up to 400 readings</p> <p>Languages Spanish, Italian, French, English and Polish</p> <p>Display Graphic, backlit liquid crystal, 128x64 dots</p> <p>Connectable sensors Conductivity cell with Pt 1000 probe, telephone connector</p> <p>Connectable peripherals CRISON magnetic stirrer. Printer or PC. External PC keyboard or barcode reader</p> <p>Directive low voltage and EMC According to 2004/95/EC. According to 2004/108/EC.</p> <p>Power supply External plug-in power supply 220VCA/12 VDC, 3.3 W.</p> <p>Materials Enclosure, ABS and PC. Keypad, PET with protective treatment.</p> <p>Physical parameters Weight:1100 g. Size: 350 x 200 110 mm.</p>
Conductivity	0.001* μ S...1000 ** mS/cm																								
Salinity	5.85 mg/l... 311.1 g/l NaCl																								
T.D.S.	0 mg/l ...500 g/L																								
Temperature	-20.0 ... 150.0 °C (-4 ... 302 °F)																								
	Measurement error	Reproducibility																							
Conductivity	$\leq 0.5\%$	$\pm 0.1\%$																							
Salinity and T.D.S.	$\leq 0.5\%$	$\pm 0.1\%$																							
Temperature	≤ 0.2 °C (0.36 °F)	± 0.1 °C(0.18)°F																							
Conductivity cell																									
<table style="width: 100%; border-collapse: collapse;"> <tr> <td style="width: 50%;">Approximate constant</td> <td style="width: 50%;">Electrode material</td> </tr> <tr> <td>0.7 cm⁻¹</td> <td>Platinum electrodes</td> </tr> <tr> <td>Measurement scale</td> <td>Electrodes number</td> </tr> <tr> <td>0.2 μS/cm... 200</td> <td>3</td> </tr> <tr> <td>Working temperature (°C)</td> <td>Temperature sensor</td> </tr> <tr> <td>-30 ... 85 °C</td> <td>Pt 1000</td> </tr> <tr> <td>Material</td> <td>Minimum dive</td> </tr> <tr> <td>Glass body</td> <td>25mm</td> </tr> </table>	Approximate constant	Electrode material	0.7 cm ⁻¹	Platinum electrodes	Measurement scale	Electrodes number	0.2 μ S/cm... 200	3	Working temperature (°C)	Temperature sensor	-30 ... 85 °C	Pt 1000	Material	Minimum dive	Glass body	25mm									
Approximate constant	Electrode material																								
0.7 cm ⁻¹	Platinum electrodes																								
Measurement scale	Electrodes number																								
0.2 μ S/cm... 200	3																								
Working temperature (°C)	Temperature sensor																								
-30 ... 85 °C	Pt 1000																								
Material	Minimum dive																								
Glass body	25mm																								

761 Compact IC Chromatographs

<p>High - pressure pump</p> <p>Type Serial dual piston pump with two valves</p> <p>Pump capacity</p> <p>Flow range 0.20...2.5 mL/min</p> <p>Maximum error <± 2% of set value</p> <p>Flow constancy < 0.5% of set value</p> <p>Reproducibility of eluent flow typ. Better than ± 0.1%</p> <p>Pressure measurements</p> <p>Pressure range 0...25.0 MPa(0...250 bar)</p> <p>Residual pulsation < 1% (at 1mL/min water and 10 MPa pressure, without pulsation dampener)</p> <p>Measurement principle Piezoresistive measurement</p> <p>Response time:3 ms</p> <p>Measurement volume: ca. 50 µL</p> <p>Maximum error ± 3% of set value</p> <p>Resolution 0.1 MPa (conductivity measurements)</p> <p>0.01 MPa (pressure measurements)</p> <p>Sampling rate 1 measurement/piston stroke (pump running)</p> <p>1 measurement/s (pump not running)</p> <p>10 measurements/s (pressure measurements)</p> <p>Safety shutdown</p> <p>Function Automatic shutdown when upper and lower pressure limits violated</p> <p>Maximum pressure limit Adjustable between 0.1...25.0 MPa (1...250 bar), Response time: 1 pump cycle</p> <p>Minimum pressure limit Adjustable between 0.1...25.0 MPa (1...250 bar), Inactive at 0 MPa</p> <p>Response time: 5 pump cycles</p> <p>Pump head</p> <p>Pump head volumes Main piston : 40µL</p> <p>Priming piston: 20 µL</p> <p>Pump displacement Main piston: 28.5 µL</p> <p>volumes Priming piston: 14.25 µL</p> <p>Length of stroke Main piston: 3.6 mm</p> <p>Priming piston: 1.8 mm</p>	<p>Injection valve</p> <p>Actuator switching duration 100...150 ms)</p> <p>Pressure resistance 25 MPa (250 bar)</p> <p>Suppressor module (only in anions detection)</p> <p>Switching duration140 ms</p> <p>Pressure resistance2.5 MPa (25 bar)</p> <p>Leak detector</p> <p>Type Detector with 2 electrodes approx. 1mm above base of interior</p> <p>Response level Resistance < 1MΩ (for deion. water)</p> <p>Peristaltic pump</p> <p>Type 2-channel peristaltic pump</p> <p>Pump capacity</p> <p>Rotational speed 20 U/min at 50 Hz</p> <p>24 U/min at 60 Hz</p> <p>Flow range 0.5...0.6 mL/min</p> <p>Maximum error ± 5%</p> <p>Maximum pressure 0.4 MPa (4 bar)</p> <p>Pumpable liquids Clear liquids with no solid contents</p> <p>Pump tubing material PP (polypropylene)</p> <p>Conductivity detector</p> <p>Construction Thermostatted conductivity detector with 2ring- shaped steel electrodes</p> <p>Measurement Alternating current measurement with principle 1kHz frequency and ca. 1.7 V amplitude</p> <p>Effective cell volume 0.8 µL</p> <p>Cell constant Approx. 17/cm</p> <p>Operating temperature Adjustable in steps of 5°C from 25... 45°C</p> <p>Max temperature ± 2.5°C</p> <p>Deviation</p>
--	--

<p>Carrier material Polyvinyl alcohol with quaternary ammonium groups</p> <p>Column capacity 37 µmol (Cl⁻)</p> <p>Column dimensions 250 x 4.0 mm</p> <p>Eluents</p> <p>Phthalate eluent (standard eluent)</p> <p>Without chemical suppression</p> <p>Phthalic acid: 5.0 mmol/L; 1.660 mg/2L</p> <p>TRIS: pH= 4.4</p> <p>Carbonate eluent (standard eluent)</p> <p>Withchemical suppression</p> <p>Sodium hydrogen carbonate: 1.7 mmol/L; 286 mg/2 L</p> <p>Sodium carbonate: 1.8 mmol/L; 382 mg/2 L</p> <p>Carbonate eluent, modified</p> <p>Sodium hydrogen carbonate: 4.0 mmol/L; 672 mg/ 2L</p> <p>Sodium carbonate: 1.0 mmol/L; 212 mg/2 L</p> <p>Housing material PEEK</p> <p>Max. pressure 12 MPa</p> <p>Maximum flow 2.0 mL/min</p> <p>Organic modifier 0-100% (particularly acetone, acetonitrile, methanol)</p> <p>Particle size 9 µm</p> <p>pH range 3...12</p> <p>Standard flow 1.0 mL/min</p>	<p>Cations Column : Metrosep C3 - 250/4.0</p> <p>Polyvinyl alcohol with carboxyl groups</p> <p>30µmol (K⁺)</p> <p>250 X 4.0 mm</p> <p>Nitric acid eluent (standard eluent)</p> <p>Nitric acid /c= 1 mol/L): 5.0 mmol/L; 10 mL/2L (column temperature 40°C)</p> <p>Nitric acid/ crown ether eluent</p> <p>Nitric acid (c= 1 mol/L): 3.5 mmol/L; 7mL/2L 18-crown-6:0.5 mmol/L; 264 mg/2L (column temperature 40°C)</p> <p>PEEK</p> <p>15 MPa</p> <p>1.5 mL/min</p> <p>0 – 50% acetonitrile, 0-30% acetone, no methanol</p> <p>5 µm</p> <p>2...12</p> <p>1.0 mL/min</p>
--	--

Bibliography and sitography

- [1] J. M. P. Q. Delgado, A. S. Guimarães, V. P. de Freitas, I. Antepará, V. Kočí, R. Černý, *Salt Damage and Rising Damp Treatment in Building Structure*, Advances in Materials Science and Engineering, 2016, 1-13.
- [2] <https://sdfoundation.org.uk/downloads/BSI-White-Paper-Moisture-In-Buildings.PDF>
- [3] E. Borrelli, Arc Laboratory Handbook, *Conservation of Architectural Heritage, Historic Structures and Materials*, ICCROM, 1999.
- [4] J. F. Straube, *Moisture in buildings*, Ashrae Journal, 2002.
- [5] Dr Z. Zhang, *A Review of Rising Damp in Masonry Buildings*, Advanced Polymer and Composites (APC) Research Group Department of Mechanical and Design Engineering University of Portsmouth, Anglesea Building, Portsmouth, Hampshire, 2014.
- [6] E. Franzoni, *Rising damp removal from historical masonries: A still open challenge*, Construction and Building Materials, 2014, 54; 123–136.
- [7] K. Agyekum, B. Salgin, *Diagnosing rising damp in residential buildings: lessons from three cases*, ANNALS of Faculty Engineering Hunedoara, International Journal of Engineering, 2017.
- [8] C. Hall, W. D. Hoff, *Rising damp: capillary rise dynamics in walls*, Proceedings of the royal society A, 2007, 463;1871–1884.
- [9] B. Lubelli, R.P.J. van Hees, J. Bolhuis, *Effectiveness of methods against rising damp in buildings: Results from the EMERISDA project*, Journal of Cultural Heritage, 2018; 315: 512-522.
- [10] <https://www.buildingconservation.com/articles/risingdamp/risingdamp.htm>
- [11] M. Gacic´, I.M. Mosquera, V. Kovacevic, A. Mazzoldi, V. Cardin, F. Arena, G. Gelsi, *Temporal variations of water flow between the Venetian lagoon and the open sea*, Journal of Marine Systems 2004; 51:33–47.
- [12] L. Carbognin, P. Teatini, A. Tomasin, L. Tosi, *Global change and relative sea level rise at Venice: what impact in term of flooding*, 2010, 35; 1039-1047.
- [13] G. Gambolati, P. Teatini, *Venice Shall Rise Again*, Chapter 3- The Venice Lagoon, First Edition, Elsevier Insights, United States of America, 2013.
- [14] A. Casasso, A. Di Molfetta, R. Sethi, *Groundwater monitoring at a building site of the tidal flood protection system “MOSE” in the Lagoon of Venice, Italy*, Environmental Earth Sciences, 2015;73: 2397-2408.
- [15] <http://www.corila.it>
- [16] P. Caloi, *Sulle cause delle “acque alte” nell’ Adriatico settentrionale, con particolare riguardo alla Laguna di Venezia*, Annals of Geophysics, 1973; 26: 2-3.
- [17] E. Di Sipio, F. Zezza, *Present and future challenges of urban systems affected by seawater and its intrusion: the case of Venice, Italy*, Hydrogeology Journal, 2011; 19: 1387-1401.
- [18] A. Brambati, L. Carbognin, T. Quaia, P. Teatini, L.Tosi, *The Lagoon of Venice: geological setting, evolution and land subsidence*, Episodes, 2003; 26: 264-268.
- [19] <https://www.venezia.isprambiente.it>
- [20] <https://www.comune.venezia.it/>
- [21] P. Foraboschi, *Specific structural mechanics that underpinned the construction of Venice and dictated Venetian architecture*, Engineering Failure Analysis, 2017; 78: 169-195.
- [22] S. Munaretto, P. Vellinga, H. Tobi, *Flood Protection in Venice under Conditions of Sea-Level Rise: An Analysis of Institutional and Technical Measures*, Coastal Management, 2012;40:355-380.
- [23] G. Bertagnoli, C. Anerdi, M. Malavisi, N. Zoratto, *Autogenous Crak Control during Construction Phases of MOSE Venice Dams*, IOP Conf. Series: Materials Science and Engineering, 2017; 245: 1-10.
- [24] P. Foraboschi, A. Vanin, *Experimental investigation on bricks from historical Venetian buildings subjected to moisture and salt crystallization*, Engineering Failure Analysis, 2014; 45:185-203.

- [25] E. Goldin, *L'umidità di risalita a Venezia - analisi dei meccanismi che influiscono sul fenomeno di risalita dell'acqua salina e sugli effetti di degrado che questa ha sui materiali edili veneziani*, Bachelor Thesis in Technologies for Conservation and Restoration, Ca' Foscari University, Venice, Italy A.Y. 2014/2015.
- [26] F.C.Izzo, G. Biscontin, C.Bini, *Indagini sul terreno* in G. Biscontin, F. Izzo, E. Rinaldi, *Il sistema delle fondazioni lignee a Venezia*, CORILA 2009, Venezia, 65-78.
- [27] V. Apih, M. Makarovic, *Development of a method for drying out the damp walls of buildings in Venice*, Transactions on the Built Environment Institute for Testing and Research in Materials and Structures (ZRMK), 1993; 4, Ljubljana, Slovenia.
- [28] A.Bakolas, G.Biscontin, A. Moropoulou, E. Zendri, *Salt impact on brickwork along the canals of Venice*, Materials and Structures, 1996; 29: 47-55.
- [29] G. Torraca *Porous building materials: Materials Science for Architectural Conservation*, ICCROM, 2005.
- [30] E. Rirsch, Z. Zhang, *Rising damp in masonry walls and the importance of mortar properties*, Construction and building materials, 2010 ; 24:1815-1820.
- [31] <http://venice.umwblogs.org/exhibit/>
- [32] P. Lopez- Arce, E. Doehne, J. Greenshields, D. Benavente, D. Young, *Treatment of rising damp and salt decay: the historic masonry buildings of Adelaide, South Australia*, Materials and Structures, 2009; 42 :827-848.
- [33] A. E. Charola, C. Bläuer, *Salts in Masonry: An Overview of the Problem*, Restoration of Buildings and Monuments, 2015; 21: 119-135.
- [34] G. Alfano, C. Chiancarella, E. Cirillo, I. Fato, F. Martellotta, *Long-term performance of chemical damp-proof courses: Twelve years of laboratory testing*, Building and environment 2006; 41:1060-1069.
- [35] G. Pia, *Aspetti innovativi per la valutazione e la misura della porosità nei materiali dell' edilizia antica e moderna*, Doctoral Thesis, Supervisor: Prof. Ulrico Sanna, Assistant Supervisor: Dr. Cirillo Atzeni, Alma Mater Studiorum Università di Bologna, A.Y 2007/2008.
- [36] <https://science.jrank.org/pages/1182/Capillary-Action.html>
- [37] G.S. Barozzi, D. Angeli, *A note on capillary rise in tubes*, Energy Procedia 2014 ;45 :548-557.
- [38] L. Falchi, D. Slanzi, E. Balliana, G. Driussi, E. Zendri, *Rising damp in historical buildings; A Venetian perspective*, Building and Environment, 2018 ;131:117-127.
- [39] A.E. Charola, *Salts in the Deterioration of Porous Materials: An Overview*, Journal of the American Institute for Conservation, 2013; 39 :327-343.
- [40] A. Sardella, P. De Nuntiis, C. Giosuè, F. Tittarelli, A. Bonazza, *Diagnosis and methods against rising damp in industrial heritage buildings :a case study in Italy*, IMEKO International Conference on Metrology for Archaeology and Cultural Heritage Lecce, Italy, October 23-25,2017.
- [41] M. Collepardi, S. Collepardi, R. Troli, *Salt Weathering of Masonry Walls The Venice Experience*, 2000.
- [42] V. Voronina, L. Pel, K. Kopinga, *Effect of osmotic pressure on salt extraction by a poultice*, Construction and Building Materials, 2014; 53: 432–438.
- [43] S. Gupta, H. P. Huinink, M. Prat, L. Pel, K. Kopinga, *Paradoxical drying of a fired-clay brick due to salt crystallization*, Chemical Engineering Science, 2014; 109: 204–211.
- [44] L. B. Mayer, G. Baronio, *Indagine sull' aderenza tra legante e laterizio in malte ed intonaci di coccio pesto*, Ministero per i Beni e le Attività Culturali-Bollettino d'Arte 109-115.
- [45] R. T. Kreh, Sr, *Masonry Skills*, Fifth Edition Thomson Delmar Learning, United States of America, 2003.
- [46] M. Realini, Lucia Toniolo, *II International Symposium " The Oxalate Films in the Conservation of Works of Art" Proceedings: Centro CNR "Gino Bozza" Per lo studio delle cause di deperimento e dei metodi di conservazione delle opere d'arte*, Politecnico di Milano, Milan, March 25-27, EDITEAM, 1996.
- [47] K. Zehnder, *Salt Weathering on Monuments*, Conference: 1st international symposium on the conservation of monuments in the Mediterranean Basin, Bari,7-10 June,1989.

- [48] Emerisda, *Summary report on existing techniques, procedures and criteria for assessment of effectiveness of interventions*, D2.3 FINAL version, 2014.
- [49] P. Gasparoli, F. Trovò, *Venezia fragile. Processi di usura del sistema urbano e possibili mitigazioni*, Altralinea, Firenze, 2014.
- [50] I. Nardini, E. Zendri, G. Biscontin, A. Brunetin, *Analytical methods for the characterization of surface finishing in bricks*, *Analytica Chimica Acta*, 2006; 577:276-280.
- [51] <http://sistemavenezia.regione.veneto.it/content/legge-speciale-venezia>
- [52] http://www.monitoraggio.corila.it/Docs/Monografia-MOSE_Completo.pdf
- [53] <http://smu.insula.it/index.php.html>
- [54] E. Di Sipio, F. Zezza, *Present and future challenges of urban systems affected by seawater and its intrusion: the case of Venice, Italy*, *Hydrogeology Journal*, 2011; 19: 1387-1401.
- [55] *The future of Venice and its Lagoon in the context of global change*
http://www.unesco.org/new/fileadmin/MULTIMEDIA/FIELD/Venice/pdf/rapporto1_very%20high%20res.pdf
- [56] A. Varrani, M. Nones, *Vulnerability, impacts and assessment of climate change on Jakarta and Venice*, *International Journal of River Basin Management*, 2018; 16: 439-447.
- [57] A. Zirinoa, H. Elwanya, C. Neiraa, F. Maicu, G. Mendoza, L. A. Levina *Salinity and its variability in the Lagoon of Venice, 2000–2009*, *Advances in Oceanography and Limnology*, 2014; 5:41-59.
- [58] F. Biasolo, *Valutazione e monitoraggio dello stato di conservazione di superfici lapidee veneziane attraverso l'analisi di immagini*, Bachelor Thesis in Technologies for Conservation and Restoration, Ca' Foscari University of Venice, Italy, Supervisor Prof. Elisabetta Zendri, Supervisor Assistant: Dr. Laura Falchi, A.Y 2017/2018.
- [59] https://cpn.canon-europe.com/it/content/product/cameras/powershot_g12.do
- [60] <http://www.albumdivenezia.it>
- [61] https://www.unive.it/pag/fileadmin/user_upload/comunicazione/tour/documenti/fondo_storico/Profilo_eng_appr..pdf
- [62] <http://www.veneziatoday.it/attualita/ca-bottacin-restaurato-venezia.html>
- [63] [https://www.unive.it/pag/14024/?tx_news_pi1\[news\]=6857&cHash=335b8aee4b46663b889b76e75f44e908](https://www.unive.it/pag/14024/?tx_news_pi1[news]=6857&cHash=335b8aee4b46663b889b76e75f44e908)
- [64] <https://www.conoscerevenezia.it/?p=44585>
- [65] https://www.unive.it/pag/fileadmin/user_upload/ateneo/spazi/schedestoriche/scheda_cenni_storici_sangiobbe_eng.pdf
- [66] <http://www.iuav.it/Ateneo1/Sedi/Sedi-venez/palazzo-Ba/>
- [67] <http://www.iuav.it/Ateneo1/Sedi/Sedi-venez/ca--Tron/>
- [68] http://www.palazzomalipiero.com/sito_statico/storia.htm
- [69] <https://www.labiennale.org/it/bacheca/515>
- [70] <https://venicere.wordpress.com/2014/04/11/propagation-of-energy-festival-a-palazzo-malipiero-propagation-ofenergy-festival-at-palazzo-malipiero->
- [71] Summary report on existing techniques, procedures and criteria for assessment of effectiveness of interventions, D2.3 FINAL version, 2014. https://www.emerisda.eu/wp-content/uploads/2014/07/D-2_3.pdf
- [72] S.K.Babu, Matthew C. Y. Chan, *Testing of Wall tiles using Infrared Thermography*, 2004.
- [73] E. Grinzato, *IR Thermography Applied to the Cultural Heritage Conservation*, Constructions Technology Institute (ITC), National Research Council (CNR), 18th World Conference on Non destructive Testing, 16-20 April 2012, Durban, South Africa.
- [74] J.Spodek, E. Rosina *Application of Infrared Thermography to Historic Building Investigation*, , *Journal of Architectural Conservation*, March 2009; 15: 65-81..
- [75] <https://www.flir.com/discover/instruments/moisture-restoration/thermal-imaging-cameras-help-preserve-italys-cultural-heritage/>
- [76] UNI 11085:2003 Beni culturali – Materiali lapidei naturali ed artificiali – Determinazione del contenuto d'acqua: Metodo ponderale
- [77] Emerisda, *Summary report on existing techniques, procedures and criteria for assessment of effectiveness of interventions*, DL2.4 FINAL version, 2015.

- [78] Standard salt solutions for humidity calibration, IUPAC recommendation
- [79] UNI 11087:2003 Beni culturali – Materiali lapidei naturali ed artificiali – Determinazione del contenuto di sali solubili
- [80] <http://www.crisoninstruments.com/it>
- [81] <https://www.sigmaaldrich.com/italy.html>
- [82] <https://www.metrohm.com/it-it>
- [83] D. Camuffo, C. Bertolin, P. Schenal, *A novel proxy and the sea level rise in Venice, Italy, from 1350 to 2014* Dario Camuffo, Climatic Change. 2017; 143:73–86.
- [84] http://www.iitk.ac.in/ce/test/Material%20Characterisation_Low%20Cost%20Housing_Dr.%20V%20singhal%20_%20H.Basha.pdf
- [85] M. Raimondo, M.Dondi, F.Mazzanti, P.Stefanizzi, P.Bondi, *Equilibrium moisture content of clay bricks: The influence of the porous structure*, Building and Environment, 2007; 42: 926-932.
- [86] J.Tuna, J. Feitera, I. Flores-Colen, J. de Brito, M.F.C. Pereira, *In Situ Characterization of Damaging Soluble Salts in Wall Construction Materials*, Journal of Performance of Constructed Facilities, October 2014.
- [87] , A.N. Adazabra, G. Viruthagiri, N. Shanmugam *Infrared analysis of clay bricks incorporated with spent shea waste from the shea butter industry*, Journal of Environmental Management, 2017; 191: 66-74.
- [88] P. Sathya, G. Velraj, S. Meyvel, *Fourier transform infrared spectroscopic study of ancient brick samples from Salavankuppam Region, Tamilnadu, India*, Advances in Applied Science Research, 2012; 3 :776-779.
- [89] MdRaheijuddin, A.Gohain , *X-Ray diffraction and Fourier transform infrared spectra of the bricks of the Kamakhya temple* , Indian Journal of Pure & Applied Physics, 2013; 51: 745-748.
- [90] A. Sultana, A.Valouma, G. Bartzas, K. Komnitsas *Properties of inorganic polymers produced from brick waste and metallurgical slag* , Minerals 2019;9:551:1-17.
- [91] S. Sivakumar , R.Ravisankar, Y. Raghu , A. Chandrasekaran , J. Chandramohan, *FTIR Spectroscopic Studies on Coastal Sediment Samples from Cuddalore District, Tamilnadu, India* , Indian Journal of Advances in Chemical Science 2012; 1: 40-46.
- [92] F. Zambon, *Il processo di risalita capillare nelle murature: studio del degrado chimico-fisico legato alla migrazione dei Sali*, Master Thesis in Industrial Chemistry, Ca' Foscari University of Venice, supervisor G. Biscontin, Venice, Italy A.Y. 1981-1982.
- [93] M. R. Derrick, D. Stulik ,J.M. Landry, *Infrared Spectroscopy in Conservation Science*. Scientific Tools for Conservation, The Getty Conservation Institute, , Los Angeles, 1999.